Cross-talk of protein kinase B (PKB/Akt) with the transcription factor NFAT and the Src kinase Fyn in T lymphocytes

Dissertation

zur Erlangung des akademischen Grades

doctor rerum naturalium

(Dr. rer. nat.)

genehmigt durch die Fakultät für Naturwissenschaften

der Otto-von-Guericke-Universität Magdeburg

von Diplom-Biologe Thomas Drewes

geb. am 22.06.1975 in Steinheim

Gutachter: PD Dr. Ursula Bommhardt

Prof. Dr. Lars Nitschke

eingereicht am: 12.02.2010

verteidigt am: 16.09.2010

Acknowledgement

First, I like to thank my mentor PD Dr. Ursula Bommhardt for coaching and her outstanding engagement. I am grateful for her inexhaustible, continuous support and the fact that she always had time for me, my questions and discussion from the first day of my work at Magdeburg until the defense of my thesis.

Next, I want to thank my colleagues Mandy Pierau, Swen Engemann, Stefanie Holze and Gabi Weitz with whom I worked together in the lab day by day. Especially, I want to thank for their help, patience and friendliness.

I am grateful to Dr. Michal Smida and Dr. Jonathan Lindquist for supporting me and my work by providing antibodies, reagents and helpful advice.

I like to thank Prof. Burkhart Schraven for providing the possibility to work in his institute, for helpful scientific discussion and advice and for providing DNA-constructs.

I am grateful to Prof. Dirk Reinhold for supervising my radioactive work and calling me ‘Bürgermeister von Stralsund’.

I want to mention Tina Krieger and Dr. Bhavani Kowtharapu who introduced me into the usage of the Kodak quantification software.

I also want to thank all technicians of the institute who helped me concerning protocols and reagents and all scientists for helpful professional discussion and advice.

Finally, I like to thank all members of the Institute for Molecular and Clinical Immunology for providing a good, collegial atmosphere. I remember the parties I joined, showing me that there is also life besides work.

1 Summary

Protein kinase B (PKB), a ubiquitously expressed serine/threonine kinase, has central impact on several cellular processes including survival, proliferation and differentiation. In T cells, PKB is activated by growth factors, cytokines as well as TCR and CD28 stimulation. Previous studies performed with PKB transgenic (tg) mice, expressing a constitutively active version of PKBα (myrPKB) in the T cell lineage, revealed active PKB to influence TCR proximal signaling events. The aim of this study was to characterize the cross-talk of PKB with the transcription factor NFAT and the Src kinase Fyn at the biochemical and molecular level.

Expression of a hyperactive form of the phosphatase calcineurin (ΔCam) in thymocytes increased nuclear NFAT levels and caused a block in early thymocyte differentiation. Co-expression of PKB in ΔCam tg thymocytes reduced NFAT activity, induced Rag and TCR β-chain expression and abrogated the block in thymocyte differentiation. Rag2 promoter activity assays showed that NFATc1 as well as NFATc2 regulates the Rag2 promoter, NFAT factors thus being among the few transcription factors so far known to be involved in the regulation of *rag* expression in T cells. IL-2 promoter activity induced by NFAT was also down-modulated by active PKB. Furthermore, myrPKB enhanced the inhibition of NFAT activation in concert with the NFAT kinases PKA and GSK3 or the transcription factor Foxp3. Since recombinant PKB phosphorylated NFATc1 at (at least) two sites within the NFAT regulatory domain, NFAT could be a direct substrate of PKB. However, despite several mutations in GST-NFAT fusion proteins encompassing the regulatory domain, no single PKB site(s) could be elucidated, suggesting that a complex interplay of several residues is needed for NFAT phosphorylation by PKB.

Compared to wild type cells, peripheral myrPKB tg $CD4^+$ T cells showed enhanced proliferation after CD3 stimulation and in the presence of pharmacological Src kinase and MEK inhibitors. In addition, western blot analysis revealed enhanced Erk activity in myrPKB tg $CD4^+$ T cells and *in vitro* kinase assays (IVKs) showed increased Fyn activity in myrPKB tg $CD4^+$ T cells and thymocytes. By generating several GST-Fyn fusion proteins and mutagenesis of prospective PKB phosphorylation sites, a PKB phosphorylation site was identified in N-terminal Fyn, Fyn thus being a novel substrate of PKB *in vitro*. Furthermore, in transfected HEK 293T cells PKB and Fyn co-immunoprecipitated, supporting a direct interaction of PKB and Fyn *in vivo*. Interestingly, Fyn hyperactivity in PKB tg cells was not correlated with increased phosphorylation of the adapter molecule PAG at Y314, a known Fyn phosphorylation site and anchor for the recruitment of the kinase Csk, which inhibits Src kinase activity and, thereby, leads to the shut-down of T cell receptor signaling.

It is known that increased Fyn activity causes/coincides with T cell anergy. Interestingly, in the model of ionomycin induced anergy, myrPKB tg $CD4^+$ T cells were less susceptible to anergy induction. Whereas anergy, i.e. lack of proliferation after CD3 Ab restimulation, in wild type $CD4^+$ T cells correlated with enhanced Fyn activity, in comparison to untreated wild type cells, ionomycin treatment of myrPKB tg $CD4^+$ T cells did not enhance Fyn activity. Altogether the data reveal a novel interaction and impact of PKB on Fyn activity. PKB mediated changes in Fyn activity, possibly also resulting in altered interaction of Fyn with certain substrates, may be important in regulatory processes like anergy, as our initial results indicate. Finally, the cross-talk of PKB with Fyn, both known proto-oncogenes, could also be important for transformation and tumorigenesis.

2 Zusammenfassung

Proteinkinase B (PKB), eine ubiquitär exprimierte Serin/Threonin-Kinase, hat zentralen Einfluss auf verschiedene zelluläre Prozesse, wie Überleben, Proliferation, Wachstum und Differenzierung. In T-Zellen erfolgt PKB-Aktivierung über Wachstumsfaktoren, Zytokine sowie TCR- und kostimulatorische CD28-Signale. Vorherige Arbeiten zur Rolle von PKB in transgenen (tg) Mäusen, die eine konstitutiv aktive Form der PKBα (myrPKB) in der T-Zelllinie exprimieren, zeigten, dass aktive PKB proximale T-Zellrezeptor-Signale beeinflusst. In der vorliegenden Dissertationsarbeit sollte die Interaktion von PKB mit dem Transkriptionsfaktor NFAT und der Src Kinase Fyn auf biochemischer und molekularer Ebene untersucht werden.

Verstärkte Aktivität der Phosphatase Calcineurin (ΔCam) und damit einhergehende erhöhte nukleäre NFAT-Aktivität in frühen Thymozyten führte zu einem Differenzierungsblock der Thymozyten, der durch fehlende Rag- und TCRβ-Ketten-Expression bedingt ist. Koexpression von myrPKB in ΔCam transgenen Thymozyten verminderte die NFAT-Aktivierung, induzierte Rag-Expression und ermöglichte die Weiterdifferenzierung der Thymozyten. Es konnte diesbezüglich gezeigt werden, dass die Rag2-Promotoraktivität durch NFATc1 sowie NFATc2 reguliert wird, NFAT-Faktoren somit zu den wenigen bisher bekannten Transkriptionsfaktoren gehören, welche die Rag-Genexpression in T-Zellen steuern. NFAT-induzierte IL2-Promotoraktivität wurde durch myrPKB ebenfalls inhibiert und im Zusammenspiel mit den NFAT-Kinasen PKA und GSK3 sowie dem Transkriptionsfaktor Foxp3 steigerte myrPKB deren inhibitorischen Effekt auf die NFAT-Aktivierung. Eine direkte Regulation der NFAT-Aktivierung durch PKB erscheint möglich, da rekombinante PKB NFATc1 in der regulatorischen NFAT-Domäne an mindestens zwei Stellen *in vitro* phosphoryliert. Allerdings konnte trotz etlicher GST-NFATc1-Mutanten für potenzielle PKB-Phosphorylierungsstellen in der regulatorischen NFAT-Domäne keine „einzelne“ PKB-Stelle identifiziert werden. Nur bei Kombination mehrerer Mutationen wurde die NFAT-Phosphorylierung durch PKB unterbunden, was auf ein komplexes Zusammenspiel mehrerer Aminosäurereste für die NFAT-Phosphorylierung durch PKB hinweist.

MyrPKB tg $CD4^+$ T-Zellen zeigten gegenüber Wildtyp-Zellen eine verstärkte Proliferation nach TCR/CD3-Stimulation und eine deutlich erhöhte „Resistenz“ gegenüber pharmakologischen Src Kinase- und MEK-Inhibitoren. Dahingehend wurde in Western Blot-Analysen nach CD3/CD4-Stimulation eine deutlich erhöhte Erk-Aktivierung in myrPKB tg $CD4^+$ T-Zellen nachgewiesen. *In vitro* kinase assays (IVKs) belegten, dass die Fyn-Aktivität, d. h. Fyn-Autophosphorylierung an Y417 sowie Fyn-Transphosphorylierungsaktivität, in PKB tg $CD4^+$ T-Zellen erhöht ist. Anhand mehrerer Fyn-GST-Fusionsproteine und entsprechender Mutagenese wurde sodann im N-terminalen Bereich von Fyn eine PKB-

Phosphorylierungsstelle identifiziert. Somit ist Fyn ein neues Substrat der PKB *in vitro*. Da in transfizierten HEK 293T-Zellen PKB und Fyn koimmunopräzipitiert werden konnten, scheint eine direkte Interaktion beider Kinasen *in vivo* gegeben.

Fyn-Hyperaktivität wurde auch in myrPKB tg Thymozyten nachgewiesen. Interessanterweise korreliert die erhöhte Fyn-Aktivität nicht mit vermehrter Phosphorylierung des Adaptermoleküls PAG an Tyrosin 314, welches durch Fyn phosphoryliert wird und sodann zur Rekrutierung der Kinase Csk führt, die wiederum Fyn/Lck inhibiert und derart zum Abschalten der T-Zellrezeptorsignalgebung führt. Analyse der *lipid raft* Fraktionen aktivierter Thymozyten zeigte in PKB tg Zellen eine deutlich erhöhte Menge an Y147 phosphorylierter aktiver Fyn, aber keine einhergehende erhöhte PAG Y314-Phosphorylierung. Erhöhte PKB-Signale führen daher nicht zu einer Sequestrierung von Fyn und PAG, fördern aber sehr wohl die Fyn-Aktivität, die aber nicht in die Negativregulation der TCR-Signalgebung über PAG-Csk einzufließen scheint.

Anerge T-Zellen sind areaktiv gegenüber TCR-Signalen und produzieren kein IL-2. T-Zell-Anergie wurde mit erhöhter Fyn-Aktivität korreliert. In dem durch Ionomycin-Behandlung induzierten Anergiemodellsystem zeigten myrPKB tg $CD4^+$ T-Zellen eine deutlich „abgeschwächte“ Anergie, da sie im Gegensatz zu den entsprechenden Wildtyp-T-Zellen bei TCR/CD3-Restimulation wesentlich stärker proliferierten. Während anergisierte Wildtyp-T-Zellen im Vergleich zu den DMSO-behandelten Kontrollzellen eine höhere Fyn-Aktivität aufwiesen, im Einklang publizierter Daten, war die Fyn-Aktivität in Ionomycin-behandelten myrPKB tg T-Zellen nicht gesteigert. Insgesamt zeigen die gewonnenen Daten, dass erhöhte PKB-Signale die Fyn-Aktivität wesentlich beeinflussen und PKB über die Regulation von Fyn beim Abschalten ungewollter T-Zellaktivierung, z. B. bei der Anergie, eine zentrale Rolle spielen könnte. Der aufgezeigte *cross-talk* von PKB mit Fyn, zwei ausgewiesenen Protoonkogenen, könnte auch bei der Tumorbildung von entscheidender Bedeutung sein.

3 Introduction

3.1 The immune system

The physiological function of the immune system is to protect organisms against infection. To achieve this goal it has to distinguish between self and non-self and to eliminate pathogens. The immune response encompasses an unspecific (innate) and a specific (adaptive) effector arm. The innate immune response is the first defense against an infection, does not involve specific recognition of the pathogen and does not provide specific protection against reinfection. It comprises physical barriers such as the skin and mucous membranes, physiological defense mechanisms such as the low pH in the stomach and soluble components like acute-phase proteins, interferons and lysozyme. The complement system and various cell types also contribute to innate immunity, like monocytes, macrophages and granulocytes, which mediate their function by phagocytosis (Ezekowitz 1998; Janeway and Medzhitov 2002). In contrast, the adaptive immune response is characterized by specific recognition of pathogens and by generation of an immunological memory, thus providing enhanced protection against re-infection. Adaptive immunity can be divided into two major arms: the humoral immune response, constituted by B cells producing antibodies, and the cellular immune response, which is executed by T lymphocytes. The adaptive immune system is not present in animals derived from ancestors older than jawed fish (Flajnik and Du Pasquier 2004; Pancer and Cooper 2006).

3.1.1 Cells of the immune system

All cells of the immune system originate from a common progenitor in the bone marrow, the hematopoietic stem cell (HSC). HSCs develop into stem cells with a more limited potential: mast cells, macrophages and granulocytes derive from myeloid progenitor cells, whereas lymphoid progenitor cells differentiate into T cells, B cells and natural killer (NK) cells. Monocytes are precursors of macrophages and are thus derived from the myeloid progenitor. Dendritic cells, which function as potent antigen presenting cells (APCs), are also derived from bone marrow precursors. T and B cells are the two major types of lymphocytes. B cells develop in the bone marrow, mature in the spleen and after activation of their B cell receptor (BCR) differentiate into antibody producing plasma cells. T cells are defined by their development in the thymus and the presence of T cell receptors (TCRs). Most T cells possess α/β heterodimeric TCRs (α/β T cells), but about 5% of T cells bear γ/δ heterodimeric TCRs. The different subtypes of T cells are specialized to serve special functions.

T helper (Th) cells express the CD4 co-receptor and recognize peptides presented by MHC II molecules. These peptides are derived from proteins taken up by the APC via endocytosis.

Th cells thus respond to antigens from extracellular sources (Germain 1994). Engagement of TCRs by cognate peptide/MHC II complexes results in the activation and proliferation of Th cells, which then differentiate into specialized Th subsets dependening on the activation signals and the cytokine milieu. Th1 cells mainly produce IFN-γ, IL-2 and TNF-β and stimulate macrophage activity and the proliferation of cytotoxic $CD8^+$ T cells. Th2 cells produce IL-4, IL-5, IL-6, IL-10 and IL-13 and stimulate the proliferation and differentiation of B cells, resulting in enhanced and specific antibody production. Th17 cells are a more recently identified population of Th cells, which produce IL-17 and serve important functions in inflammatory and autoimmune diseases (Harrington, Hatton et al. 2005; Stockinger and Veldhoen 2007). TGF-β, IL-6, IL-21 and IL-23 are known to be involved in the induction of Th17 cells in mice and humans (Dong 2008; Manel, Unutmaz et al. 2008). Regulatory T cells (Tregs) inhibit T cell activity to downmodulate immune reactions and suppress auto-reactive T cells. So called naturally occurring $CD4^+CD25^+$ Tregs (nTregs) develop in the thymus, whereas adaptive Tregs are generated in the periphery during an immune response. A hallmark of murine Tregs is the expression of the transcription factor Foxp3, which determines Treg function. Follicular T helper cells (ThFs) are $CD4^+$ T cells, which had contact with antigen and reside in lymph node follicles (Akiba, Takeda et al. 2005).

Cytotoxic T cells (CTLs) express the CD8 co-receptor and recognize peptides presented by MHC I molecules, which are predominantly loaded with peptides derived from intracellular proteins, e.g. viral proteins (York and Rock 1996). Cells infected with virus as well as tumor cells are targets of CTLs, which are also critically involved in transplant rejection. Cytotoxicity is mediated by the production of granzymes and perforin and the interaction of Fas with Fas ligand (FasL) (Kagi, Vignaux et al. 1994).

3.1.2 T cell receptor (TCR) signaling

The TCR is a heterodimeric protein consisting of an α and β or γ and δ subunit, which themselves are unable to transduce signals. The TCR is associated with one γ, one δ and two ε chains, commonly referred to as CD3 complex, and a homodimer of two ζ chains (Samelson, Harford et al. 1985; Clevers, Alarcon et al. 1988). The cytosolic domains of the ζ chains contain three, and each of the γ, δ and ε chains possess one immunoreceptor tyrosine based activation motif (ITAM) (Reth 1989; Letourneur and Klausner 1992; Irving, Chan et al. 1993). The ITAM consensus sequence is $YXXL/I/VX_{(6-8)}YXXL/I/V$, where X denotes any amino acid. TCR engagement by cognate peptide/MHC initiates a signaling network leading to T cell activation (Smith-Garvin, Koretzky et al. 2009), and nowadays logical computer models are employed to describe the complexity of biochemical events initiated by TCR and co-receptor triggering (Saez-Rodriguez, Simeoni et al. 2007).

The TCR initiated signaling cascade starts with phosphorylation of the tyrosine residues (Y) within the ITAMs by activated Src kinases, p56-Lck and p59-Fyn (Abraham, Miceli et al. 1991; Cooke, Abraham et al. 1991; Weiss and Littman 1994; Latour and Veillette 2001). Lck and Fyn are inactivated by phosphorylation at Y505 (Lck) and Y528 (Fyn) by the C-terminal Src kinase (Csk) and activated by dephosphorylation by the phosphatase CD45 (Figure 3.1). The phosphorylated ITAMs within the ζ chains provide docking sites for the Syk family tyrosine kinase zeta-associated protein of 70 kDa (ZAP-70), which is then phosphorylated and activated by Lck (Chan, Dalton et al. 1995; van Oers, Killeen et al. 1996). Substrates for active ZAP-70 are the adapter proteins linker for activation of T cells (LAT) (Zhang, Sloan-Lancaster et al. 1998) and Src homology 2 (SH2) domain-containing leukocyte protein of 76 kDa (SLP76) (Bubeck Wardenburg, Fu et al. 1996).

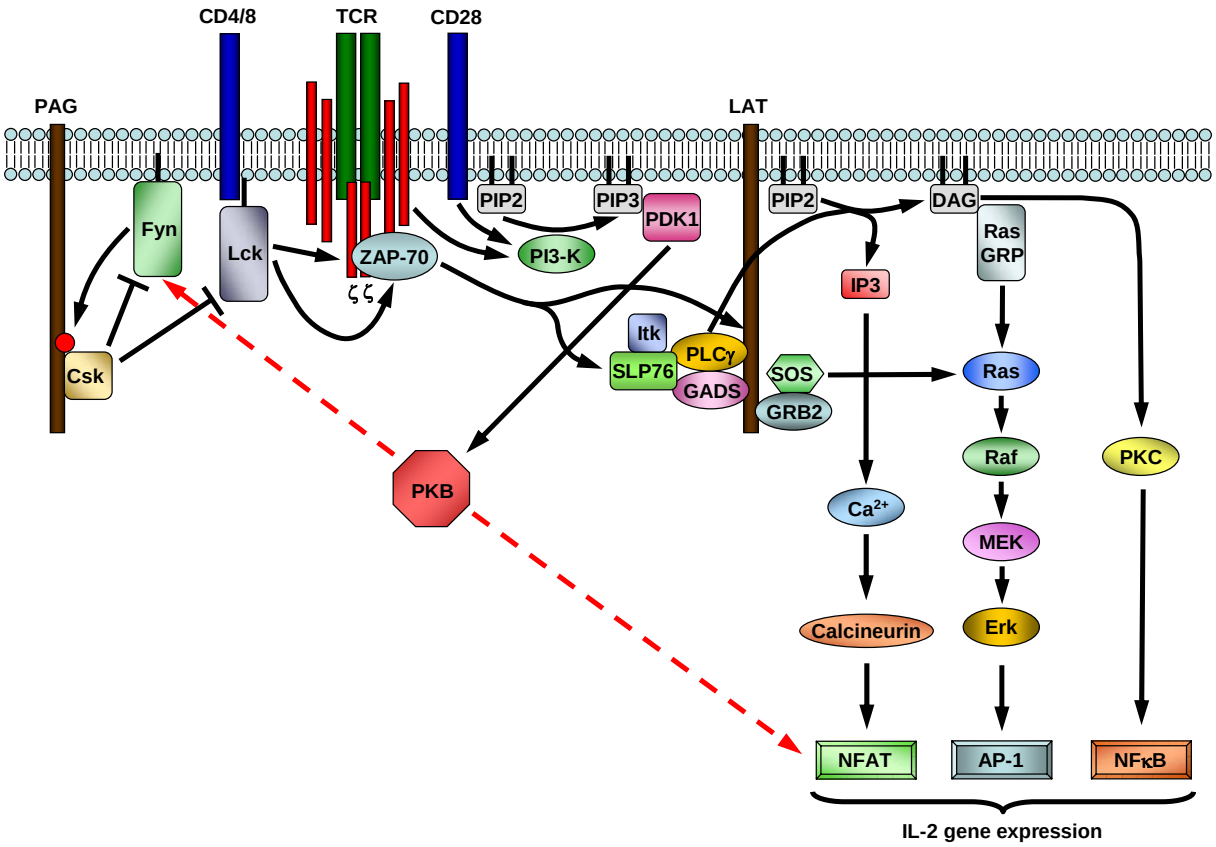

Figure 3.1 Model of selected early signaling events after TCR/CD28 stimulation
The cross-talk of activated PKB with NFAT and Fyn is indicated by dashed red lines. For a detailed explanation see section 3.1.2.

Phosphorylation of LAT induces the formation of a multiprotein signaling complex at the plasma membrane including Grb2-related adapter downstream of Shc (GADS), SLP76, phospholipase Cγ1 (PLCγ1), the Tec kinase IL-2 inducible T cell kinase (Itk), the adapter protein growth-factor-receptor-bound protein 2 (GRB2) and the guanine nucleotide exchange factor (GEF) son of sevenless (SOS) (Samelson 2002). This leads to the activation of PLCγ1

involving phosphorylation by Itk (Berg, Finkelstein et al. 2005). Active PLCγ1 cleaves phosphatidylinositol-4,5-bisphosphate (PIP2) to yield diacylglycerol (DAG) and inositol-1,4,5-trisphosphate (IP3). IP3 induces the release of intracellular Ca^{2+} from the endoplasmatic reticulum (ER), which triggers external Ca^{2+} influx through calcium-release-activated calcium (CRAC) channels. Increased calcium levels lead to activation of the phosphatase calcineurin (CN), which dephosphorylates and thus activates the transcription factor nuclear factor of activated T cells (NFAT) (Oh-hora and Rao 2008). DAG is associated with the activation of the serine/threonine kinase protein kinase C (PKC) and thus with the activation of the transcription factor nuclear factor kappa-light-chain-enhancer of activated B cells (NFκB).

The major mechanism in T cells leading to the activation of the small G protein Ras is mediated by the GEF Ras guanyl nucleotide-releasing protein (RasGRP), which is recruited to the plasma membrane by binding to DAG (Ebinu, Bottorff et al. 1998; Cantrell 2003; Roose, Mollenauer et al. 2005). Additionally, the GEF SOS, which is constitutively associated with the adapter protein GRB2, is recruited to LAT after TCR triggering, where it contributes to the activation of Ras (Zhang, Sloan-Lancaster et al. 1998). Generation of RasGTP triggered by RasGRP was found to enhance the activation of SOS (Roose, Mollenauer et al. 2007; Chakraborty, Das et al. 2009; Das, Ho et al. 2009). This positive feedback loop results in robust Ras activation after TCR triggering. Ras activation initiates the Ras/Raf/MEK/Erk pathway. Active extracellular signal-regulated kinase (Erk) causes activation of the transcription factor Elk1, which regulates expression of Fos. The transcription factor activator protein-1 (AP-1) consists of Fos and Jun, and Erk enhances AP-1 activation via Fos.

TCR stimulation also triggers the activation of phosphatidylinositol 3-kinase (PI3-K) leading to activation of phosphoinositide-dependent kinase-1 (PDK1) and the serine/threonine kinase protein kinase B (PKB). The activation of PKB is described in more detail in section 3.2.3. PI3-K/PKB signals also result from engagement of CD28 and other co-stimulatory molecules. The activation of the transcription factors NFAT, NFκB and AP-1 after TCR/CD28 triggering is important for the expression of interleukin-2 (IL-2), the IL-2 receptor α chain (CD25) and CD69, which mark early T cell responses.

The influence of active PKB on NFAT and Fyn activation and their molecular interaction, which is indicated by dashed red arrows in Figure 3.1, was the focus of this thesis.

3.2 PKB

3.2.1 Identification of PKB

PKB research was initiated in 1977 by Staal and co-workers, who identified a leukemia virus which induced spontaneous lymphoma in mice. The retrovirus was able to transform the cell line CCL-64 (mink epithelial cells) and was called AKT8 (Staal, Hartley et al. 1977). The AKT8 virus induced thymic lymphomas when inoculated into mice, and the cell-derived *akt* sequence of the virus was shown to be present in the DNA of virus-induced tumors. Thus, the *akt* sequence of the AKT8 virus was responsible for tumorigenesis (Staal and Hartley 1988). The virus genome consisted of both viral and nonviral, cell-related sequences. The nonviral sequence was called *akt*, the presumed viral oncogene of the AKT8 virus. Two human homologues of *akt*, PKBα and PKBβ, were identified by screening of a human genomic library with a probe specific for *akt*. One part of the PKBα gene was shown to be amplificated in human gastric adenocarcinoma and thus PKB could play a role in cancerogenesis (Staal 1987).

Despite these findings, the exact genetic identity of *akt* was not known until three groups independently identified genes coding for Akt in 1991. Jones et al. isolated full-length cDNA clones by screening libraries derived from the human cell lines MCF-7 and WI38 with a probe specific for a protein kinase related to the A and C kinases (rac), which later was given the name Akt1/PKBα. DNA analysis identified an open reading frame of 1440 base pairs coding for a protein of 480 amino acids. The protein was immunoprecipitated and shown to possess specific kinase activity phosphorylating histone H1 and myelin basic protein (MBP) *in vitro* (Jones, Jakubowicz et al. 1991 Proc Natl Acad Sci USA).

Bellacosa et al. cloned *v-akt*, consisting of the viral gag protein fused to Akt1/PKBα (Bellacosa, Testa et al. 1991). The viral gag protein is myristoylated at its N-terminus and localized at the plasma membrane, whereas PKB mainly resides in the cytoplasm. Thus, the fused gag protein targets v-Akt to the plasma membrane, which could influence kinase activity (Ahmed, Franke et al. 1993). PCR screening technology was applied to identify an open reading frame coding for a 479 amino acid protein that showed similarity to protein kinase A (PKA) and protein kinase C (PKC) and was thus named protein kinase B (PKB) (Coffer and Woodgett 1991). PKBβ was identified by screening cDNA libraries from the human cell lines MCF-7 and WI38 applying the procedure used for identification of PKBα (Jones, Jakubowicz et al. 1991 Cell Regul). PKBγ, the third PKB gene, was cloned in 1995 from rat (Konishi, Kuroda et al. 1995) and in 1999 from human cells (Brodbeck, Cron et al. 1999; Nakatani, Sakaue et al. 1999).

In mammals, the three PKB proteins are ubiquitously expressed, but the intensity of expression differs assessing different tissues. PKBα is strongly expressed in many tissues, whereas PKBβ is predominantly expressed in skeletal muscle, liver, kidney and heart (Altomare, Guo et al. 1995). PKBγ is dominant in brain and testis, and low expression is found in adult pancreas, kidney and heart (Konishi, Matsuzaki et al. 1996; Brodbeck, Cron et al. 1999; Nakatani, Sakaue et al. 1999). The human gene coding for PKBα/Akt1 is localized on chromosome 14q32.32-q32.33, the gene for PKBβ/Akt2 is localized on chromosome 19q13.1-q13.2 and the gene for PKBγ/Akt3 on chromosome 1q44. The three PKB/Akt genes show about 85% sequence similarity and code for proteins with similar domain-organization.

3.2.2 Domain structure of PKB

PKBα, PKBβ and PKBγ display structural similarity within their conserved domains:
a pleckstrin homology (PH) domain at the N-terminus, a kinase domain and a regulatory domain at the C-terminus. The regulatory domain includes a hydrophobic motif conserved in AGC kinases with the consensus sequence FXXF/YS/TY/F (X represents any amino acid). The PH domain mediates membrane targeting of PKB by interaction with phosphorylated membrane lipid molecules, e.g. phosphatidylinositol-3,4,5-trisphosphate (PIP3) produced by activated PI3-K (James, Downes et al. 1996). The structure of the kinase domain is conserved within the family of AGC kinases, including PKB (Peterson and Schreiber 1999). Phosphorylation of PKB in the kinase domain and the hydrophobic motif leads to activation of the enzyme.

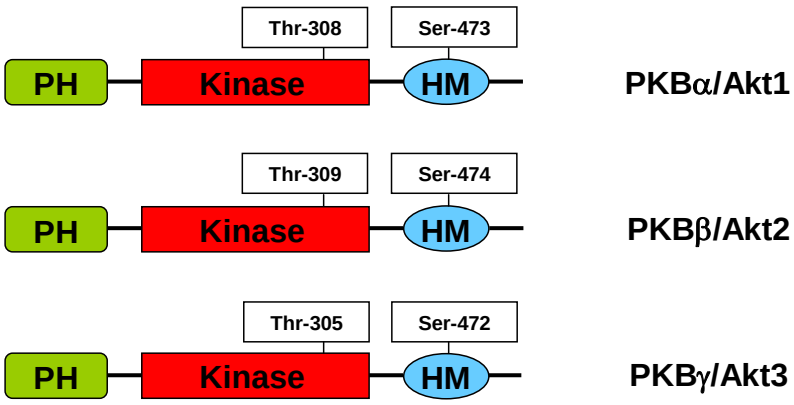

Figure 3.2 Domain structure of human PKB
PKB consists of three domains: an N-terminal pleckstrin homology (PH) domain, a central kinase domain and a regulatory domain harboring a hydrophobic motif (HM) at the C-terminus. Activation of PKB requires phosphorylation of the indicated threonine in the kinase domain and of the indicated serine in the hydrophobic motif (modified after: Kandel and Hay 1999; Hanada, Feng et al. 2004).

3.2.3 Regulation of PKB activity

PKB is activated by insulin and various other growth and survival factors. In T cells, activation of PKB is triggered by TCR ligation, several co-stimulatory molecules like CD28, cytokines and chemokines, among others. Active PI3-K produces PIP3 and interaction with PIP3 via its PH domain recruits PKB to the plasma membrane, where it is activated by phosphorylation at T308 and S473 (see Figure 3.3) (Alessi, Andjelkovic et al. 1996). These phosphorylations are inhibited by the PI3-K inhibitors LY294002 and wortmannin, and exchange of these two residues to alanine abrogates PKB activity. Phosphorylation at T308 in the activation loop of PKB is mediated by PDK1 (Brazil and Hemmings 2001). The kinase responsible for phosphorylation at S473 is mammalian target of rapamycin (mTOR), in a complex with rictor and Sin1, called mTORC2 complex (Sarbassov, Guertin et al. 2005; Jacinto, Facchinetti et al. 2006).

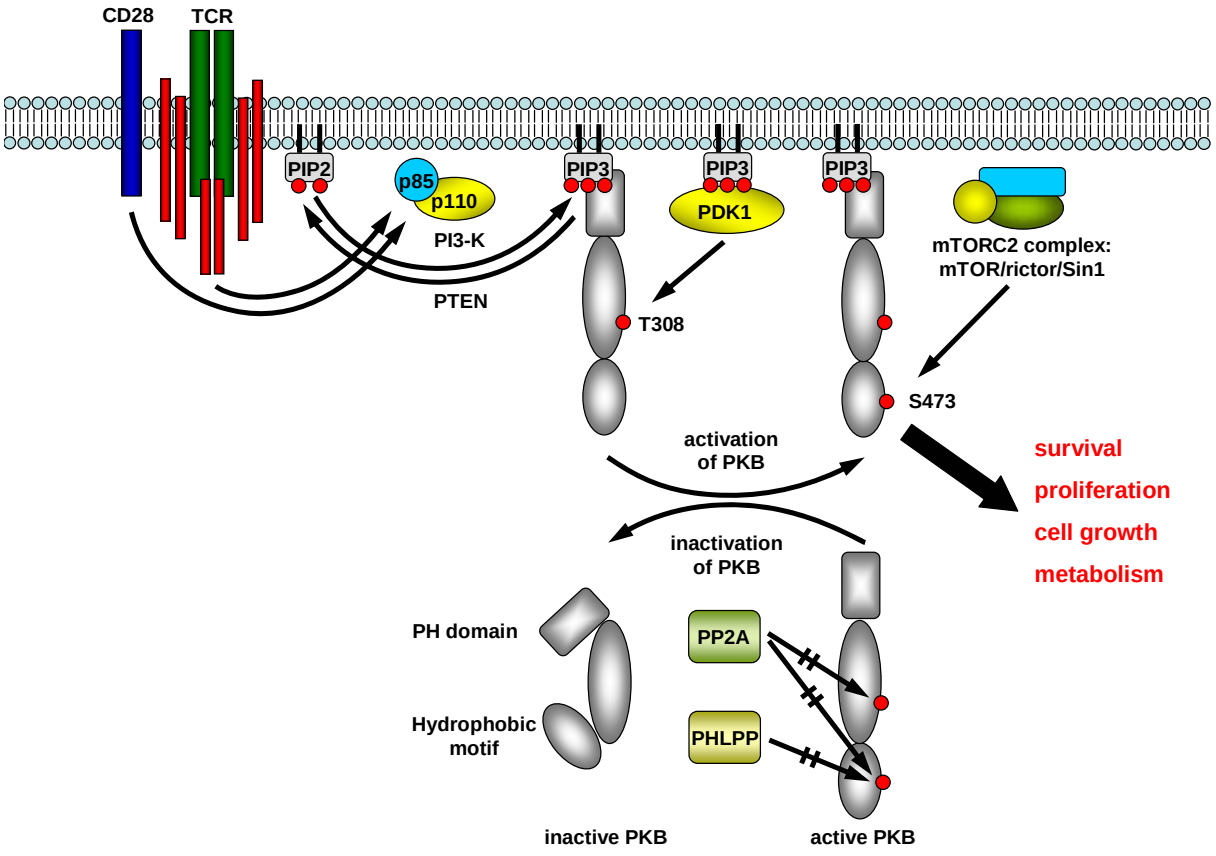

Figure 3.3 Model for regulation of PKB activity
Triggering of the TCR and/or the co-receptor CD28 leads to the activation of PI3-K, which generates PIP3 by phosphorylation of PIP2. PKB is recruited to the plasma membrane by binding to PIP3 via its pleckstrin homology (PH) domain followed by phosphorylation of T308 in the kinase domain by PDK1 and S473 in the hydrophobic motif of the regulatory domain by the mTORC2 complex, leading to its activation. Dephosphorylation of T308 and S473 by PP2A and of S473 by PHLPP or activation of PTEN, which depletes PIP3, leads to PKB inactivation (modified after: Brazil and Hemmings 2001).

PKB is inactivated by phosphatases such as protein phosphatase 2A (PP2A), which dephosphorylate T308 and S473, converting PKB to its inactive conformation

(Andjelkovic, Jakubowicz et al. 1996; Meier, Thelen et al. 1998). PH domain leucine-rich repeat protein phosphatase (PHLPP) was found to dephosphorylate PKB at S473 (Gao, Furnari et al. 2005). A tumor suppressor gene located on chromosome 10q13 was identified in 1997, which was given the name phosphatase and tensin homologue localized on chromosome ten (PTEN). Since PIP3 is a substrate of PTEN (Maehama and Dixon 1998), active PTEN counteracts PKB activation via dephosphorylation of PIP3, a membrane lipid required for membrane targeting and activation of PKB.

3.2.4 Physiological functions of PKB

The various physiological functions of PKB include cell survival, proliferation, cell growth and differentiation, mediated by several downstream targets, more than 40 so far. The first direct target of PKB identified in cells was glycogen synthase kinase-3 (GSK-3) (Cross, Alessi et al. 1995). Using synthetic peptide sequences based on the PKB phosphorylation site of GSK-3, the PKB phosphorylation motif was defined: RXRXXS/T, where X represents any amino acid and S/T the PKB phosphorylation site. Figure 3.4 shows major PKB phosphorylation targets, which are inhibited via phosphorylation.

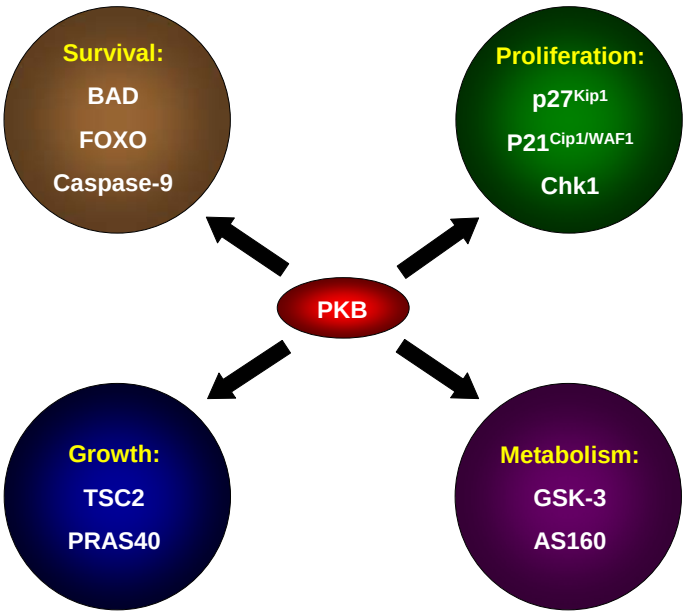

Figure 3.4 PKB regulates survivval, proliferation, growth and metabolism
Some direct substrates of PKB are indicated.

PKB and cell survival

PKB is known as ‘survival kinase’ because it inhibits the function of several pro-apoptotic proteins. For instance, Bcl-2 homology domain 3 (BH3)-only proteins, which are downmodulated in their expression or function by PKB, enhance apoptosis by inactivation of pro-survival Bcl-2 family proteins. The BH3-only protein BAD is directly regulated by PKB. PKB phosphorylates BAD at S136, thereby generating a binding site for 14-3-3 proteins causing dissociation of BAD from its target proteins and promoting survival

(Datta, Dudek et al. 1997; Datta, Katsov et al. 2000). PKB also interacts with transcription factors of the forkhead box family, which regulate the expression of BH3-only proteins. T24, S256, and S319 of FOXO1 and the corresponding amino acids of FOXO3a and FOXO4 are phosphorylated by PKB (reviewed in Tran, Brunet et al. 2003). Phosphorylation of T24 and S256 promotes nuclear export of FOXOs by providing docking sites for 14-3-3 proteins. There is also evidence that PKB phosphorylates S196 on human pro-caspase-9, which is associated with reduced caspase-9 activity *in vitro* and reduced cell death (Cardone, Roy et al. 1998).

PKB and cell proliferation

PKB is also critically involved in cell cycle regulation. Phosphorylation of the cyclin-dependent kinase inhibitor $p27^{Kip1}$ at T157 by PKB triggers binding of 14-3-3 proteins causing nuclear export and reduction of cell-cycle inhibition by $p27^{Kip1}$ (Liang, Zubovitz et al. 2002; Sekimoto, Fukumoto et al. 2004). Another PKB phosphorylation target is the cyclin-dependent kinase inhibitor $p21^{Cip1/WAF1}$, which upon phosphorylation at T145 by PKB localizes in the cytoplasm (Zhou, Liao et al. 2001). Furthermore, downmodulation of GSK-3 activity via phosphorylation by PKB has also impact on the cell cycle. Molecules involved in cell cycle progression from G1 to S phase, such as cyclin D and cyclin E and the transcription factors c-Jun and c-Myc, are driven to degradation in proteasomes by phosphorylation via GSK-3 (Diehl, Cheng et al. 1998; Welcker, Singer et al. 2003; Yeh, Cunningham et al. 2004; Wei, Jin et al. 2005). Thus, inactivation of GSK-3 by PKB reduces degradation of these proteins and fosters cell cycle progression. PKB facilitates progression of mitosis even when DNA is damaged (Kandel, Skeen et al. 2002; Shtivelman, Sussman et al. 2002). The DNA damage checkpoint kinase Chk1 is phosphorylated by PKB at S280 (King, Skeen et al. 2004), causing Chk1 ubiquitination and its translocation to the cytosol leading to abrogation of checkpoint function. Cells with damaged DNA therefore proliferate (Puc, Keniry et al. 2005), one mechanism among others by which dysregulated PKB fosters transformation and tumorigenesis (Carpten, Faber et al. 2007; Tokunaga, Oki et al. 2008).

PKB and cell growth, metabolism

PKB promotes cell growth via activation of the mTOR complex 1 (mTORC1), which is also known as mTOR-raptor complex and is regulated by growth factors and nutrients. mTORC1 regulates the initiation of translation and the synthesis of ribosomes. mTORC1 activation by PKB is mediated via the tuberous sclerosis complex 2 (TSC2), also termed tuberin, which negatively regulates mTOR signal transduction. PKB phosphorylates TSC2, inhibits its function (Potter, Pedraza et al. 2002) and thereby causes increased mTORC1 activity and cell growth. The proline-rich Akt substrate of 40 kDa (PRAS40) negatively regulates mTORC1 (Sancak, Thoreen et al. 2007) and is phosphorylated by PKB at T246

(Kovacina, Park et al. 2003). T246A mutants of PRAS40 led to the suggestion that phosphorylation of PRAS40 at T246 by PKB enhances mTOR signaling.

GSK-3 phosphorylates and inactivates glycogen synthase after stimulation of cells with insulin. Phosphorylation of GSK-3α at S21 and of GSK-3β at S9 by PKB inactivates GSK-3 leading to enhanced glycogen synthesis (Cross, Alessi et al. 1995; Lafont, Astoul et al. 2000; Ohteki, Parsons et al. 2000).

PKB also increases glucose uptake of cells after stimulation with insulin. PKBβ was associated with vesicles containing the glucose transporter 4 (Glut4) in adipocytes, which were stimulated with insulin (Calera, Martinez et al. 1998). Furthermore, it was shown that PKB activation results in translocation of Glut4 to the plasma membrane (Kohn, Summers et al. 1996). A 160-kDa protein called AS160 and harboring a GTPase activating domain for Rab G proteins, which are important for membrane trafficking, was identified as a phosphorylation target of PKB and found to be involved in Glut4 membrane translocation (Sano, Kane et al. 2003; Eguez, Lee et al. 2005). PKB also influences transcription and translation of the gene coding for Glucose tansporter 1 (Glut1), which mediates glucose transport in many cell types (Taha, Liu et al. 1999), and PKB enhances the rate of glycolysis in cancer cells (Elstrom, Bauer et al. 2004).

3.2.5 PKB deficient and transgenic mice

To date more than 40 proteins have been described to be regulated by PKB. Whether all of these proteins are PKB targets in immune cells is not yet clear. To resolve the physiological functions of PKB in whole organisms and specifically in the immune system, PKB knockout (ko) and PKB transgenic (tg) mice with deletion or overexpression of PKB genes in all cells or specifically in T cells were established. PKB$\alpha^{-/-}$ mice display increased apoptosis in the thymus and show reduced body size (Chen, Xu et al. 2001; Cho, Thorvaldsen et al. 2001). PKB$\beta^{-/-}$ mice are also viable but suffer from severe diabetes (Cho, Mu et al. 2001; Garofalo, Orena et al. 2003), indicating an essential function of PKBβ in glucose metabolism. Adult PKB$\alpha^{-/-}$ mice display decreased thymic cellularity but overall normal thymic subsets, and thymocyte development in PKB$\beta^{-/-}$ mice is normal. In contrast, thymi from PKB$\alpha^{-/-}/\beta^{-/-}$ mice have a 8-fold reduction of thymic cell number and a higher percentage of cells at the double negative (DN)3 stage of thymocyte differentiation, indicating a defect in pre-TCR selection (Juntilla, Wofford et al. 2007). Analysis of PKB$\gamma^{-/-}$ mice revealed an about 25% reduction of brain weight and size in adult mice, indicating a central function of PKBγ in brain development (Tschopp, Yang et al. 2005). The viability and mild phenotype of mice with a single PKB deletion suggest that PKBα, PKBβ and PKBγ can functionally compensate for each other. This is supported by the fact that PKB$\alpha^{-/-}/\beta^{-/-}$ mice quickly die after birth and show

a strong reduction in body size. Furthermore, skin and bone development are defective, skeletal muscles display atrophy and adipogenesis is reduced (Peng, Xu et al. 2003). PKB$\alpha^{-/-}/\gamma^{-/-}$ double ko mice are embryonic lethal (Yang, Tschopp et al. 2005) suggesting that PKBα has an important function in embryogenesis and survival after birth. Mice which solely express PKBα, such as PKB$\beta^{-/-}/\gamma^{-/-}$ or PKB$\alpha^{+/-}/\beta^{-/-}/\gamma^{-/-}$ mice, are viable, although total PKB expression is strongly reduced in many tissues. Finally, PKB$\alpha^{-/-}/\beta^{-/-}/\gamma^{-/-}$ mice are not viable and show embryonic lethality (Dummler, Tschopp et al. 2006). The analysis of PKB ko mice revealed the importance of the three PKB forms in growth, proliferation and differentiation of cells as well as glucose metabolism. PKBα is especially important in embryonic growth, development and survival, PKBβ serves unique functions in glucose metabolism and PKBγ has specifically impact on brain development.

An inducible PKB$\alpha^{-/-}$ mouse was generated by usage of the Lck-Cre-lox system. Since the expression of Lck starts at the DN2 stage of thymocyte development, PKBα expression is decreased at the DN3 stage and eliminated at the DN4 stage of thymocyte differentiation. Crossing PKB$\alpha^{-/-}$ mice with PKB$\beta^{-/-}$, PKB$\gamma^{-/-}$ or PKB$\beta^{-/-}/\gamma^{-/-}$ mice resulted in the generation of viable PKB double and triple ko mice. PKB$\beta^{-/-}/\gamma^{-/-}$ mice show basically normal thymocyte development, but PKB$\alpha^{-/-}/\beta^{-/-}$ mice display a reduction of thymic cellularity and a block in the transition from the DN4 to the double positive (DP) stage. PKB$\alpha^{-/-}/\gamma^{-/-}$ mice also show reduced thymic cellularity and a partial block in the transition from the DN4 to the DP stage. Combined deletion of all PKB genes in thymocytes (PKB$\alpha^{-/-}/\beta^{-/-}/\gamma^{-/-}$ mice) inhibited the survival of DN thymocytes. From analysis of these mice can be concluded that all three forms of PKB contribute to thymocyte development, although PKBα seems to be most important (Mao, Tili et al. 2007).

The first PKB tg mouse described harbored a membrane targeted and thus constitutively active gag-PKBα expressed under the CD2 promoter (Jones, Parsons et al. 2000). Peripheral T cells and thymocytes from these mice showed increased viability in culture. Furthermore, an increase in NFκB activation after stimulation of peripheral T cells and increased levels of the anti-apoptotic protein Bcl-X_L were detected in T cells and thymocytes from gag-PKB tg mice. In aged gag-PKB tg mice, accumulation of $CD4^+$, $CD8^+$ and B cells caused lymphadenopathy and splenomegaly and several organs were infiltrated by lymphocytes. A defect in Fas-mediated apoptosis was found in gag-PKB tg T cells and B cells from these mice showed enhanced proliferation after IgM $F(ab')_2$ and CD40 stimulation. Thus, expression of a constitutively active form of PKB in T cells has an impact on T as well as B cell homeostasis (Parsons, Jones et al. 2001). Additional studies revealed that the recruitment of pro-caspase-8 to the death-inducing signaling complex (DISC) associated with Fas receptors is impaired in gag-PKB tg T cells causing reduced activation of caspase-8, the

pro-apoptotic Bcl-2 protein BID and caspase-3 leading to a reduction of Fas-induced apoptosis (Jones, Elford et al. 2002). Later studies showed that NFκB is necessary to avoid Fas-induced apoptosis via constitutively active gag-PKB. Gag-PKB-mediated survival after cytokine withdrawal was independent of protein synthesis and NFκB (Jones, Saibil et al. 2005). The function of PKB in survival of $CD4^+$ and $CD8^+$ T cells was examined in gag-PKB tg mice deficient for PKCθ. The survival of splenic $PKC\theta^{-/-}$ $CD4^+$ T cells was slightly affected but a strong survival defect occurred in splenic $PKC\theta^{-/-}$ $CD8^+$ T cells. Furthermore, PKCθ deficiency caused reduced expression levels of the anti-apoptotic protein $Bcl\text{-}X_L$ in CD3+CD28 Ab-stimulated $CD4^+$ and $CD8^+$ T cells. Active gag-PKB rescued the expression of $Bcl\text{-}X_L$ in $PKC\theta^{-/-}$ $CD8^+$ cells but not in $PKC\theta^{-/-}$ $CD4^+$ cells and increased the viability of $PKC\theta^{-/-}$ $CD4^+$ T cells but not of $PKC\theta^{-/-}$ $CD8^+$ T cells. A proliferation defect was observed in peptide-stimulated P14 TCR $PKC\theta^{-/-}$ T cells and this defect was not rescued by gag-PKB. Thus, $CD4^+$ and $CD8^+$ T cell survival is regulated differentially and PKB specifically contributes to this regulation (Saibil, Jones et al. 2007).

Thompson et al. generated tg mice expressing a myristoylated constitutively active form of murine PKBα in T cells under control of the Lck promoter and CD2 enhancer. Naive T cells from these mice displayed increased cell size, glucose metabolism and viability in *in vitro* culture. Additionally, myrPKB tg T cells were less dependent on CD28 co-stimulation for induction of cell growth and cytokine secretion. Increased numbers of $CD4^+$ T cells and B cells were present in one year old myrPKB tg mice compared with wt mice. Additionally, induction of autoimmunity with immunoglobulin accumulations in kidney glomeruli and a higher number of lymphomas were found in aged myrPKB tg mice (Rathmell, Elstrom et al. 2003).

Cell growth is associated with increased energetic and biosynthetic activity. T cell activation is limited by the amount of glucose consumed and CD28 co-stimulation is crucial for maximal glucose uptake via triggering expression and cell surface translocation of the Glut1 glucose transporter. Constitutively active myrPKB enhanced glucose consumption of resting T cells by promoting Glut1 cell surface trafficking (Jacobs, Herman et al. 2008). PKB is also important for glucose uptake of lymphocytes driven by IL-7. IL-7 induces transcriptional activity of signal transducer and activator of transcription 5 (STAT5) and leads to activation of PKB, which regulates Glut1 membrane trafficking and thereby influences glucose consumption. No component of this signaling pathway seems to be dispensable, because deletion of PKBα, inhibition of PI3-K or downmodulation of STAT5 by siRNA inhibited IL-7-driven glucose uptake (Wofford, Wieman et al. 2008).

Similar mice expressing a myristoylated human PKBα under the CD2 promoter and locus control region (LCR) were generated by Bommhardt et al. and used for experiments in this

thesis. PKB is constitutively recruited to the membrane via the N-terminal *lck* myristoylation/palmitoylation signal (MGCWCSSNPEDD) and constitutively active (Avota, Avots et al. 2001). Previous studies on these mice showed that myrPKB tg thymocytes display enhanced and prolonged activation of the Src kinase Lck and the Raf/MEK/Erk signaling pathway associated with hyperproliferation of thymocytes after TCR stimulation. In addition, proliferation of myrPKB tg thymocytes was less sensitive to inhibition by CsA or FK506. Concerning thymocyte selection, myrPKB tg thymocytes showed enhanced positive selection towards the CD4 lineage and an increased CD4:CD8 ratio in the peripheral organs. With respect to negative selection, myrPKB was shown to enhance, to reduce or to have no effect on negative selection depending on the system of negative selection analyzed (Na, Patra et al. 2003). MyrPKB tg peripheral T cells showed reduced nuclear translocation of NFATc1, NFATp, NFκB p65 and RelB proteins after CD3 Ab and CD3+CD28 Ab stimulation, although they proliferated faster and produced more cytokines. Since NFAT and PKB co-immunoprecipitate in $CD4^+$ T cells, PKB could regulate NFAT activation via direct mechanisms (Patra, Na et al. 2004). Wt and myrPKB tg mice were also analyzed under septic conditions. MyrPKB tg mice showed enhanced survival which correlated with reduced apoptosis of lymphocytes and altered IFN-γ and IL-4 production (Bommhardt, Chang et al. 2004).

3.3 NFAT

3.3.1 The NFAT family of transcription factors

NFAT was identified as a transcription factor binding to the IL-2 promoter of activated T cells (Shaw, Utz et al. 1988; Randak, Brabletz et al. 1990). The binding of NFAT to the IL-2 promoter was shown to be sensitive to CsA treatment (Emmel, Verweij et al. 1989; Randak, Brabletz et al. 1990; Serfling, Berberich-Siebelt et al. 2000). NFAT is expressed in several tissues and involved in the regulation of many processes such as development of the embryonic heart, angiogenesis, the growth of neuronal axons and bone development (Hogan, Chen et al. 2003; Macian 2005). The family of NFAT factors includes NFATc1 (NFAT2 or NFATc), NFATc2 (NFAT1 or NFATp), NFATc3 (NFAT4 or NFATx), NFATc4 (NFAT3) and NFAT5. The oldest member of the NFAT family, NFAT5, appeared as early as *Drosophila* in evolution and developed from the REL transcription factor family. NFAT5 is broadly expressed and activated by osmotic stress (Lopez-Rodriguez, Aramburu et al. 1999; Miyakawa, Woo et al. 1999). NFATc1-c3 are expressed in T cells, whereas NFATc4 is mainly expressed outside the immune system. NFATc1-c4 are regulated by calcium signaling via the Ca^{2+}/calmodulin-dependent phosphatase calcineurin (CN). CN dephosphorylates at least 13 residues within the regulatory domain of NFAT, stimulating its

nuclear translocation, a process which is inhibited by CsA and FK506 (Okamura, Aramburu et al. 2000; Serfling, Berberich-Siebelt et al. 2000; Kaminuma 2008).

3.3.2 Domain structure of NFAT

The domain structure of NFAT is crucial for its function and characterized by the presence of an N-terminal transactivation domain (TAD), a regulatory domain, also termed NFAT-homology region (NHR), a DNA-binding domain, known as REL-homology region (RHR) and a C-terminal domain (Figure 3.5).

Regulatory domain (NFAT-homology region NHR)

An important function of the regulatory domain is the control of the nuclear and cytoplasmic localization of NFAT transcription factors. Phosphorylation of serines positioned within the regulatory domain of NFAT causes cytosolic localization in resting T cells. These serines are mainly positioned in conserved sequence motifs: two serine-rich regions (SRR) and three serine-proline (SP) boxes. The regulatory domain also harbors binding sites for NFAT kinases and CN, which regulate the activation of NFAT factors by phosphorylation and dephosphorylation of the serines. Additionally, a nuclear localization sequence (NLS) is localized in the NHR (Okamura, Aramburu et al. 2000).

DNA-binding domain (REL-homology region RHR)

The REL-homology region is a characteristic feature of NFAT proteins. The name is due to its sequence similarity (15-17%) to the DNA-binding domains of the NFκB/Rel family of transcription factors. NFATc1-c4 depict 60-70% sequence similarity in the DNA binding domains and the NFAT5 DNA binding domain shows about 40% sequence similarity compared with the other family members. Conservation of the DNA-binding domain results in similarity in DNA-binding specificity that characterizes NFAT transcription factors. The consensus NFAT binding site for several promoters is GGAAAA (Serfling, Avots et al. 1995; Chen, Glover et al. 1998).

Transactivation domain (TAD) and C-terminal domain

Transactivation domains contributing to the regulation of NFAT activity were identified at the N-terminus and the C-terminus of NFAT (Luo, Burgeon et al. 1996). NFATc1-c4 harbor transactivation domains at the N-terminus and NFATc1-c3 additionally possess transactivation domains at the C-terminus.

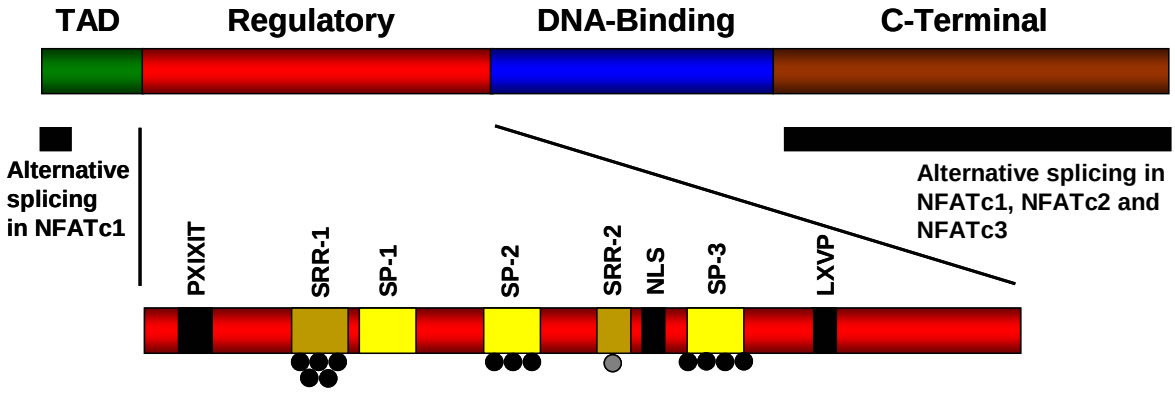

Figure 3.5 Domain structure of NFAT proteins and phosphorylation pattern of the regulatory domain
NFAT proteins consist of an N-terminal transactivation domain (TAD), a regulatory domain, a DNA-binding domain and a C-terminal domain, which also harbors transactivation domains in NFATc1-c3. N- and C-terminal domains are alternatively spliced in different NFAT isoforms. An enlarged version of the regulatory domain is shown including the conserved serine-rich regions (SRR-1 and SRR-2) and the conserved serine-proline boxes (SP-1, SP-2 and SP-3). The calcineurin binding site with the sequence PXIXIT (X depicts any amino acid), the second calcineurin binding site with the sequence LXVP and a nuclear localization signal (NLS) are also indicated. Phosphorylated serines in conserved sequence motifs are represented by circles. Black circles indicate phosphorylations that get lost after activation, whereas the gray circle represents a constitutively phosphorylated serine (modified after: Macian, Lopez-Rodriguez et al. 2001; Lee and Park 2006).

3.3.3 Regulation of NFAT activity

Activation of NFAT proteins is induced by ligation of the TCR, which leads to increase of intracellular Ca^{2+} levels via CRAC channel activation. Binding of the Ca^{2+}/calmodulin complex activates CN, which subsequently dephosphorylates and thus activates NFAT (Shaw, Ho et al. 1995; Okamura, Aramburu et al. 2000). The binding sites for CN with the sequence motifs PXIXIT and LXVP are present in the regulatory domain (Aramburu, Garcia-Cozar et al. 1998; Garcia-Cozar, Okamura et al. 1998; Martinez-Martinez, Rodriguez et al. 2006). NFAT kinases are crucial regulators of NFAT activity, because they control nuclear shuttling of this transcription factor. GSK-3, p38, casein kinase 1 (CK1), JUN N-terminal kinase (JNK) and dual-specificity tyrosine-phosphorylation regulated kinase (DYRK) (Gwack, Sharma et al. 2006) have been reported to phosphorylate NFAT. Maintenance kinases phosphorylate NFAT proteins in the cytosol and thus stabilize the cytosolic localization, whereas export kinases phosphorylate nuclear NFAT proteins and thereby enhance nuclear export. GSK-3 acts as an export kinase (Beals, Sheridan et al. 1997). In NFATc1, the GSK-3 phosphorylation sites with the consensus sequence S/TXXXpS are generated after priming by protein kinase A (PKA), which phosphorylates serines or threonines within the consensus sequence RRXS/TY (Sheridan, Heist et al. 2002). CK1 serves as an export and maintenance kinase for the SRR-1 region of NFAT (Zhu, Shibasaki et al. 1998). Mitogen-activated protein

kinases (MAPKs) also phosphorylate various NFAT proteins. JNK phosphorylates NFATc1 (Chow, Dong et al. 2000), and p38 phosphorylates NFATc2 (Gomez del Arco, Martinez-Martinez et al. 2000). The fact, that different kinases phosphorylate various serine-rich motifs in NFAT proteins provides a molecular basis for the spacial and temporal regulation of NFAT family members. PKB is known to phosphorylate and thus inactivate GSK-3. Since GSK-3 functions as an export kinase for NFATc1 and NFATc2 and inactivates NFAT, one could speculate that PKB stimulates NFAT activation by phosphorylation of GSK-3. Indeed, enhanced NFAT activation was found after CD28 co-stimulation (Siefken, Klein-Hessling et al. 1998; Diehn, Alizadeh et al. 2002), which would lead to PKB activation.

NFATc1 is not only regulated by phosphorylation and dephosphorylation in its regulatory domain, but additionally on the transcriptional level by a positive feedback loop. The expression of the splice variant NFATc1A is transcriptionally controlled by a promoter which is switched on by NFAT itself (Chuvpilo, Zimmer et al. 1999; Chuvpilo, Jankevics et al. 2002; Zhou, Cron et al. 2002; Serfling, Chuvpilo et al. 2006).

CBP and p300 are co-factors of diverse transcription factors and function as adapter proteins. Additionally, CBP and p300 can acetylate histones and enhance transcription by this mechanism. CBP and p300 bind to the N-terminal transactivation domain of NFAT and enhance NFAT activity (Avots, Buttmann et al. 1999).

NFATc1C and NFATc2 are also regulated by sumoylation. Addition of small ubiquitin-like modifier (SUMO) molecules to NFATc2 causes nuclear localization (Terui, Saad et al. 2004). Sumoylation of NFATc1C results in its localization in promyelocytic leukemia nuclear bodies (PML-nbs), where it interacts with histone deacetylases. Subsequent histone deacetylation results in the generation of transcriptionally inactive chromatin, which is associated with reduced IL-2 production. Thus, sumoylation of NFATc1C converts this transcription factor from a transcriptional activator to a repressor of IL-2 gene expression (Nayak, Glockner-Pagel et al. 2009).

NFAT was also found to co-immunoprecipitate with the cytoplasmic scaffolding proteins Homer2 and Homer3, which belong to the Homer family. This interaction diminishes binding of CN to NFAT and thus reduces dephosphorylation of NFAT by CN, leading to reduced NFAT activity. Thus, Homer molecules act as negative regulators of TCR signaling. Active PKB reduces the binding of Homer2 and Homer3 to NFAT, which results in enhancement of NFAT activity and thus TCR signaling. Since PKB is activated by CD28 as well as TCR stimulation, the impact of active PKB on the interaction of Homer with NFAT seems to be one mechanism by which CD28 co-stimulation enhances TCR signaling and T cell activation (Huang, Huso et al. 2008).

3.3.4 Transcriptional partners of NFAT

NFAT proteins interact with a variety of other transcription factors. The main interaction partner of NFAT after T cell activation is activator protein-1 (AP-1). This cooperative transcriptional activity provides a molecular basis for the interplay between calcium and Ras/MAPK signaling. Increased intracellular Ca^{2+} leads to NFAT activation and Ras/MAPK signaling triggers AP-1 formation (Jain, McCaffrey et al. 1992). Complexes of NFAT and AP-1 bind with high affinity to the consensus sequence 5' –GGAAAaxxxxTGAxTCA-3' (Kel, Kel-Margoulis et al. 1999). Activation of the IL-2 promoter is a prominent example for transcriptional interaction of NFAT and AP-1 (Serfling, Berberich-Siebelt et al. 2000).

Other transcriptional partners of NFAT comprise ICER (Bodor and Habener 1998), Maf (Ho, Hodge et al. 1996) and p21SNFT (Iacobelli, Wachsman et al. 2000), which are members of the basic region-leucine zipper (bZIP) family to which AP-1 belongs as well. Egr (Decker, Nehmann et al. 2003) and GATA (Avni, Lee et al. 2002) are zink finger proteins, and HNF3 (Furstenau, Schwaninger et al. 1999), Oct (Duncliffe, Bert et al. 1997) and IRF-4 (Rengarajan, Mowen et al. 2002) belong to the helix-turn-helix-domain proteins, which interact with NFAT. The nuclear receptor PPARγ (Yang, Wang et al. 2000) and the MADS-box protein MEF2 (McKinsey, Zhang et al. 2002) are also interaction partners of NFAT.

Foxp3 belongs to the forkhead-winged-helix family of transcription factors. It is a specific marker of murine Tregs and has impact on the phenotype and function of these cells (Fontenot, Rasmussen et al. 2005). Foxp3 was initially identified as the gene which causes autoimmunity in scurfy mice (Brunkow, Jeffery et al. 2001). T helper cells from scurfy mice possess enhanced activity of the transcription factors NFAT and NFκB, which is essential for cytokine production. Reconstitution of functional Foxp3 in scurfy-derived T cells reduces transcriptional activity of NFAT and NFκB. Foxp3 and NFATc1A were shown to interact physically in lysates of transfected HEK 293T cells (Bettelli, Dastrange et al. 2005). Foxp3 has influence on gene expression in Tregs by interaction with NFATc2 and the interaction was found to be mandatory for the suppressive function of Tregs *in vivo*. Depending on the promoter, the interaction with Foxp3 enhances or reduces NFATc2 driven transcription. Foxp3 can inhibit IL-2 promoter activity driven by NFATc2-AP-1 complexes but not by NFAT dimers (Wu, Borde et al. 2006). Thus, interaction with various transcription factors enables NFAT proteins to integrate different signaling pathways and to serve different functions.

3.3.5 NFAT in T cells

NFAT is crucial for the activation of the IL-2 promoter and other cytokine genes and thus for T cell activation (Shaw, Utz et al. 1988; Serfling, Avots et al. 1995; Luo, Burgeon et al. 1996).

Genetic data from two human families indicate the importance of NFAT for T cell activation, because impaired activation of NFAT caused by a defect in calcium influx coincided with severe immunodeficiency (Feske, Draeger et al. 2000).

Mice deficient for single NFAT proteins display only weak changes in immune functions. However, elimination of more than one NFAT factor has a strong impact on immune cells and their functions. Mice deficient for NFATc1 and NFATc2 in T cells show reduced production of the cytokines IL-2, IL-4, IL-5, IL-10, IFN-γ, GM-CSF and TNF-α (Peng, Gerth et al. 2001).

Distinct functions of the NFAT family members in Th1 and Th2 cell differentiation were proposed as NFATc2$^{-/-}$ mice display a weak preference to differentiate into Th2 cells, probably mediated by prolonged IL-4 production (Hodge, Ranger et al. 1996; Kiani, Viola et al. 1997) and reduced IFN-γ production of Th1 cells (Kiani, Garcia-Cozar et al. 2001). NFATc2$^{-/-}$/c3$^{-/-}$ mice show increased Th2 responses and cytokine production (Rengarajan, Tang et al. 2002). NFATc1$^{-/-}$ T cells are characterized by a block of IL-4 production and decreased titers of IgE and IgD (Ranger, Hodge et al. 1998). These data indicate that NFATc1 promotes Th2 differentiation and NFATc2 and NFATc3 give rise to Th1 differentiation. On the contrary, overexpression of constitutively active NFATc1 as well as NFATc2 in Th1 and Th2 cells induces transcription of Th1 and Th2 cytokines to the same extent (Monticelli and Rao 2002; Porter and Clipstone 2002). NFATc2 binds to the IL-4 and IFN-γ promoter in activated Th1 and Th2 cells (Avni, Lee et al. 2002). These data contradict the effects seen in NFATc1$^{-/-}$ and NFATc2$^{-/-}$ mice. Thus, NFATc1 and NFATc2 could serve redundant functions in T cell differentiation without being exclusively restricted to the Th1 or Th2 branch.

3.4 Fyn

3.4.1 Fyn, a member of the Src family of tyrosine kinases

Fyn belongs to the family of Src kinases (Resh 1998), which consists of nine members in mammals: Fyn, Src, Fgr, Yes, Lck, Hck, Blk, Lyn and Frk. Fyn is ubiquitously expressed and FynT expression is restricted to hematopoietic cells. FynT harbors an alternatively spliced variant of exon 7, which codes for a part of the kinase domain (Cooke and Perlmutter 1989).

3.4.2 Domain structure of Fyn

Fyn is a 59 kDa protein with a domain organization typical for Src kinases and harbors the following domains: attachment sites for ligation of saturated fatty acids at the N-terminus, a unique region, a Src-homology 3 (SH3) domain, a Src-homology 2 (SH2) domain, a tyrosine kinase domain, also termed SH1 domain, and a negative regulatory domain at the C-terminus (Boggon and Eck 2004) (see Figure 3.6).

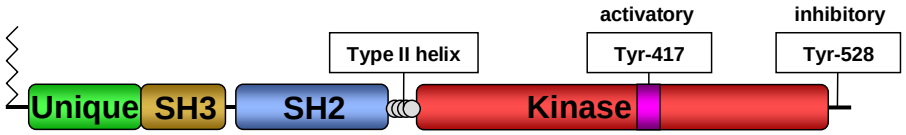

Figure 3.6 Domain structure of Fyn
A myristyl residue bound to a fatty acid attachment site at the N-terminus of the molecule is indicated by a black zick-zack line. The unique region, SH3 domain, SH2 domain and the kinase domain are represented by colored boxes. The linker region between the SH2 domain and the kinase domain, which constitutes a polyproline type 2 helix, is indicated. The pink rectangle in the kinase domain represents the activation loop (A-loop) with the activatory tyrosine 417. The inhibitory tyrosine 528 next to the C-terminus is also indicated (modified after: Boggon and Eck 2004).

N-terminal fatty acid attachment

A glycine residue at position 2 directly behind the start methionine is present in all Src kinases. The methionine residue is cut off and myristate is attached to glycine during translation, a hydrophobic residue which enables Src kinases to attach to membranes (Johnson, Bhatnagar et al. 1994). In addition, Fyn is reversibly palmitoylated at cysteine 3 and cysteine 6 (Koegl, Zlatkine et al. 1994).

Unique region

The function of the unique domain of Fyn is not known. The unique domain of Lck mediates its interaction with CD4 and CD8 and thus influences its cellular localization (Turner, Brodsky et al. 1990).

SH3 domain and SH2 domain

SH domains of Fyn contribute to the regulation of its activity by mediating interactions with other binding partners and within the molecule. SH3 domains bind to proline-rich proteins, preferentially to PXXP motifs. The SH3 domain of Fyn can associate with the proline-independent motif PKXXYXXY of the adapter protein Src kinase-associated phosphoprotein of 55 kDa (SKAP55) (Kang, Freund et al. 2000). The activity of Fyn is also regulated by binding of its SH3 domain to the SLAM-associated protein (SAP) (Chan, Lanyi et al. 2003; Latour, Roncagalli et al. 2003). The SH3 domain of Fyn mediates an intramolecular interaction with the linker region between the SH2 and kinase domains, contributing to Fyn

inactivation. The structure of SH2 domains is characterized by two pockets. One pocket binds phosphorylated tyrosines and the other typically mounts hydrophobic residues (Eck, Shoelson et al. 1993; Waksman, Shoelson et al. 1993). The SH2 domain of Fyn binds to phosphorylated tyrosine 528 localized at the C-terminus of Fyn, causing catalytic inactivation.

Tyrosine kinase domain

The bilobal structure of the kinase domain is a characteristic feature of all serine/threonine and tyrosine kinases and also shared by Fyn. (Knighton, Zheng et al. 1991). The small N-terminal lobe is formed by one α-helix and five β-strands, whereas the large C-terminal lobe, which harbors the activation loop (A-loop) with the tyrosine for activatory phosphorylation, is mainly constituted by α-helices. The transfer of the phosphate group to the substrate takes place in the groove between these two lobes.

3.4.3 Regulation of Fyn activity

Fyn kinase activity is regulated by conformational changes modulated by binding of ligands to the SH3 and SH2 domains and by the phosphorylation status of Y417 (mouse FynT) in the tyrosine kinase domain and of Y528 (mouse FynT). The C-terminal Y528 of Fyn is phosphorylated by the C-terminal src kinase (Csk) and then inhibits Fyn activity (Takeuchi, Kuramochi et al. 1993) by intramolecular binding to the SH2 domain of Fyn causing an inactive conformation (Sicheri and Kuriyan 1997). Intramolecular interactions between the SH3 domain and the polyproline type II helix positioned in the linker region between the SH2 and kinase domains of Fyn cause further stabilization of the inactive conformation. Tyrosine 417 in the activation loop of the catalytic domain of Fyn enhances kinase activity when phosphorylated and thereby acts as an activatory tyrosine (see Figure 3.7).

In the unphosphorylated state the activation loop is in an α-helical conformation, which occupies the catalytic cleft and thereby inhibits the kinase. Activation of Fyn leads to opening of the kinase domain. This is achieved by changing the position of the A-loop in a way that the activatory tyrosine 417 can undergo autophosphorylation. The phosphorylated A-loop stabilizes the catalytic cleft and thereby facilitates the activity of Fyn (Palacios and Weiss 2004; Salmond, Filby et al. 2009). Src phosphorylation at Y215 in its SH2 domain after cell stimulation with platelet-derived growth factor (PDGF) or epidermal growth factor (EGF) is associated with an increase in the kinase activity of Src (Stover, Furet et al. 1996; Vadlamudi, Sahin et al. 2003). Y215 of Fyn was found to be hyperphosphorylated in anergic human T cells in association with enhanced Y529 phosphorylation giving rise to a hyperactive conformation of Fyn (Smida, Posevitz-Fejfar et al. 2007).

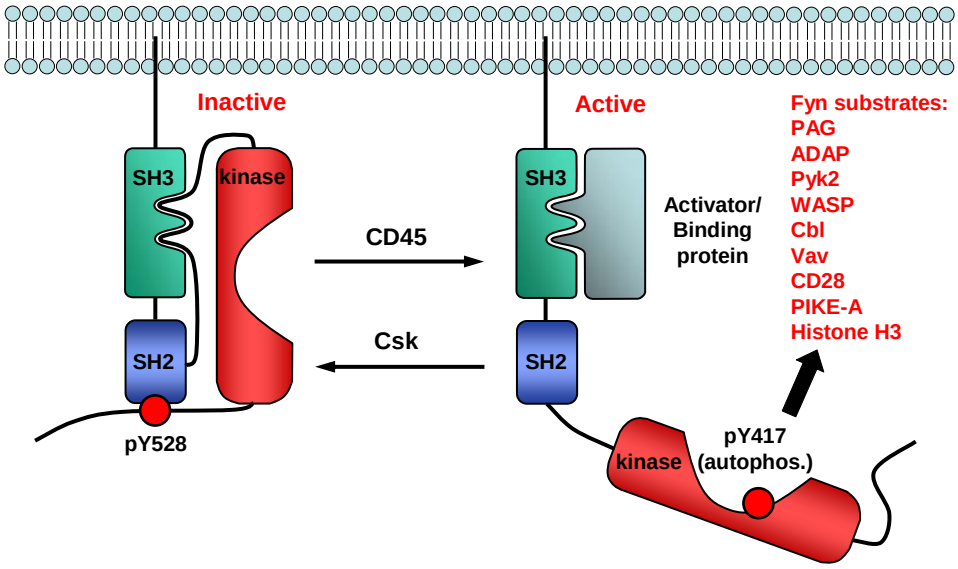

Figure 3.7 Model for regulation of Fyn activity
Phosphorylation of Y528 of Fyn mediated by Csk induces an inactive, closed conformation of Fyn. pY528 interacts with the SH2 domain of Fyn and the linker region between the SH2 and the kinase domains forms contact with the SH3 domain. Dephosphorylation of the inhibitory pY528 by CD45 results in an active, open conformation of Fyn. Binding of proteins to the SH3 domain promotes the active conformation of Fyn and autophosphorylation at Y417 enhances kinase activity. Substrates of Fyn are listed on the right (modified after: Salmond, Filby et al. 2009).

Fyn is dephosphorylated at the inhibitory Y528 by the hematopoietic-specific tyrosine phosphatase CD45, which leads to Fyn activation (Mustelin, Pessa-Morikawa et al. 1992; Hermiston, Xu et al. 2003). Correspondingly, Fyn is hyperphosphorylated at Y528 in CD45-deficient T cell lines, which display a strong reduction in tyrosine phosphorylation after TCR stimulation (Ostergaard, Shackelford et al. 1989; Koretzky, Picus et al. 1991; Stone, Conroy et al. 1997). A proline-enriched protein tyrosine phosphatase (PEP) is associated with the SH3 domain of Csk (Cloutier and Veillette 1996) and PEP causes dephosphorylation of the activatory Y417 of FynT in transfected Cos-1 cells (Cloutier and Veillette 1999). PEP also reduces the phosphorylation of the activatory Y394 in the kinase domain of Lck in transfected JCam1.6 cells stimulated with CD3 Ab (Gjorloff-Wingren, Saxena et al. 1999). Receptor protein tyrosine phosphatase α (PTPα) deficiency in thymocytes results in increased phosphorylation of Fyn at the inhibitory Y528 and the activatory Y417, indicating that PTPα might be responsible for dephosphorylation of these tyrosines. Furthermore, PTPα deficiency caused Fyn hyperactivity (Maksumova, Le et al. 2005).

Binding of Fyn to the protein Uncoordinated 119 (Unc119) or SAP was also shown to cause increased Fyn activity (Gorska, Stafford et al. 2004; Simarro, Lanyi et al. 2004). Fyn and Lck associate in lipid rafts (Filipp, Moemeni et al. 2008) and Lck is necessary for Fyn activation in lipid rafts (Filipp, Zhang et al. 2003). These data indicate that Lck could also serve a function in the regulation of Fyn activity.

The localization of Csk is crucial for Fyn activity, because Csk phosphorylates the inhibitory Y528 causing reduced Fyn activity (Okada, Nada et al. 1991). In resting T cells, Csk is positioned in close proximity to Fyn by the transmembrane adapter protein phosphoprotein associated with glycosphingolipid-enriched microdomains (PAG) (Brdicka, Pavlistova et al. 2000; Kawabuchi, Satomi et al. 2000). Fyn was shown to phosphorylate PAG at Y314 (Yasuda, Nagafuku et al. 2002; Filby, Seddon et al. 2007) causing increased binding of Csk and thus subsequent inactivation of Fyn. After TCR stimulation, PAG is dephosphorylated at Y314 causing dissociation of Csk and thus results in increased Src kinase activity (Torgersen, Vang et al. 2001; Davidson, Bakinowski et al. 2003).

3.4.4 Binding partners and substrates of Fyn

Fyn interferes with lymphocyte signaling on many levels. Fyn is associated with the intracellular part of the TCR, although this interaction is of low stoichiometry (Samelson, Phillips et al. 1990; Timson Gauen, Kong et al. 1992). Since Fyn is the kinase phosphorylating PAG at Y314, elimination of Fyn in T cells abolishes Csk recruitment to PAG and thus decreases phosphorylation of the inhibitory Y505 of Lck. These effects are associated with enhanced proliferation and cytokine production (Filby, Seddon et al. 2007). Fyn associates with PI3-K (Prasad, Janssen et al. 1993) and phosphorylates CD28 (Raab, Cai et al. 1995). Other targets of Fyn are the casitas B-lineage lymphoma proto-oncogene (Cbl) (Tsygankov, Mahajan et al. 1996; Elly, Witte et al. 1999; Hunter, Burton et al. 1999) and the guanine nucleotide exchange factor (GEF) Vav (Huang, Tilly et al. 2000). An association of Fyn with ZAP-70 was detected in a murine hybridoma cell line and transfected COS cells (Fusaki, Matsuda et al. 1996). Furthermore, TCR stimulation enhances tyrosine phosphorylation of the focal adhesion kinase Pyk2 in Jurkat cells, which is critically dependent on Fyn activity (Qian, Lev et al. 1997). Fyn is also involved in signal transduction initiated by the signaling lymphocyte activation molecule (SLAM) co-receptor. Fyn associates with the adapter protein SAP, which increases Fyn activity (Simarro, Lanyi et al. 2004) and recruits Fyn to SLAM (Latour, Gish et al. 2001; Chan, Lanyi et al. 2003). Absence or deficiency of SAP is associated with X-linked lymphoproliferative syndrome (XLP) (Coffey, Brooksbank et al. 1998; Nichols, Harkin et al. 1998; Sayos, Wu et al. 1998). Interactions of Fyn with CD2, the IL-2 receptor and the cell death protein Fas were also reported (Beyers, Spruyt et al. 1992; Kobayashi, Kono et al. 1993; Atkinson, Ostergaard et al. 1996).

Fyn also influences the organization of the cytoskeleton. The Wiskott-Aldrich syndrome protein (WASP), which has an impact on actin polymerization in T cells by regulation of the Arp2/3 complex, was shown to be a phosphorylation target of Fyn (Badour, Zhang et al. 2004). Fyn influences the reorganization of the tubulin cytoskeleton, as T cells from $Fyn^{-/-}$ mice do not rearrange their cytoskeleton after stimulation with CD3 Ab coated beads

(Martin-Cofreces, Sancho et al. 2006). Furthermore, an association of Fyn with phosphorylated α-tubulin was detected in T cells (Marie-Cardine, Kirchgessner et al. 1995).

Molecules crucial for T cell adhesion are also associated with Fyn like the adapter protein SKAP55 (Marie-Cardine, Bruyns et al. 1997) and the adhesion and degranulation promoting adapter protein (ADAP) (da Silva, Li et al. 1997), which constitutively associate with each other in T cells (Liu, Kang et al. 1998; Marie-Cardine, Hendricks-Taylor et al. 1998). ADAP, also termed SLP76 associated protein (SLAP) or Fyn binding protein (FYB), is phosphorylated by Fyn (Geng, Raab et al. 1999). ADAP and SKAP55 are essential for integrin clustering and T cell adhesion (Griffiths, Krawczyk et al. 2001; Peterson, Woods et al. 2001; Simeoni, Kliche et al. 2004; Jo, Wang et al. 2005; Kliche, Breitling et al. 2006).

Interestingly, Fyn phosphorylates the phosphatidylinositol 3-kinase enhancer-activating Akt (PIKE-A) at Y682 and Y774, thereby inhibiting apoptotic cleavage of PIKE-A. The kinase activity of PKB is enhanced by binding of PIKE-A, and apoptosis is reduced via this mechanism (Tang, Feng et al. 2007). Fyn and Src homology 2 domain containing transforming protein (Shc) co-immunoprecipitate (Wary, Mariotti et al. 1998), and the protein Src associated in mitosis 68 kDa (Sam68) was co-immunoprecipitated with the SH2 and SH3 domains of Fyn (Fusaki, Iwamatsu et al. 1997). In mast cells, GRB2-associated binding protein 2 (Gab2) associated with Fyn (Parravicini, Gadina et al. 2002) and Histone H3 was found to be phosphorylated by Fyn at serine 10 (He, Cho et al. 2005).

Thus, Fyn has various important physiological functions depending on its binding partners and substrates.

3.4.5 Src kinases in T cell activation

The phosphorylation of tyrosine residues within the ITAMs of the CD3 and ζ chains, which are among the first detectable biochemical events after TCR stimulation, are performed by Fyn and Lck. Analysis of a Lck-deficient human Jurkat T cell line, J.CaM.1, revealed reduced tyrosine phosphorylation after TCR stimulation (Straus and Weiss 1992). $Lck^{-/-}$ mice display a severe block in T cell development and $Lck^{-/-}$ thymocytes show a lack in phosphorylation of the ITAMs of the TCR ζ-chains resulting in reduced recruitment and phosphorylation of ZAP-70 (van Oers, Killeen et al. 1996). Lck function in peripheral T cells was analyzed by an inducible Lck transgenic mouse system on $Lck^{-/-}$ background (Legname, Seddon et al. 2000). Lack of Lck expression caused reduced ZAP-70 phosphorylation and activation after CD3+CD4 Ab stimulation, but slight ZAP-70 activity was still present in $Lck^{-/-}$ cells and some LAT phosphorylation was detectable as well. Only elimination of Fyn in addition to Lck caused complete abrogation of LAT phosphorylation. However, Fyn was not able to compensate the loss of Lck function concerning activation of PLCγ1 and induction of calcium

flux. Thus, Fyn has an impact on proximal TCR signaling, but seems to play a minor role than Lck. On the other hand, phosphorylation of Erk after CD3 Ab and CD3+CD4 Ab stimulation proceeded in the absence of Lck and was only abolished when both Lck and Fyn were deleted. Thus, Fyn can induce phosphorylation of Erk independently of Lck (Lovatt, Filby et al. 2006).

$Fyn^{-/-}$ mice do not show severe abnormalities in thymic development with the exception of NK cells (Eberl, Lowin-Kropf et al. 1999). The activation of peripheral $Fyn^{-/-}$ T cells was reduced after CD3 Ab stimulation, and activation via antigen presenting cells was not impaired. A strong proliferative defect was found in $Fyn^{-/-}$ thymocytes after stimulation with CD3 Ab and PMA (Appleby, Gross et al. 1992; Stein, Lee et al. 1992; Sugie, Jeon et al. 2004). In this context, Fyn was shown to be important for proliferation induced by low affinity TCR ligands (Utting, Teh et al. 1998) and T cell stimulation with low affinity antagonistic ligands preferentially led to activation of Fyn (Huang, Tilly et al. 2000).

Fyn and Lck are not solely positive regulators of TCR signaling, but they are involved in negative regulation of TCR signaling as well. $Fyn^{-/-}$ mice display reduced tyrosine phosphorylation of PAG (Yasuda, Nagafuku et al. 2002), especially at Y314 (Filby, Seddon et al. 2007). Because phosphorylated Y314 of PAG is the anchor for binding of Csk, the amount of Csk bound to PAG was reduced in the absence of Fyn and, thereby, phosphorylation of the inhibitory Y505 of Lck by Csk was impaired. However, the physiological relevance of reduced PAG function in $Fyn^{-/-}$ cells remains questionable, because T cells from $PAG^{-/-}$ mice display normal TCR signaling (Dobenecker, Schmedt et al. 2005; Xu, Huo et al. 2005), possibly by the existence of additional mechanisms for the recruitment of Csk into the proximity of Src kinases.

Lck and Fyn also seem to be involved in the activation of the PI3-K pathway after TCR stimulation, but the exact mechanisms are not unraveled yet. Fyn associated with PI3-K in the T-lymphoblastoid cell line HPB-ALL (Prasad, Janssen et al. 1993) and both kinases increase the interaction of PI3-K and GRB2 with CD28 by phosphorylation of CD28 at Y191 (Raab, Cai et al. 1995). However, Y191 of CD28 seems to be dispensable for CD28/PI3-K induced PIP3 generation at the immunological synapse (Garcon, Patton et al. 2008).

3.5 Anergy

3.5.1 Definition of anergy

Anergy is defined as a hyporesponsive state of T cells. Anergic T cells display impaired proliferation and cytokine production after exposure to the cognate antigen and especially a prominent block in IL-2 production (Jenkins, Pardoll et al. 1987). Anergy persists for a long time after induction and is not an early step on the way to cell death (Quill and Schwartz 1987). After the first description of anergy in mouse and human $CD4^+$ T cell clones (Lamb, Skidmore et al. 1983; Jenkins and Schwartz 1987), the term anergic has been used to describe different unresponsive states *in vitro* and *in vivo*. For instance, regulatory T cells (Tregs) were shown to display a hyporesponsive phenotype similar to anergic T cells (Hickman, Yang et al. 2006).

Clonal anergy is a growth arrest which is associated with markedly reduced production of specific cytokines (IL-2 and IL-3) after TCR stimulation. Antigen is not required to maintain this state and it can be abrogated by IL-2 (Beverly, Kang et al. 1992; Schwartz 1996) or stimulation with phorbol esters and ionomycin (Fields, Gajewski et al. 1996; Li, Whaley et al. 1996). Clonal anergy is characterized by a block in Ras activation and thus inactivation of the Ras/MEK/Erk signaling cascade (Fields, Gajewski et al. 1996; Li, Whaley et al. 1996; Chiodetti, Choi et al. 2006; Smida, Posevitz-Fejfar et al. 2007).

Adaptive tolerance (*in vivo* tolerance) is associated with decreased production of all cytokines driven by TCR-stimulation and antigen persistence is obligatory to maintain this state. Furthermore, it is not reversed by treatment with IL-2 (Tanchot, Barber et al. 2001; Schwartz 2003; Singh and Schwartz 2003). Adaptive tolerance is characterized by a block in TCR signaling at the level of LAT phosphorylation by ZAP-70 (Chiodetti, Choi et al. 2006). This proximal block in TCR signaling causes downmodulation of the NFAT and NFκB pathways but results in weak reduction of Erk phosphorylation.

3.5.2 *In vitro* induction of anergy

Initially, anergy was induced by triggering the TCR with agonist peptides presented by MHC molecules without additional co-stimulation via antigen presenting cells (APCs) (Quill and Schwartz 1987; Boussiotis, Freeman et al. 1993) or by partial agonist peptides with additional co-stimulation mediated by APCs (Sloan-Lancaster, Evavold et al. 1993). Furthermore, other methods can be used such as TCR cross-linking with plate-bound CD3 Ab (Jenkins, Chen et al. 1990), self-presentation of agonist peptides by T cells possessing MHC II molecules (Lamb, Skidmore et al. 1983) and incubation of T cells with ionomycin (Macian, Garcia-Cozar et al. 2002; Heissmeyer, Macian et al. 2004). Application of CTLA4-Ig

to block CD28 co-stimulation in combination with soluble CD3 Ab and splenic APCs also induces anergy (King, Buckler et al. 2008).

3.5.3 *In vivo* induction of anergy

Initially, *in vivo* induction of anergy was performed by injection of superantigens (Rellahan, Jones et al. 1990). Additionally, intravenous injection of CD3 Ab into mice resulted in unresponsiveness of T cells (Hirsch, Eckhaus et al. 1988; Ben-Amor, Leite-De-Moraes et al. 1996). Antigen-specific anergy models were established with TCR tg T cells triggered by intravenous injection of the peptide specific for the tg TCR (Kearney, Pape et al. 1994; Frauwirth, Alegre et al. 2001) or TCR tg T cells were transferred into T cell depleted mice expressing the cognate antigen (Rocha and von Boehmer 1991; Lanoue, Bona et al. 1997; Adler, Huang et al. 2000; Tanchot, Barber et al. 2001). In oral tolerance models, TCR tg mice were fed with high concentrations of the cognate antigen (Asai, Hachimura et al. 2002). Importantly, the model systems do not only differ in the procedure of anergy induction but also in their biochemical features. The experimental work done to analyze anergy resulted in the generation of the two-signal model of T cell activation. Signaling through the antigen receptor alone (signal 1) causes anergy, whereas signal 1 in combination with appropriate co-stimulation (signal 2) induces activation of T cells. Programmed death 1 (PD-1) is a receptor molecule with inhibitory function, which belongs to the CD28 superfamily and is expressed on T cells after antigen stimulation (Okazaki and Honjo 2006). PD-L1 and PD-L2 are ligands of PD-1 and PD-1 interaction with PD-L1 is important for the induction of anergy in lymphoid organs (Tsushima, Yao et al. 2007). Tissue-resident signals generated by PD-L1 contribute to the maintenance of tolerance in the pancreas (Martin-Orozco, Wang et al. 2006). Thus, not only the dialogue between a T cell and the antigen presenting cell is important for induction or maintenance of an anergic phenotype, but interactions of T cells with other cell types are also important.

3.5.4 Fyn and anergy

Fyn is involved in different anergy models. When an allogen specific human T cell clone was co-cultured with cells presenting the cognate antigen in the absence of CD80 expression enhanced Fyn activity was detected in the anergized cells (Boussiotis, Freeman et al. 1997). In another study, primary human T cells were anergized by stimulation with plate-bound CD3 Ab and enhanced Fyn activity in anergic cells was associated with hyperphosphorylation of PAG at Y317 leading to enhanced Csk recruitment (Smida, Posevitz-Fejfar et al. 2007). Furthermore, anergy in mouse Th1 cells induced by stimulation with plate-bound CD3 Ab coincided with decreased expression of Lck and increased levels of Fyn. Consistent with the differences in protein expression, autophosphorylation activity of Lck was reduced, whereas autophosphorylation activity of Fyn was enhanced (Quill, Riley et al. 1992). An increase in

the expression level of Fyn was associated with anergy in $CD4^-CD8^-$ T cells from TCR tg mice (Utting, Teh et al. 2000), and deletion of Fyn recovered the T cell proliferation defect in this anergy system (Utting, Priatel et al. 2001). Increased FynT association with PAG was found in T cells, which were anergized *in vitro* by ionomycin. Tg expression of a PAG molecule able to interact with FynT but not with Csk, because of elimination of the Csk binding site at Y314, caused enhanced calcium fluxes after TCR stimulation and increased anergy (Davidson, Schraven et al. 2007). Increased Fyn expression was also detected in several other anergy systems (Gajewski, Qian et al. 1994; Gajewski, Fields et al. 1995; Welke and Zavazava 2002; Chiodetti, Choi et al. 2006).

Since CsA has the potential to inhibit anergy induction, experiments were performend to analyze whether calcium signaling alone is sufficient to induce anergy (Jenkins, Pardoll et al. 1987). Overnight treatment of T cells with ionomycin induced an unresponsive state, and NFAT activation without AP-1 interaction was crucial for this anergy, which was associated with a specific gene expression pattern (Macian, Garcia-Cozar et al. 2002). One of the genes induced was diacylglycerol kinase-α (DGK-α), which catalyzes the degradation of DAG to phosphatidic acid (PA) and leads to reduced activation of Ras (Zha, Marks et al. 2006). Ionomyin induced anergy is also associated with increased expression of the E3 ubiquitin ligases Grail, Cbl-b and Itch and the ubiquitin binding protein Tsg101. Stimulation of anergic cells resulted in the localization of Itch and Nedd4, which is related to Itch, to the plasma membrane and in the degradation of PKCθ and PLCγ1. Anergized cells also displayed a decreased calcium flux after TCR stimulation and an impaired stability of immunological synapses (Heissmeyer, Macian et al. 2004).

3.6 Aim of the study

Previous studies showed that myrPKB affects thymocyte selection, proliferation and survival of peripheral T cells. Although myrPKB tg T cells are hyperproliferative and produce more cytokines, they display a strong reduction in nuclear levels of the transcription factor NFAT. Interaction of PKB with NFAT was detected *in vivo* by co-immunoprecipitation experiments. These data suggest that NFAT could be a direct target of PKB.

Elevated PKB signals in thymocytes also affected early TCR signaling events leading to enhanced Lck and Erk activity. Since both Src kinases, Lck and Fyn, initiate proximal TCR signaling and after TCR stimulation co-localize in lipid rafts, as does activated or myrPKB, the hypothesis arose that myrPKB could modify Lck activity either directly by binding and phosphorylation or by indirect mechanisms like modifying Fyn or Csk activity, the kinase negatively regulating Lck/Fyn activity.

Based on above results, the aims of the thesis were:

1) to characterize the interaction of PKB with NFAT in early T cell development and at the molecular level

2) to investigate a possibly novel interaction of PKB with Lck/Fyn or Csk in T cell activation.

4 Materials and Methods

4.1 Materials

4.1.1 Bacteria

E. coli BL21	
E. coli SURE	
E. coli XL10-Gold	QuikChange® Multi Site-Directed Mutagenesis Kit Stratagene (# 200514)
E. coli XL1-Blue	QuikChange® Site-Directed Mutagenesis Kit Stratagene (# 200518)

4.1.2 Cell lines

EL4	murine T lymphoblast cell line
HEK 293T	human embryonic kidney cell line

4.1.3 Mice

C57BL/6 mice	bred at the animal facility of the Medical Faculty of the Otto-von-Guericke University
human CD2-myrPKBα (myrPKB) transgenic mice	bred at the animal facility of the Medical Faculty of the Otto-von-Guericke University

4.1.4 Miscellaneous

ø 60 x 15 mm cell culture dishes	TPP 93060
1.5 ml reaction tubes	Eppendorf
6 well plates	Corning Incorporated (costar® 3516)
12 well plates	Corning Incorporated (costar® 3513)
15 ml tubes	Greiner Bio-One (cat. no.188271)
75 cm^2 cell culture flasks	Corning Incorporated (cat. no.: #430641)
175 cm^2 cell culture flasks	Corning Incorporated (cat. no.: #431080)
50 ml tubes	Greiner Bio-One (cat. no. 227261)
96 well plates	TPP 92096
Amersham Hyperfilm™ ECL (X-RAY FILM)	GE Healthcare (prod code: 28906837)
Cell scraper	Corning Incorporated (costar® 3010)
Cell strainer 100 μm Nylon BD Falcon™	BD Biosciences (REF 352360)

FUJI MEDICAL X-RAY FILM 100 NIF 18 x 24	A. Hartenstein (N0. RF12)
Nitrocellulose (Hybond™-C Extra)	Amersham Biosciences (cat. no.:RPN 303E)
Pasteur pipettes	Roth (art. no.: 4518)
SORVALL®PA THINWALL TUBE 4,4 ML Ultra centrifugation tubes	Kendro Laboratory Products (cat. no.: 03955)
Syringe filters 0.22 μm	TPP (99722)
Tubes for luciferase measurement 5 ml, 75 x 12 mm ø	SARSTEDT (No.REF 55.467)

4.1.5 Instruments

AutoMacs	Miltenyi Biotech
Balance	Kern & Sohn GmbH (Kern 440)
Cell homogenizer DOUNCE TISSUE GRINDER 2 ML	WHEATON
Centrifuge 5415D (table centrifuge)	Eppendorf
Centrifuge Micro 200R (table centrifuge)	Hettich
Centrifuge Multifuge 3S-R	Heraeus
CO_2 incubator	Binder
Compact incubator	Heraeus (Typ B 15)
Film developing machine	CAWO GmbH (CAWOMAT 2000 IR)
Flake ice machine	Thermo Electron Corporation
Gel documentation station	Herolab
Gel dryer	BIO RAD (Model 583)
Liquid scintillator 1450 Microbeta Wallac	Perkin Elmer
Luminometer	Berthold (Lumat LB 9507)
Magnetic stirrer	IKA®-Labortechnik (MSH)
Microscope Axioskop 2 plus	Zeiss
Microwave	AEG (MICROMAT)
Mini Trans-Blot® Electrophoretic Transfer Cell	BIO RAD
Mini-PROTEAN® 3 Cell	BIO RAD
PCR machine PTC-200 Peltier Thermal Cycler	MJ RESEARCH
PCR machine T3000 Thermocycler	Biometra

PHD cell harvester	Inotech AG
pH meter	Ino lab
Precision balance	OHAUS
RC-5 Superspeed Refrigerated Centrifuge	Kendro Laboratory Products
Rotor GSA (r: 14.56 cm)	Kendro Laboratory Products
Rotor SORVALL® TH-660 (r: 12.15 cm)	Kendro Laboratory Products
Safety cabinet	Heraeus (Hera Safe HS 12)
Shaker	Heidolph Duomax 1030
Shaking incubator	GFL (3032)
Shaking water bath	GFL 1083
Spectrophotometer	Ultrospec 3000 Pharmacia Biotech
Steam sterilizer	Thermo Scientific (VARIOKLAV®)
Sub-Cell® GT Agarose Gel Electrophoresis System	BIO RAD
Thermomixer	Eppendorf (5436)
Transilluminator	Messinstrumentebau GmbH Erlangen Germany
Ultracentrifuge Combi Sorvall®	Du Pont Company (OTD-COMBI)
UP50H Ultrasonic Processor (sonifier)	Hielscher Ultrasound Technology
Vortexer	IKA®-Labortechnik (VF2)
Water de-ionizer	TKA-LAB (Typ HP 5UF)

4.1.6 Chemicals and reagents

[γ-^{32}P]-ATP	GE Healthcare (PB 10168-500UCI) Perkin Elmer (prod. no.: NEG002A500UC)r
[^{3}H]-thymidine	MP Biomedicals Europe
100 bp DNA ladder	Invitrogen (cat. no.: 15628-019)
2-[N-Morpholino] ethanesulfonic acid (MES)	SIGMA (M-3023)
2-Mercaptoethanol	SIGMA (M3148)
2-Mercaptoethanol 50 MM	GIBCO (cat. no.: 31350-010)
5 x Green Go Taq® Flexi Buffer	Promega (cat. no.: M891A)
Acetic acid	J.T. Baker (cat. no.: 6052)
Acetone p. a. 8002	J.T. Baker
Adenosine 5'-Triphosphate (ATP)	SIGMA (A-2383)
Agarose NEEO Ultra-Quality	Roth (art. no.: 2267.4)
Akt kinase	Cell Signaling (cat. no.: #7500)

Ammoniumperoxodisulfate (APS)	Roth (art. no.: 9592.3)
Ampicillin	Roth (art. no.: K029.1)
β-glycerophosphate	SIGMA (G-6251)
Brij 58 (Surfact-Amps® 58)	Pierce (prod. # 28336)
Brilliant Blue R250	Roth (art. no.: 3862.1)
BSA (Albumine Fraction V)	Roth (art. no.: 8076.2)
$CaCl_2$	Roth (art. no.: A119.1)
Cholera Toxin B Subunit, Peroxidase from *Vibrio cholerae*	SIGMA (C4672)
Deoxycholate	SIGMA (D-2510)
D(+)-Glucose	Roth (art. no.: X997.1)
Dimethylsulfoxide (DMSO)	Aldrich (cat no.: 276855)
Dithiothreitol (DTT)	SIGMA (D-9779)
D-Luciferin	SIGMA (L9504)
D(+)-Saccharose	Roth (art. no.: 4621.1)
Enolase from rabbit muscle	SIGMA (#E0379)
Ethanol (drained)	Pharmacy University Hospital Magdeburg
Ethidium bromide solution 1% (10 mg/ml)	Roth (art. no.: 2218.1)
Ethylenediaminetetraacetic acid (EDTA)	SIGMA (E6758)
Ethylenediaminetetraacetic acid (EDTA) [titration complex 3]	Roth (art. no.: 2218.1)
FuGENE6 Transfection Reagent	Roche (cat. no.: 11814443001)
GIBCO™ MEM Non-Essential Amino Acids Solution 10 mM (100x)	Invitrogen (cat. no.: 11140076)
Glutathione Sepharose™4B	GE Healthcare (cat. no.:17-0756-01)
Glycerol	Pharmacy University Hospital Magdeburg
Glycine	Roth (art. no.: T873.2)
Go Taq® Flexi DNA Polymerase	Promega (cat. no.: M8305)
HEPES	Roth (art. no.: 9105.4)
Hydrochloric acid (HCl) 3% p.a.	Roth (art. no.: 4625.1)
Ionomycin calcium salt from *Streptomyces conglobatus*	SIGMA (I0634)
Isopropanol	Pharmacy University Hospital Magdeburg
Isopropyl-β-D-thiogalactopyranoside (IPTG)	Fermentas (#R0392)
Kaliumdihydrogenphosphate (KH_2PO_4)	Roth (art. no.: 3904.2)
Kanamycin sulfate	Roth (art. no.: T832.1)
LB Agar (Lennox)	Roth (art. no.: X965.1)

LB Broth (Lennox)	International Diagnostics Group plc (idg)
L-Glutamine 200 mM (100 x)	GIBCO (25030)
L-Glutathione reduced	SIGMA (G4251)
Magnesium acetate [Mg $(OAc)_2$]	SIGMA (M-5661)
Manganese chloride ($MnCl_2$)	SIGMA (M-8530)
Methanol	J.T. Baker (cat. no.: 8045)
Milk powder	Roth (art. no.: T145.2)
Murine IL-2	BIOCHROM AG (#W1505.960.005)
n-Dodecyl-β-D-maltoside (LM)	Calbiochem (cat. no.: 324355)
NP-40 (IGEPAL Ca 630)	SIGMA (I-3021)
Page Ruler™ Prestained Protein Ladder	Fermentas (#SMO671)
PD98059 (MEK inhibitor)	Calbiochem (cat. no.: 513000)
Penicillin-Streptomycin	Invitrogen (cat. no.: 15140-122)
Phenylmethylsulfonylfluoride (PMSF)	Roth (art. no.: 6367.2)
Phorbol 12-myristate 13-acetate (PMA)	SIGMA (P8139)
Polyethylenimine (PEI)	Aldrich (408727)
Ponceau S	SIGMA-ALDRICH (P3504)
PP2	Calbiochem (cat. no.: 529573)
Protein G Sepharose™ 4 Fast Flow	GE Healthcare (cat. no.: 17-0618-01)
Proteinase inhibitor mix complete	Roche (cat. no.: 11697498001)
Proteinase K	Roth (art. no.: 7528.1)
Roti®- Load 1 (4x)	Roth (art. no.: K929.1)
Rotiphorese® Gel 40 37,5:1 (acrylamide N, N methylenebisacrylamide)	Roth (art. no.: T802.1)
Rotisol	Roth (art. no.:7917.1)
Sodium acetate	Roth (art. no.:6773.1)
Sodium azide	Roth (art. no.: K305.1)
Sodium chloride (NaCl)	Roth (art. no.: 3957.1)
Sodium dodecyl sulfate (SDS)	SIGMA (L-4390)
Sodium fluoride (NaF)	Roth (art. no.: P756.1)
Sodium orthovanadate (Na_3VO_4)	SIGMA (S6508)
Sodium pyrophosphate	SIGMA (S-6422)
Sodium pyruvate	Roth (art. no.: 8793.2)
Streptavidin	Dianova (cat no.: 016-000-084)
Streptavidin MicroBeads	Miltenyi Biotech (# 130-048-101)

Super Signal® West Pico Chemiluminescent Substrate (ECL substrate)	Thermo SCIENTIFIC (prod # 34077)
TEMED	Roth (art. no.: 2367.3)
Trichloroacetic acid (TCA)	Aldrich (cat. no.: 116114)
Tris	Roth (art. no.: 5429.3)
TritonX100	Roth (art no.: 3051.2)
Trypan blue	Roth (art. no.: CN76.1)
Tween®20	Roth (art. no.: 9127.1)
UO126 (MEK inhibitor)	Calbiochem (cat. no.: 662005)

4.1.7 Kits

BCA™ Protein Assay Kit	Thermo SCIENTIFIC (prod #23225)
Dual-Luciferase® Reporter Assay System	Promega (E1910)
HiSpeed Plasmid Maxi Kit	Qiagen (cat no.: 12663)
peq GOLD Plasmid Miniprep Kit I	PEQLAB (order no.: 12-6942-02)
Quik Change® Multi Site-Directed Mutagenesis Kit	Stratagene (cat. no.: 200514)

4.1.8 Vectors

pGEX-3X	Amersham Biosciences (27-4803-01)
pGEX-4T-1	Amersham Biosciences (27-4580-01)

4.1.9 Antibodies

Stimulation

Biotin-CD4 clone GK1.5 (rat monoclonal)	Becton Dickinson (mat. no.: 553728)
Biotin-CD3ε clone 145-2C11 (hamster monoclonal)	Becton Dickinson (mat. no.: 553060)
CD28 clone 37.51 (hamster monoclonal)	Becton Dickinson (mat. no.: 553295)
CD3ε clone 145-2C11 (mouse monoclonal)	Becton Dickinson (mat. no.: 553058)

Immunoprecipitation

Akt1 (2H10) (mouse monoclonal)	Cell Signaling (cat. no.: #2967)
Fyn15 (mouse monoclonal)	Santa Cruz (sc-434)
PAG IG452 (rabbit polyclonal)	ImmunoGlobe (cat. no.: # 0062-10)

Control antibodies for immunoprecipitation

Rabbit IgG control Ab (rabbit polyclonal)	Dianova (code no.: DLN-13121)
AffiniPure mouse anti-rat IgG (H+L) (mouse polyclonal)	Dianova (code no.: 212-005-168)

Western blotting (primary antibodies)

4G10 (mouse monoclonal)	prepared from hybridoma by AG Bommhardt
Actin (mouse monoclonal)	SIGMA (A3853)
Akt (rabbit polyclonal)	Cell Signaling (cat. no.: #9272)
Csk C-20 (rabbit polyclonal)	Santa Cruz (sc-286)
FLAG (rabbit polyclonal)	SIGMA (F7425)
Fyn01 (mouse monoclonal)	provided by Vaclav Horejsi, Prague
Fyn3 (rabbit polyclonal)	Santa Cruz (sc-16)
PAG IG452 (rabbit polyclonal)	ImmunoGlobe (cat. no.: # 0062-10)
pAkt (Ser473) (rabbit monoclonal)	Cell Signaling (cat. no.: #4060)
pErk Phospho-p44/42 Map Kinase (Thr202/Tyr204) (rabbit polyclonal)	Cell Signaling (cat. no.: #9101)
pY314 PAG (rabbit polyclonal)	Rabbit anti-phospho-PAG (pY314) was generated by immunizing rabbits with the peptide KEISAMpYSS (gift from Dr. J. Lindquist).
Src pY418 (rabbit polyclonal)	BIOSOURCE (cat. no.: 44-660G)

Western blotting (secondary antibodies)

Peroxidase-conjugated AffiniPure Goat Anti-Mouse IgG (H+L)	Dianova (code no.: 115-035-146)
Peroxidase-conjugated AffiniPure Goat Anti-Rabbit IgG (H+L)	Dianova (code no.: 111-035-003)

4.1.10 Solutions, buffers and media

Dulbecco's MEM	BIOCHROM AG (cat. no.: FG 0435)
FCS	PAN BIOTECH GmbH (cat. no.: 3702-P211312)
OPTI MEM® 1x	GIBCO (31985)
PBS Dulbecco w/o Ca^{2+}, Mg^{2+}	BIOCHROM AG (cat. no.: L 1825)
RPMI 1640 medium	BIOCHROM AG (cat. no.: FG 1215)
TBS	137 mM NaCl 20 mM Tris pH 7.6
TBST	TBS 0.05% (v/v) Tween®20
Trypsin/EDTA solution	BIOCHROM AG (cat. no.: L2163)

4.2 Methods

4.2.1 Bacterial cell culture

Liquid culture

Liquid culture was performed to gain sufficient amounts of bacteria for subsequent plasmid isolation or protein expression. Bacteria were cultured in LB medium containing antibiotics for selection of clones harboring the plasmid of interest. Ampicillin and kanamycin were used at a concentration of 100 μg/ml. Bacteria were cultured at 37°C and shaken at 225 rpm.

LB agar plates

Plate culture of bacteria was performed to separate single clones. LB Agar was autoclaved and 100 μg/ml ampicillin or kanamycin was added to the liquid agar before casting into petri dishes. Plates were inoculated with liquid bacteria culture and incubated at 37°C. Plates carrying single colonies were stored at 4°C.

4.2.2 DNA isolation and precipitation

DNA isolation from bacteria was performed using the peq GOLD Plasmid Miniprep Kit I from PEQLAB or the HiSpeed Plasmid Maxi Kit from Qiagen according to the manufacturer's instructions. DNA used for transfections was precipitated by the following procedure:

- addition of ddH_2O to a final volume of 500 μl
- addition of 1/10 vol (50 μl) 3 M sodium acetate pH 5.2 and 2.5 vol (1375 μl) ethanol
  => mixing by inverting tube
  => incubation at -20°C (at least 1 h)
- centrifugation at 18620 g (14000 rpm in a table centrifuge) for 20 min at 4°C
  => discard supernatant
- washing of pellet (2 x)
  => addition of 500 μl 70% ethanol
  => centrifugation at 18620 g for 10 min at 4°C
  => discard supernatant
- drying of pellet at RT or at 50°C in a heating block
- resuspension of dry pellet in ddH_2O

4.2.3 DNA quantification

The concentration of the purified DNA was measured by spectrophotometry. Nucleic acids possess an absorption maximum at 260 nm. An optical density (OD) of 1 indicates a DNA concentration of 50 μg/ml. The absorption at 280 nm represents contamination by proteins and the absorption at 230 nm represents contamination by peptides, aromatic compounds

and carbohydrates. Thus, the quotients OD_{260}/OD_{280} and OD_{260}/OD_{230} provide information concerning the purity of DNA as indicated in Table 4.1.

Table 4.1 Spectralphotometric analysis of concentration and purity of nucleic acids

	OD_{260}=1	**pure DNA $OD_{260}/OD_{280} \geq$**	**pure DNA $OD_{260}/ OD_{230} \geq$**
dsDNA	50 $^{\mu g}/_{ml}$	1.8	2.2

4.2.4 PCR mutagenesis and DNA sequencing

Mutagenesis PCRs were performed using the Quik Change® Multi Site-Directed Mutagenesis Kit from Stratagene according to the manufacturer's instructions. PCR primers were prepared by APARA BIOSIENCE GmbH (Denzlingen, Germany). Isolation of DNA from transformed E. coli XL10-Gold was done with the peq GOLD Plasmid Miniprep Kit I from PEQLAB. Mutagenesis was monitored by sequencing the appropriate DNA segments by GATC BIOTECH AG (Konstanz, Germany).

4.2.5 Transformation of bacteria

Proteins were expressed in E. coli BL21 bacteria optimized for protein expression.
Transformation of bacteria was performed as follows:

- thawing of an aliquot (50 µl) of competent bacteria on ice
- addition of DNA and careful mixing
  (E. coli SURE and E. coli XL1-Blue: 50 ng DNA; E. coli BL21: 500-1000 ng DNA)
- 30 min incubation on ice
- 90 sec heat shock at 42°C (E. coli SURE),
  45 sec heat shock at 42°C (E. coli XL1-Blue; E. coli BL21)
- 2 min incubation on ice
- addition of 1 ml LB medium (sterile and without antibiotics)
- 1 h incubation at 37°C with shaking at 225 rpm
- plating on LB agar plates with appropriate antibiotic for selection of the plasmid:
  => 30 µl of LB culture
  => centrifuge rest of culture at 750 g (2800 rpm in a table centrifuge)
  for 5 min at RT
  => discard supernatant, carefully resuspend bacteria in 50 µl LB and plate
  (equivalent to 970 µl)

4.2.6 Bacterial GST-fusion protein expression and harvest via glutathione columns

Elution buffer:
50 mM Tris/HCl pH 8.0
10 mM reduced glutathione

A 5 ml LB culture with ampicillin (100 μg/ml) and the appropriate bacterial clone was grown overnight. 1/50 vol of this culture was used for inoculation of 100 ml LB containing 50 μg/ml ampicillin and 20 mM glucose. The culture was incubated at 37°C with shaking at 200 rpm until an OD_{600} of 0.6–0.8 was reached, which indicated entry into the exponential growth phase. At this stage, the expression of the GST-fusion protein was induced by adding 1 mM IPTG to the culture and 600 μl proteinase-inhibitor solution (prepared as recommended by the manufacturer Roche) was added, followed by an incubation at 30°C for 2 h with shaking at 200 rpm. Thereafter, the culture was transferred into two 50 ml tubes and centrifuged at 3000 g (3600 rpm in Heraeus Multifuge 3S-R) for 5 min at 4°C. The supernatants were discarded and the cell pellets were resuspended in 5 ml PBS 0.1% TritonX100 (v/v). Each sample was sonified with a Hielscher UP50H ultrasonic processor (100% amplitude, cycle 1) for 3 min, subsequently stored on ice and centrifuged at 16264 g (10000 rpm in RC-5 Superspeed Refrigerated Centrifuge) for 20 min at 4°C. The supernatants were transferred into a 15 ml tube and 500 μl washed Glutathione Sepharose™4B suspension was added. The mix was incubated at 4°C with gentle rotation for 1 h or overnight. The GST-fusion proteins should bind to the Glutathione Sepharose™4B during this incubation.

Glutathione Sepharose™4B was washed as follows: 2 x 600 μl Glutathione Sepharose™4B were transferred into two 1.5 ml reaction tubes and briefly centrifuged at 18620 g (14000 rpm in a table centrifuge). The supernatants were discarded and the pellets were washed three times with 1 ml PBS 0.1% TritonX100 (v/v).

After incubation, samples were centrifuged at 380 g (1300 rpm in Heraeus Multifuge 3S-R) for 5 min at 4°C and washed three times with 10 ml PBS 0.1% TritonX100 (v/v). After the last washing step, the Glutathione Sepharose™4B with bound GST-fusion proteins was resuspended in 1 ml PBS 0.1% TritonX100 (v/v) and transferred into a 1.5 ml reaction tube. After a brief centrifugation at 18620 g (14000 rpm in a table centrifuge) at 4°C, the supernatant was discarded and the pellet was resuspended in 300 μl elution buffer. After 2 min incubation at RT, the mixture was centrifuged briefly at 18620 g at RT, the supernatant was collected and after addition of 1/50 vol proteinase-inhibitor solution stored at -20°C. This procedure was repeated to obtain a second fraction of eluted proteins.

4.2.7 *In vitro* kinase assay (IVK)

10 x kinase reaction buffer:
250 mM Tris/HCl pH 7.5
100 mM $MgCl_2$
1 mM Na_3VO_4
50 mM β-glycerophosphate
20 mM DTT
Coomassie solution:
0.25% (w/v) Brilliant Blue R250
50% (v/v) methanol
12.5% acetic acid
Destaining solution:
30% (v/v) methanol
10% (v/v) acetic acid

The concentration of the eluted GST-fusion proteins (prepared as described in section 4.2.6) was quantified with the BCA™ Protein Assay Kit from Thermo SCIENTIFIC. 5 µg of protein were used to assess the phosphorylation by recombinant PKB. For the *in vitro* kinase assay (IVK), the proteins of interest were incubated for 30 min at 37°C with shaking at 600 rpm in 1 x kinase reaction buffer containing 50 ng recombinant PKB and 10 µCi [γ-^{32}P]-ATP. The reaction was terminated by addition of 1/4 vol 4 x Roti-Load followed by boiling for 5 min at 95°C with shaking at 800 rpm. Samples were run on a 10% SDS-PAGE gel. The running front of the gel, containing most unincorporated [γ-^{32}P]-ATP, was cut off and discarded and the gel was incubated in 10% (v/v) ethanol 10% (v/v) acetic acid in ddH_2O for 10 min at RT. Afterwards, the gel was stained in coomassie solution for 1 h at RT with gentle shaking, followed by an incubation in destaining solution at RT and overnight (with gentle shaking). After destaining, gels were dried and X-ray films were exposed to detect phosphorylation of the analyzed proteins by autoradiography.

4.2.8 Cell culture

EL4 lymphoma cells were grown in RPMI 1640 medium containing 10% FCS, 0.352 µM β-mercaptoethanol, 100 units/ml penicillin and 100 µg/ml streptomycin at 37°C and 5% CO_2. Cells were diluted 1:10 after 3 days to maintain optimal cell density ($1x10^5$–$1x10^6$ cells/ml).

Adherent HEK 293T cells were grown in Dulbecco's MEM containing 10% FCS, 100 units/ml penicillin and 100 µg/ml streptomycin at 37°C and 5% CO_2. Cells were diluted 1:10 in 3 day cycles to avoid confluency of the cell layer on the culture flask bottom. For splitting, adherent

cells were washed once with PBS and subsequently treated with 5 ml Trypsin/EDTA solution (0.25% trypsin/ 0.02% EDTA in PBS without Ca^{2+}, Mg^{2+}) for 1 min at RT for cell detachment. Cells were suspended and diluted 1:10 in fresh medium for culture.

4.2.9 Heat-inactivation of FCS

FCS used in media and buffers was incubated in a water bath at 56°C for 30 min to inactivate proteins of the complement system.

4.2.10 Transfection methods

FuGENE6

EL4 cells were transfected using FuGENE6 Transfection Reagent (Roche) according to the manufacturer's instructions. 50 ng murine Rag2-firefly luciferase reporter, 400 to 800 ng human NFATc1 (Chuvpilo, Jankevics et al. 2002) or NFATc2 expression construct, 50 ng ΔCam expression vector (Parsons, Wiederrecht et al. 1994) and empty vector for DNA compensation in a solution containing 1 μg DNA were mixed with 4 μl FuGENE6. Subsequently, this mixture was evenly distributed over 1.5-3.0x10^5 cells per well cultured in 12 well plates. 26 h later, cells were stimulated with ionomycin (100 ng/ml) and PMA (100 ng/ml) for 16 to 20 h. Afterwards, cells were harvested followed by assessment of luciferase activity. Luciferase expression was controlled by the TCR β-chain enhancer and part of the murine Rag2 promoter (nt -251 to nt +147) (Kishi, Wei et al. 2000).

Polyethylenimine (PEI)

Polyethylenimine was described to function as an efficient transfection reagent (Ehrhardt, Schmolke et al. 2006). 0.15x10^6 HEK 293T cells in 2 ml Dulbecco's MEM/10% FCS without antibiotics were seeded into 6 well plates the day before transfection. Cells were transfected with 1575 ng total DNA and 5 μl PEI stock solution. Stock solution of PEI was prepared as follows: 1 mg PEI was diluted in 1 ml ddH_2O and pH 7.0 was adjusted with HCl. The stock solution was sterilized by filtration through a syringe filter (0.22 μm) and aliquots were stored at -80°C. A total volume of 100 μl OPTI MEM medium containing all DNA constructs to be transfected was pipetted into 1.5 ml reaction tubes. 5 μl PEI stock solution was added to each sample, samples were vortexed for 2 sec and incubated for 10 min at RT. Afterwards, the samples were mixed by pipetting up and down two times before dropwise addition to HEK 293T cells cultured in 6 well plates. After addition of the transfection mix, 6 well plates were gently shaken several times for proper mixing of the transfection solution with the culture medium. The day after transfection, HEK 293T cells were stimulated with 100 ng/ml PMA and 747 ng/ml (1 μM) ionomycin for 6 h at 37°C followed by cell lysis and determination of luciferase activity.

Calcium phosphate

2 M $CaCl_2$

2 x HBS pH 7.05:

280 mM NaCl

10 mM KCl

1.5 mM Na_2HPO_4

12 mM glucose

50 mM Hepes

$1x10^6$ HEK 293T cells were seeded into ø 60x15 mm cell culture dishes in 4 ml Dulbecco's MEM/10% FCS/1% antibiotics the day before transfection. The cells were transfected with 5 μg total DNA. For this, DNA constructs were taken up in a total volume of 500 μl ddH_2O, and 50 μl 2 M $CaCl_2$ and 500 μl 2 x HBS buffer, adjusted to RT, were added. The mixture was vortexed followed by incubation at RT for 30 min. The cell culture medium was replaced by 4 ml fresh Dulbecco's MEM/10% FCS/1% antibiotics. Thereafter, the transfection mixture was added dropwise to the cells. The day after transfection, cells were lysed and western blot analysis was performed.

4.2.11 Luciferase assay

Harvesting buffer:

50 mM Tris

50 mM MES

0.1% (v/v) TritonX100

1 mM DTT

pH 7.8

Assay buffer:

125 mM Tris

125 mM MES

25 mM $Mg(OAc)_2$

1 pipette tip ATP powder for a total volume of 1 ml assay buffer

pH 7.8

Luciferase solution:

1 mM luciferin

5 mM KH_2PO_4 pH 7.8

Luciferase solution was prepared by dilution of 10 mM luciferin stock solution (in DMSO) in 5 mM KH_2PO_4 pH 7.8.

Luciferase assays were performed with a self-prepared harvesting buffer, assay buffer and luciferase solution. Luminescence generated by firefly luciferase (firefly luciferase activity: RLU1) was measured with a Berthold Lumat LB 9507.

Procedure with self-prepared buffers:

- transfer cells of each sample into a 1.5 ml reaction tube
- centrifugation at 300 g (1700 rpm in a table centrifuge) for 5 min at 4°C
- wash cells with 1 ml PBS (w/o Ca^{2+}, Mg^{2+})
  => centrifugation at 3000 g (5500 rpm in a table centrifuge) for 2 min at 4°C
  => discard supernatant
- resuspend cell pellet in 100 µl harvesting buffer
  => vortex 20 sec at maximum intensity
- 5 min incubation on ice
  => vortex 20 sec at maximum intensity
- centrifugation at 9500 g (10000 rpm in a table centrifuge) for 4 min at 4°C
- provide 50 µl assay buffer into wells of a 96 well plate
- add 50 µl supernatant to 50 µl assay buffer and mix by pipetting
- transfer 50 µl of the mixture into a luminometer tube and store on ice
- measure luminescence (RLU1) after injection of 50 µl luciferase solution per sample

Alternatively, the Dual-Luciferase® Reporter Assay System from Promega was used according to the manufacturer's instructions. Separate measurements of luminescence generated by firefly luciferase (firefly luciferase activity: RLU1) and of luminescence generated by renilla luciferase (renilla luciferase activity: RLU2) were performed with a Berthold Lumat LB 9507. Relative luciferase activity (RLU1/RLU2) was calculated by dividing firefly luciferase activity (RLU1) by renilla luciferase activity (RLU2).

4.2.12 Isolation of genomic DNA from mouse tail

Tail lysis buffer:
50 mM Tris pH 8.0
100 mM EDTA
100 mM NaCl
1% (w/v) SDS

Tail biopsies were used for genotyping of mice. Tail pieces were incubated in 400 µl tail lysis buffer containing 8 µl proteinase K (20 mg/ml) for overnight at 50°C with shaking at 600 rpm. The next day, lysates were centrifuged at 18620 g (14000 rpm in a table centrifuge) for 15 min at RT. Supernatants were transferred into 1.5 ml reaction tubes containing an equal

volume of isopropanol. After mixing by gently inverting the Eppendorf tube 2-3 times, DNA was harvested by pulling a bent pasteur glas pipette several times through the DNA precipitation mixture. The glas pipette tips with bound DNA were dried for 10 min at RT and washed with 70% ethanol. After drying at RT, the tips of the pasteur pipettes were broken into 1.5 ml reaction tubes, containing 200 µl ddH_2O. After incubation for 30 min at 60°C with shaking at 600 rpm, DNA solutions were used as templates in PCR reactions and stored at 4°C.

4.2.13 Genotyping mice by PCR

Primers used for genotyping myrPKB tg mice:	
F5 forward primer:	5' TGA CAC CAG GTA TTT TGA TGA 3'
6168 reverse primer:	5' TGT TGG ACC AGC TTT GCA G 3'

The genotype of mice was determined by PCR-amplification of genomic DNA obtained from mouse tails with primers specific for the myrPKB transgene cassette. Expected size of PCR fragments was 900 bp.

The PCR mixture had the following composition:

F5 forward primer	10 µM	1 µl
6168 reverse primer	10 µM	1 µl
dNTP mix	12.5 mM	0.4 µl
5 x Green Go Taq® Flexi Buffer		4 µl
$MgCl_2$	25 mM	2 µl
Go Taq® Flexi DNA Polymerase	5 units/µl	0,1 µl
Template DNA solution		1 µl
ddH_2O		10.5 µl (ad 20 µl)

The PCR reaction was peformed using the following program:

94°C 5 min		initial denaturation
94°C 1 min	32 cycles	denaturation
56°C 1 min		annealing
72°C 1 min		elongation
72°C 5 min		final elongation
4°C		storage

4.2.14 Agarose gel electrophoresis

50 x TAP buffer:	
Tris	242 g
Acetic acid	57.1 ml
EDTA (titration complex 3)	37.2 g
ddH_2O	ad 1000 ml
pH 8.0	

For agarose gels 1% (w/v) agarose was added to 1 x TAP buffer, the mixture was boiled in a microwave and 10 µl ethidium bromide (10 mg/ml) were added before casting the agarose into a gel chamber. DNA samples were run at 100 volts and recorded with an UV-gel documentation system.

4.2.15 Preparation of thymocyte and lymph node cell suspensions

Supplement complete (SC) 20x:

500 ml FCS (heat inactivated)

100 ml sodium pyruvate (100 mM)

100 ml GIBCO™ MEM Non-Essential Amino Acids Solution 10 mM (100x)

100 ml Penicillin-Streptomycin [10000 units/ml penicillin (base) and 10000 µg/ml streptomycin (base), Invitrogen (cat. no.: 15140-122)]

5 ml 2-Mercaptoethanol [50 MM; GIBCO (cat. no.: 31350-010)]

Supplemented RPMI 1640/10% FCS medium:

(75 µM final 2-Mercaptoethanol)

500 ml RPMI 1640

25 ml SC

25 ml FCS (heat inactivated)

5 ml Penicillin-Streptomycin [10000 units/ml penicillin (base) and 10000 µg/ml streptomycin (base)]

1.75 µl 2-Mercaptoethanol [14.3 M; SIGMA (M3148)]

Mice were killed with CO_2, thymi and lymph nodes were extracted and kept in supplemented RPMI 1640/10% FCS medium at RT. For preparation of single cell suspensions, thymi or lymph nodes were passed through a 100 µm plastic cell strainer in petri dishes containing supplemented RPMI 1640/10% FCS. An aliquot of cells was diluted in 0.05% trypan blue in PBS and counted in a Neubauer chamber for calculation of the cell concentration.

4.2.16 Isolation of $CD4^+$ T cells

Isolation of $CD4^+$ T cells from lymph nodes was performed with AutoMacs technology (Miltenyi Biotech, Bergisch Gladbach). Single cell suspensions were centrifuged at 300 g (1160 rpm Heraeus Multifuge 3S-R) for 10 min at 4°C and $1x10^7$ cells were resuspended in 100 µl PBS/0.5% (w/v) BSA. A mixture of the following antibodies was added to the cell suspension using 0.2 µl of each antibody for $1x10^7$ cells:

- Biotin anti-mouse CD8α; BD Pharmingen, Cat. 553029; 0.5 mg/ml
- Biotin anti-mouse I-A/I-E (2G9); BD Pharmingen, Cat. 553622; 0.5 mg/ml
- Biotin anti-mouse CD11b; BD Pharmingen, Cat. 553309; 0,5 mg/ml
- Biotin anti-mouse CD45R/B220 (RA3-6B2); BD Pharmingen, Cat. 553086; 0.5 mg/ml
- Biotin anti-mouse TER-119/erythroid cells (Ly-76); BD Pharmingen, Cat. 553672; 0.5 mg/ml
- AffiniPure mouse anti-rat IgG (H+L); Dianova, Code Number 212-005-168; 1.7 mg/ml
- AffiniPure goat anti-mouse IgG (H+L); Dianova, Code Number 115-005-166; 1.3 mg/ml

Cells were incubated for 20 min at 4°C with gentle mixing in between by inversion of the tube, followed by washing with 2 ml PBS/0.5% BSA for $1x10^7$ cells. Cells were centrifuged at 300 g (1160 rpm Heraeus Multifuge 3S-R) for 10 min at 4°C. The supernatant was discarded and the cell pellet was resuspended in 90 µl PBS/0.5% BSA for $1x10^7$ cells. For 1×10^7 cells, 10 µl Streptavidin MicroBeads were added, mixing was performed by gentle inversion of tubes and cells were incubated for 15 min at 4°C. Subsequently, cells were washed with 2 ml PBS/0.5% BSA for 1×10^7 cells. The supernatant was discarded and the cell pellet was resuspended in 1 ml PBS/0.5% BSA for $1x10^8$ cells. Negative selection was performed using the 'Deplete' program of the AutoMacs machine. Isolated $CD4^+$ T cells were spun down at 440 g (1400 rpm Heraeus Multifuge 3S-R) for 5 min at 15°C, the supernatant was discarded and cells were suspended in supplemented RPMI 1640/10% FCS medium.

4.2.17 Preparation of protein extracts

Cell lysis buffer:
1% Nonidet P-40
100 mM NaCl
50 mM Hepes pH 7.4
5 mM EDTA
1% lauryl maltoside (LM)
1 mM phenylmethylsulfonylfluoride (PMSF)
50 mM sodium fluoride
1 mM sodium orthovanadate
10 mM sodium pyrophosphate

Protein extracts were prepared from thymocytes or lymph node $CD4^+$ T cells. Single cell suspensions were washed once with cold PBS and lysed by suspension in 100 µl ice cold lysis buffer for $1x10^7$ cells. Lysates were vortexed and incubated on ice for 30 min. Thereafter, lysates were centrifuged at 18620 g (14000 rpm in a table centrifuge) for 10 min at 4°C. Supernatants were transferred into 1.5 ml reaction tubes, 1/4 vol 4 x Roti-Load was added and lysates were boiled at 95°C for 5 min with shaking at 800 rpm. Samples were stored at -20°C. The lauryl maltoside (LM) in the cell lysis buffer led to disruption of membrane lipid rafts.

4.2.18 Sodium dodecyl sulfate polyacrylamide gel electrophoresis (SDS-PAGE)

4 x Lower gel buffer (LGB):
1.5 M Tris
0.4% (w/v) SDS
pH 8.8
4 x Upper gel buffer (UGB):
0.5 M Tris
0.4% (w/v) SDS
pH 6.8
10 x Electrophoresis buffer:
0.25 M Tris Base
1.92 M Glycin
1% (w/v) SDS

Denaturating polyacrylamide gels were used for separation of protein extracts. The separating gel mixture was poured into the gel apparatus and isopropanol was pipetted on top. After gel polymerization for 30 min at RT, the isopropanol was discarded, the stacking gel mixture was poured into the apparatus and a comb was inserted. 15 min incubation at RT were sufficient for polymerization of the stacking gel.

Table 4.2 Composition of separating gel

	8%	**10%**	**12.5%**
ddH_2O	11 ml	10 ml	8.75 ml
Acrylamide/Bisacrylamide 37.5:1	4 ml	5 ml	6.25 ml
4 x LGB buffer	5 ml	5 ml	5 ml
10% APS in ddH_2O	66 µl	66 µl	66 µl
TEMED	10 µl	10 µl	10 µl

Table 4.3 Composition of stacking gel

ddH_2O	5.65 ml
Acrylamide/Bisacrylamide 37.5:1	1.15 ml
4 x UGB buffer	2.5 ml
Glycerol	700 µl
10% APS in ddH_2O	33 µl
TEMED	20 µl

Gels were loaded with protein samples and run at 100 volts in electrophoresis buffer. Proteins were transferred onto nitrocellulose membranes by wet western blotting.

4.2.19 Western blot

1 x Blotting buffer:
192 mM glycine
25 mM Tris
20% (v/v) methanol
Ponceau S solution:
0.2% Ponceau S in 3% trichloroacetic acid (TCA)
1 x TBS:
137 mM NaCl
20 mM Tris pH 7.6
Washing solution (TBST):
1 x TBS
0.05% (v/v) Tween®20

Transfer of proteins from SDS-PAGE gels onto nitrocellulose membranes was performed at 75 volts for 2 h in blotting buffer, which was cooled with ice. After the blotting procedure, nitrocellulose membranes were stained with Ponceau S solution to monitor the transfer of proteins. Destaining was performed by washing in TBST, and thereafter nitrocellulose membranes were blocked in 5% (w/v) milk powder in TBST for 2 h at RT followed by incubation with primary antibodies diluted in 5% (w/v) milk powder in TBST overnight at 4°C. The following day, nitrocellulose membranes were washed three times by shaking in TBST for 10 min. Subsequently, membranes were incubated with horseradish-peroxidase-conjugated antibodies diluted in 5% (w/v) milk powder in TBST for 1 h at RT and shaking. After washing three times with TBST, the membrane was treated with ECL solution and X-ray films were exposed.

4.2.20 Immunoprecipitation

Washing buffer:
0.05% (v/v) NP-40
5 mM EDTA
150 mM NaCl
50 mM Tris pH 7.4

For immunoprecipitation, $1x10^7$ cells were lysed in 500 µl lysis buffer as described in section 4.2.17. 50 µl lysate were mixed with 1/4 vol 4 x Roti-Load, boiled at 95°C for 5 min and then stored at -20°C. Protein G Sepharose™ 4 Fast Flow beads were washed two times in cell lysis buffer without lauryl maltoside (LM) before usage in immunoprecipitation. Centrifugation was performed at 9500 g (10000 rpm in a table centrifuge) for 2 min at RT. 10 µl washed Protein G Sepharose™ 4 Fast Flow beads were added to 450 µl protein lysate and incubated under gentle rotation for 1 h at 4°C to eliminate proteins binding unspecifically to Protein G Sepharose. After preclearing, lysates were centrifuged and the supernatants were transferred into new 1.5 ml reaction tubes containing 20 µl washed Protein G Sepharose™ 4 Fast Flow beads. 2 µg of immunoprecipitating antibody was added to each sample. Importantly, one sample was mixed with 2 µg antibody which was of the same isotype and generated in the same species as the antibody used for immunoprecipitation. Samples were incubated overnight at 4°C with gentle rotation. After centrifugation for 2 min at 4°C, supernatants were discarded and immunoprecipitates were washed four times with 800 µl washing buffer. Finally, 21 µl washing buffer and 7 µl 4 x Roti Load were added to the sepharose pellet and immunoprecipitated proteins were released from the sepharose beads by boiling of samples at 95°C for 5 min. After this step, immunoprecipitates were stored at -20°C for later western blot analysis.

4.2.21 *In vitro* kinase assay (IVK) with immunoprecipitated protein

Washing buffer:
0.05% (v/v) NP-40
5 mM EDTA
150 mM NaCl
50 mM Tris pH 7.4
Kinase reaction buffer (30 µl):
50 mM Tris/HCl pH 7.4
10 mM $MnCl_2$
0.1% (v/v) NP-40
5 µg acid-denatured enolase
5 µCi [γ-^{32}P]-ATP
Coomassie solution: see section 4.2.7
Destaining solution: see section 4.2.7

$2x10^7$ thymocytes or $1.5x10^7$ $CD4^+$ T cells were lysed as described in section 4.2.17 and immunoprecipitation was performed as described under 4.2.20. The samples were washed four times with 800 µl washing buffer (centrifugation at 9500 g for 2 min at 4°C). After the last washing step about 40% of the sepharose beads were taken, 1/4 vol 4 x Roti-Load was added and the mixture was boiled at 95°C for 5 min with shaking at 800 rpm. Samples were stored at -20°C and analyzed by western blot for the amount of immunoprecipitated protein. The other fraction of the immunoprecipitate was suspended in 30 µl kinase reaction buffer containing 5 µCi [γ-^{32}P]-ATP and 5 µg acid denatured enolase. The kinase reaction was performed for 30 min at RT and terminated by addition of 10 µl 4 x Roti-Load followed by boiling at 95°C for 5 min. Samples were run on 10% SDS-PAGE gels, gels were fixed, stained with coomassie, then dried and X-ray films were exposed for autoradiography.

4.2.22 Denaturation of enolase

Enolase stock suspension (10 mg/ml in 2.8 M ammonium sulfate containing 0.05 M imidazole and 1 mM $MgSO_4$, pH 7.5) was mixed with 1 vol 0.1 M acetic acid, vortexed and incubated at 30°C for 8 min. Thereafter, 1 vol ddH_2O was added resulting in an enolase concentration of 2.5 mg/ml. Acid denatured enolase was stored at -20°C.

4.2.23 Membrane lipid raft preparation by ultracentrifugation

Lysis buffer:
50 mM Hepes pH 7.4
100 mM NaCl
3% (v/v) Brij 58
1 mM PMSF
5 mM EDTA
1 mM sodium orthovanadate
50 mM NaF
10 mM sodium pyrophosphate

NME buffer:
25 mM MES
5 mM EDTA
150 mM NaCl

80%, 30% and 5% sucrose in NME buffer:
30% and 5% sucrose solutions were freshly prepared by dilution of 80% sucrose in NME buffer, stored at 4°C

Lipid raft preparation was performed as cold as possible:

- lysis of $1x10^7$ thymocytes in 500 µl lysis buffer followed by vortexing and storage on ice for 10 min
- mixing of lysate with 500 µl ice-cold 80% sucrose in NME buffer resulting in a 40% sucrose solution
- transfer of lysate into a cell homogenizer and performance of 10 regular thrusts
- transfer of lysate into ultracentrifugation tubes (SORVALL®PA THINWALL TUBE 4.4 ML) with pasteur pipettes
- overlay lysate with 2 ml ice-cold 30% sucrose in NME buffer followed by 1 ml ice-cold 5% sucrose in NME buffer
- centrifugation of sucrose gradient in an ultracentrifuge with TH-660 rotor at 270000 g (44000 rpm) for 20 h at 4°C without brake
- collection of 10 fractions (400 µl each) from top to bottom of the gradient

The proteins in the fractions were precipitated by the following procedure:

- addition of deoxycholate to samples in 1.5 ml reaction tubes to a final concentration of 0.02%
- 15 min incubation at RT
- addition of trichloroacetic acid (TCA), final concentration 6%
- 1 h incubation on ice
- centrifugation at 18620 g (14000 rpm in a table centrifuge) for 10 min at 4°C
  => discard the supernatant
- wash pellet with 200 µl ice-cold acetone
- 15 min incubation on ice
- centrifugation at 18620 g for 10 min at 4°C
  => discard the supernatant
- repeat washing procedure once
- dry protein pellet for 10 min at RT

Pellets were suspended in 42 µl MNE buffer and 14 µl 4 x Roti-Load were added. Boiling at 95°C for 5 min with shaking at 800 rpm was performed and protein samples were analyzed by western blot.

Lipid raft fractions were identified via the marker protein ganglioside GM1, which was detected with cholera toxin-horseradish-peroxidase fusion proteins. For this, 3 µl of each sucrose gradient fraction were spotted onto a nitrocellulose membrane, which was then dryed for 10 min at RT. Subsequently, the nitrocellulose membrane was blocked with 5% (w/v) milk in TBST at RT for 30 min with gentle shaking. Cholera toxin-horseradish-peroxidase fusion proteins diluted in 5% milk in TBST were applied overnight at 4°C with

gentle shaking. Membranes were washed three times with TBST for 10 min at RT and binding of cholera toxin to ganglioside GM1 was detected by ECL and exposure to X-ray film.

4.2.24 Anergy induction

Anergy was induced in isolated $CD4^+$ T cells with ionomycin according to the protocol used by Davidson et al. (Davidson, Schraven et al. 2007). $CD4^+$ T cells were stimulated with CD3 Ab (3 μg/ml; plate-bound) and CD28 Ab (1 μg/ml; soluble) for 48 h. Thereafter, cells were cultured in the presence of IL-2 (50 units/ml) for 72 h and anergy was induced by treatment of cells for 16 h with ionomycin (1 μM in DMSO). Control cultures were treated with the corresponding amount of DMSO only. Subsequently, cells were analyzed in proliferation assays or Fyn activity was assessed by *in vitro* kinase assays.

4.2.25 Proliferation assay

To analyze the proliferative capacity, $5x10^4$ $CD4^+$ T cells were cultured in 96 well plates in triplicates in supplemented RPMI 1640/10% FCS medium for 48 h. T cells were left untreated or stimulated with plate-bound CD3 Ab, CD3+CD28 Abs or with PMA/ionomycin in concentrations as indicated. After 48 h, cells were pulsed with 0.2 μCi [^{3}H]-thymidine for 12-16 h and [^{3}H]-thymidine incorporation into DNA was determined by liquid scintillation.

To assess the impact of the Src kinase inhibitor PP2 and the MEK inhibitors PD98059 and UO126 on proliferation, $1x10^5$ $CD4^+$ T cells from wt and myrPKB tg mice were cultured for 24 h in the presence or absence of plate-bound CD3 Ab and inhibitors. DNA synthesis was assessed by [^{3}H]-thymidine incorporation after 12-16 h.

4.2.26 Densitometric analysis

Densitometric analysis was performed by scanning X-ray films with an Epson Perfection 4990 Photo scanner followed by determination of the optical density of the bands with Kodak 1D 3.6 software.

5 Results

5.1 Cross-talk of PKB with the transcription factor NFAT

5.1.1 PKB rescues calcineurin/NFAT induced arrest of Rag expression and thymocyte development in ΔCam tg mice

Previous publication showed that TCR/CD3 stimulated myrPKB tg $CD4^+$ T cells exhibit reduced NFAT activation, although they are hyperproliferative. NFAT and myrPKB co-immunoprecipitated in wt and myrPKB tg T cells indicating that NFAT and PKB interact *in vivo* (Patra, Na et al. 2004). The cross-talk of myrPKB with NFAT during thymocyte development was analyzed in ΔCam tg mice, which express a constitutively active form of the serine threonine phosphatase calcineurin (ΔCam) leading to enhanced nuclear translocation and activity of NFAT. ΔCam induces a strong developmental arrest in thymocyte differentiation at the $CD25^+CD44^-$ double negative 3 (DN3) stage, since 90% of thymocytes in ΔCam tg mice are DN3 phenotype. This developmental block is rescued by co-expression of constitutively active myrPKB (Patra, Drewes et al. 2006), indicating that PKB signals can reverse or overcome ΔCam induced signaling events.

Signaling via the preTCR is needed for the transition of thymocytes from the DN3 to DN4 and double positive (DP) stage. Analysis of intracellular (ic) TCR β-chain expression showed a lack or strong reduction in TCR β-chain positive ΔCam tg DN3, DN4 and DP cells, but this was partially reversed by co-expression of active PKB. Rag proteins are mediating the rearrangement of TCR β-chains (Wilson, Held et al. 1994; Bassing, Swat et al. 2002) and Rag RNA and protein expression were strongly reduced in ΔCam tg thymocytes. Interestingly, co-expression of myrPKB rescued Rag expression and TCR β-chain rearrangement in ΔCam tg thymocytes (Patra, Drewes et al. 2006).

Because the nuclear localization of NFATc1 and NFATc3 were reduced in ΔCam/PKB tg DN thymocytes in comparison to ΔCam DN cells (Patra, Drewes et al. 2006), the question arose whether NFAT proteins are involved in the inhibition of *rag* expression. To test this hypothesis, EL4 cells were co-transfected with a ΔCam-expressing vector and a firefly luciferase reporter construct harboring nucleotide -251 to +147 of the murine Rag2 promoter. NFATc1, NFATc2 or vector control (vc) DNA was co-transfected and firefly luciferase activity was determined after stimulation of cells with PMA plus ionomycin. The Rag2 promoter was active in EL4 cells and NFATc1 or NFATc2 resulted in reduced Rag2 promoter activity. Thus, NFAT factors regulate Rag promoter activity *in vivo* and hyperactivity of NFAT in ΔCam DN3 cells could result in inhibition of *rag* and thus TCR β-chain expression. Reduction of NFAT

activity via myrPKB would enable optimal *rag* and ic TCR β-chain expression and, thereby, abrogate the differentiation block in ΔCam/PKB tg thymocytes.

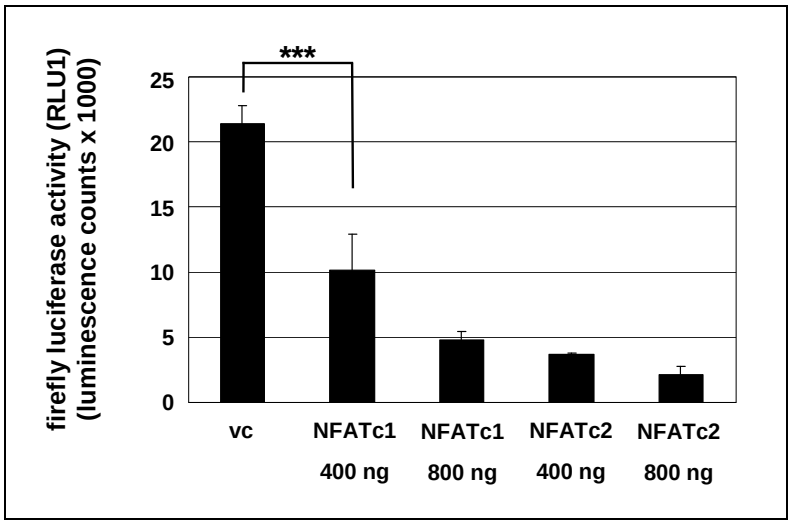

Figure 5.1 NFAT factors inhibit Rag2 promoter activity in EL4 cells (Patra, Drewes et al. 2006)
Transfection of EL4 cells was performed with a Rag2 promoter firefly luciferase reporter construct (50 ng), a vector coding for ΔCam (50 ng) and either empty vector DNA for control (vc) or NFATc1 or NFATc2 expression vectors in the given amounts. Cells were stimulated with PMA (100 ng/ml) and ionomycin (100 ng/ml) for 16-20 h and Rag2 promoter activity was assessed by measurement of luminescence generated by firefly luciferase (firefly luciferase activity: RLU1). Error bars show standard deviation of four samples of one experiment. Data were analyzed by student's t-test (*** $p<0.001$). Data are representative of 3 independent experiments.

5.1.2 MyrPKB inhibits NFAT activity in HEK 293T cells

NFAT is one of the major transcription factors involved in the activation of the IL-2 gene (Randak, Brabletz et al. 1990; Serfling, Berberich-Siebelt et al. 2000). To further substantiate the influence of PKB on NFAT activation, we analyzed the impact of myrPKB on NFATc1-induced activation of the IL-2 promoter. HEK 293T cells were transfected with NFATc1, myrPKB and a luciferase reporter construct harboring three copies of the NFAT/AP1 binding sequence (-286 to -257) of the human IL-2 gene linked to the -72 to +47 region of the human IL-2 promoter. IL-2 promoter activity was determined 6 h after stimulation of cells with PMA/ionomycin. As shown in Figure 5.2, NFATc1 induced IL-2 promoter activity and co-transfection of myrPKB resulted in a 69% reduction of IL-2 promoter activity. Thus, myrPKB inhibits NFATc1 activity in transfected HEK 293T cells.

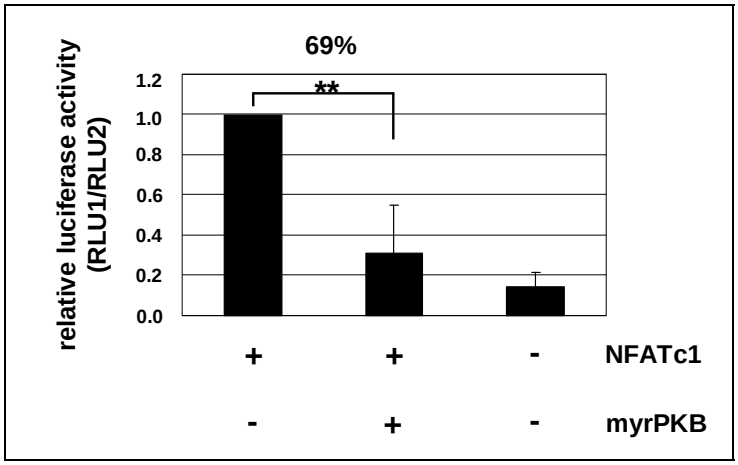

Figure 5.2 MyrPKB reduces NFATc1 activity in HEK 293T cells
HEK 293T cells were co-transfected with the IL-2 promoter firefly luciferase reporter construct (100 ng), NFATc1 (100 ng), myrPKB (75 ng) and Renilla luciferase construct (100 ng). The total amount of DNA in each transfection sample was compensated to 1575 ng with empty vector. Co-transfection of a Renilla luciferase construct was used to monitor transfection efficiency. After stimulation of cells with PMA (100 ng/ml) and ionomycin (747 ng/ml) for 6 h, IL-2 promoter activity was determined. Relative luciferase activity is given as firefly luciferase activity (RLU1) divided by renilla luciferase activity (RLU2) from 3 independent experiments. IL-2 promoter activation by NFATc1 was set as 1. Data were analyzed by student's t-test (** $p<0.01$).

5.1.3 MyrPKB enhances GSK3, PKA and Foxp3 mediated inhibition of NFAT activity

Protein kinase A (PKA) was shown to phosphorylate NFAT at S245, S269 and S294, priming for further phosphorylation of NFAT by GSK-3 at S241 and S290. These phosphorylation events lead to inactivation and cytoplasmic retention of NFAT (Sheridan, Heist et al. 2002).

We analyzed the effects of PKA and GSK-3 alone and in combination with myrPKB on NFAT activation, again using IL-2 promoter driven luciferase activity as readout. For this, HEK 293T cells were transfected with the indicated expression vectors and IL-2 promoter activity was assessed (Figure 5.3). Transfection of either myrPKB, GSK-3 or PKA alone reduced NFAT and IL-2 promoter activity. The combination of myrPKB with GSK-3 or PKA or both kinases led to a stronger reduction of IL-2 promoter activity than transfection of the single components with myrPKB/GSK-3/PKA co-transfections being most inhibitory on NFAT activation. Thus, myrPKB, GSK-3 and/or PKA expression in HEK 293T cells results in an additive reduction of NFAT activity, suggesting that elevated PKB signals provide additional inhibitory signals for inhibition of NFAT activity.

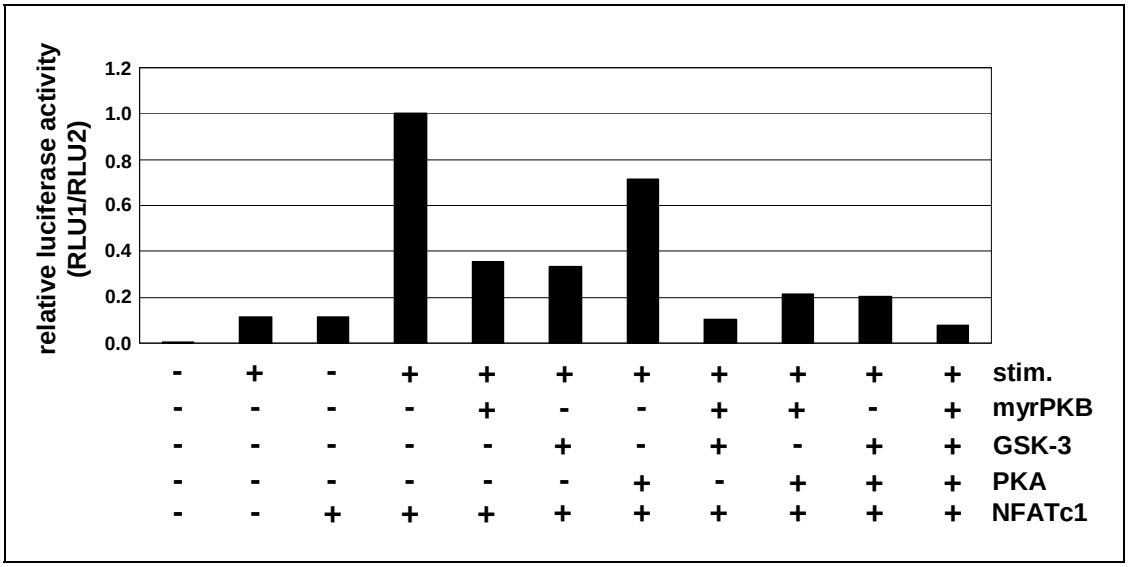

Figure 5.3 MyrPKB, GSK-3 and PKA reduce NFATc1 induced IL-2 promoter activity in HEK 293T cells
HEK 293T cells were transfected with the IL-2 promoter firefly luciferase reporter construct (100 ng), NFATc1 (100 ng), myrPKB (50 ng), GSK-3 (100 ng) and PKA (100 ng) alone or in combination. Co-transfection of a Renilla luciferase construct (30 ng) was used to monitor transfection efficiency. The total amount of DNA in each transfection sample was compensated to 1000 ng with empty DNA vector. Cells were left untreated or stimulated with PMA (100 ng/ml) plus ionomycin (747 ng/ml) for 6 h. Thereafter, IL-2 promoter activity was determined. Relative luciferase activity is given as firefly luciferase activity (RLU1) divided by renilla luciferase activity (RLU2). IL-2 promoter activation by NFATc1 in stimulated cells was set as 1.

The transcription factor Foxp3 determinates the phenotype of regulatory T cells and is involved in the shut down of IL-2 expression in Treg cells (Bettelli, Dastrange et al. 2005; Wu, Borde et al. 2006). We analyzed the effect of myrPKB on Foxp3 regulated NFAT activation. In transfected HEK 293T cells IL-2 promoter activity was reduced by Foxp3 and myrPKB alone (Figure 5.4), and the combination of Foxp3 and myrPKB resulted in a stronger reduction of IL-2 promoter activity induced by NFATc1. Altogether, these data show that myrPKB signals alone inhibit NFAT activity and enhance the inhibitory effects of PKA, GSK-3 or Foxp3 on NFAT activation.

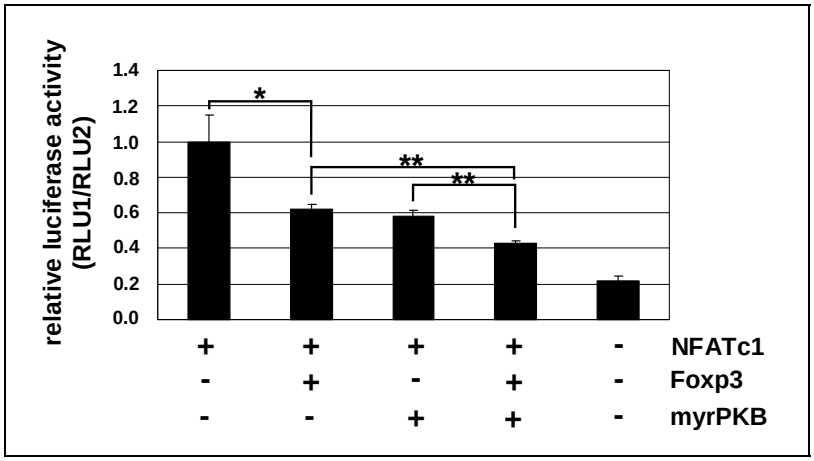

Figure 5.4 MyrPKB and Foxp3 reduce NFAT induced IL-2 promoter activity in HEK 293T cells
HEK 293T cells were co-transfected with the IL-2 promoter firefly luciferase reporter construct (100 ng), NFATc1 (100 ng), Foxp3 (1200ng), myrPKB (75 ng) and Renilla luciferase construct (100 ng). The total amount of DNA in each transfection sample was compensated to 1575 ng with empty DNA vector, if necessary. Co-transfection of a Renilla luciferase construct was used to monitor transfection efficiency. After stimulation of cells with PMA (100 ng/ml) and ionomycin (747 ng/ml) for 6 h, IL-2 promoter activity was determined. Relative luciferase activity is given as firefly luciferase activity (RLU1) divided by renilla luciferase activity (RLU2). IL-2 promoter activation by NFATc1 was set as 1. Error bars show standard deviation of three samples of one experiment. Data were analyzed by student's t-test (* $p<0.02$; ** $p<0.01$).

5.1.4 PKB phosphorylates NFAT *in vitro*

Since above data showed a strong effect of PKB signals on NFAT activation and PKB and NFAT were shown to co-immunoprecipitate in T cells (Patra, Na et al. 2004), we speculated that NFAT could be a direct target of PKB. Therefore, several GST-NFAT fusion DNA constructs were generated harboring amino acids 177-261, 262-336 and 177-336 of the regulatory domain of human NFATc1A with a GST tag fused N-terminally. Expression vectors were expressed in bacteria, and GST-NFATc1A fusion proteins were purified via glutathione columns. Additionally, several NFATc1A mutants were produced, in which potential PKB phosphorylation sites were eliminated by exchange of serine or threonine to alanine, to identify possible PKB phosphorylation sites in NFATc1A *in vitro* (see Figure 5.5). Mut A, B and W were chosen because of sequence similarity to the canonical PKB phosphorylation site. S245 is localized in the SPRASVTEES (mut D) motif, which has sequence similarity to the calcineurin binding site SPRIEIT of NFAT. Although it is not part of a PKB phosphorylation site, it was analyzed, since a mass spectrometry experiment suggested S245 as a possible PKB phosphorylation site. Additionally, T247 and S250 present in the SPRASVTEES (mut D) motif were chosen for mutation. S294, T296 and S299 in the sequence motif SPRVSVTDDS (mut C) were also mutated to alanine. T339 and S403, which are localized in canonical PKB sites indicated by black rectangles, were not analyzed, because they are positioned outside the initial GST-NFATc1A fusion proteins, which were phosphorylated by PKB.

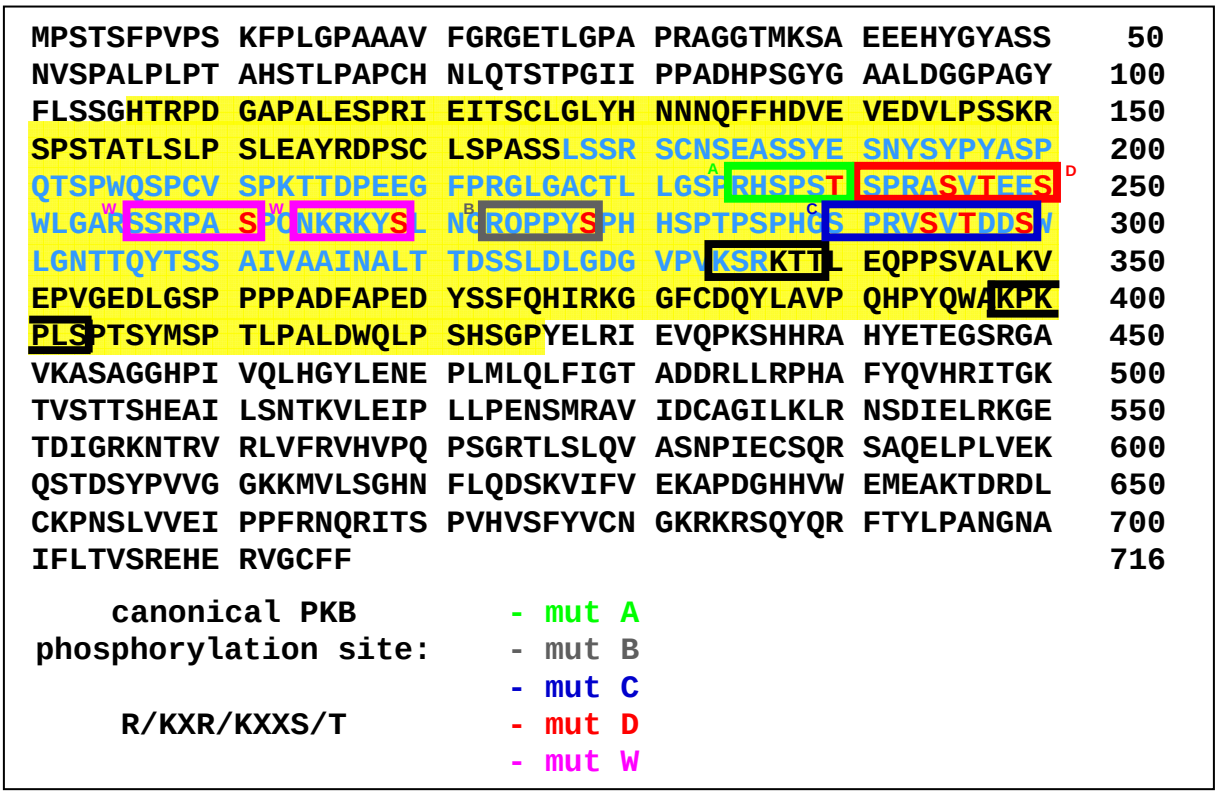

Figure 5.5 Amino acid sequence of human NFATc1A
The regulatory domain of human NFATc1A is underlaid yellow and amino acids 177-336, which are included in the GST-fusion proteins, are shown in blue. The colored rectangles mark sequences with anticipated PKB phosphorylation sites and the NFATc1A mutants A, D, W, B and C, in which S/T residues were mutated to A (indicated by red color). The black rectangles mark canonical PKB phosphorylation sites (T339 and S403).

Phosphorylation of GST-NFATc1A fusion proteins by PKB was analyzed by *in vitro* kinase assays (IVKs). Initial IVKs performed in the lab of U. Bommhardt (Figure 5.6) with GST-NFATc1A fusion proteins harboring amino acids 177-261, 262-336 and 177-336 of the regulatory domain of hNFATc1A showed that all three GST-NFATc1A fusion proteins were phosphorylated by PKB *in vitro*. Thus, potential PKB phosphorylation sites are present in the aa 177-261 as well as aa 262-336 part of the NFATc1A regulatory domain.

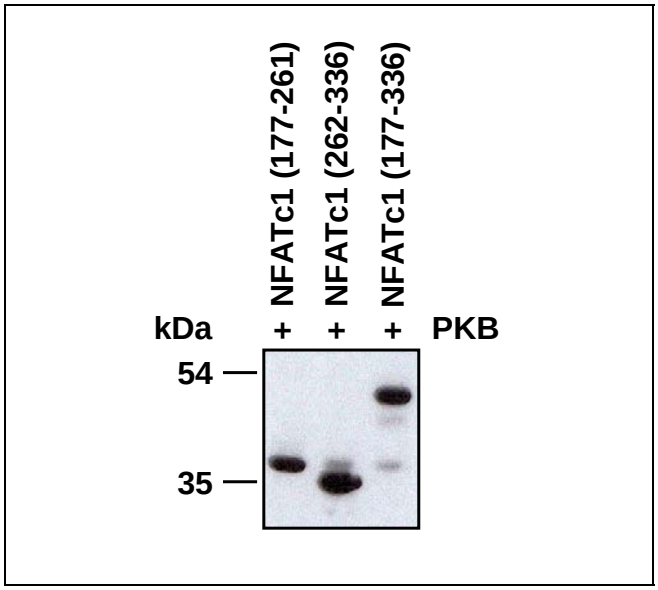

Figure 5.6 PKB phosphorylates NFATc1A within the regulatory domain *in vitro*
The indicated GST-NFATc1A fusion proteins were analyzed for phosphorylation by PKB by *in vitro* kinase assays. 5 μg of GST-NFATc1A fusion protein of interest were incubated at 37°C for 30 min in kinase reaction buffer containing 50 ng recombinat PKB and 10 μCi [γ-^{32}P]-ATP. The reaction was terminated by addition of 1/4 vol 4 x Roti-Load followed by boiling at 95°C for 5 min. Samples were run on a SDS-PAGE gel, the gel was dried and analyzed by autoradiography.

To determine the specific PKB sites within the NFATc1A regulatory domain, we next performed IVKs with various NFAT mutants (Figure 5.7). The amount of NFATc1A substrate used in each reaction was controlled by coomassie staining of the gel. Phosphorylation of the known PKB substrate GSK-3 was used as positive control for PKB activity. GST was not phosphorylated by PKB, indicating that phosphorylation of GST-NFATc1A fusion proteins was not localized in their GST part. A sample without protein was included, and no background signals were produced by the reaction mixture itself. The wt GST-NFATc1A fusion protein (aa 177-336) was phosphorylated in the presence, but not absence of PKB. The combined mutation of the serines and threonines in the sequences of mut W, A and B to alanine, which are indicated by red color in Figure 5.5, had no effect on NFAT phosphorylation (Figure 5.7 A). The mutation of S245, T247 and S250 to alanine in the sequence of mut D in addition to the mutations in the sequences of mut W, A and B (GST-NFATc1A fusion protein labeled mut W + A + B + D) caused a reduced phosphorylation. A drastic reduction of NFAT phosphorylation was found when S294, T296 and S299 in the sequence of mut C were mutated to alanine in addition to all the mutations inserted in the sequences of mut W, A, B and D (GST-NFATc1A fusion protein labeled mut W + A + B + D + C) (Figure 5.7 A and B, see red rectangle). This suggested that PKB phosphorylation sites are positioned within the mut C and mut D sequences of the NFATc1A regulatory domain.

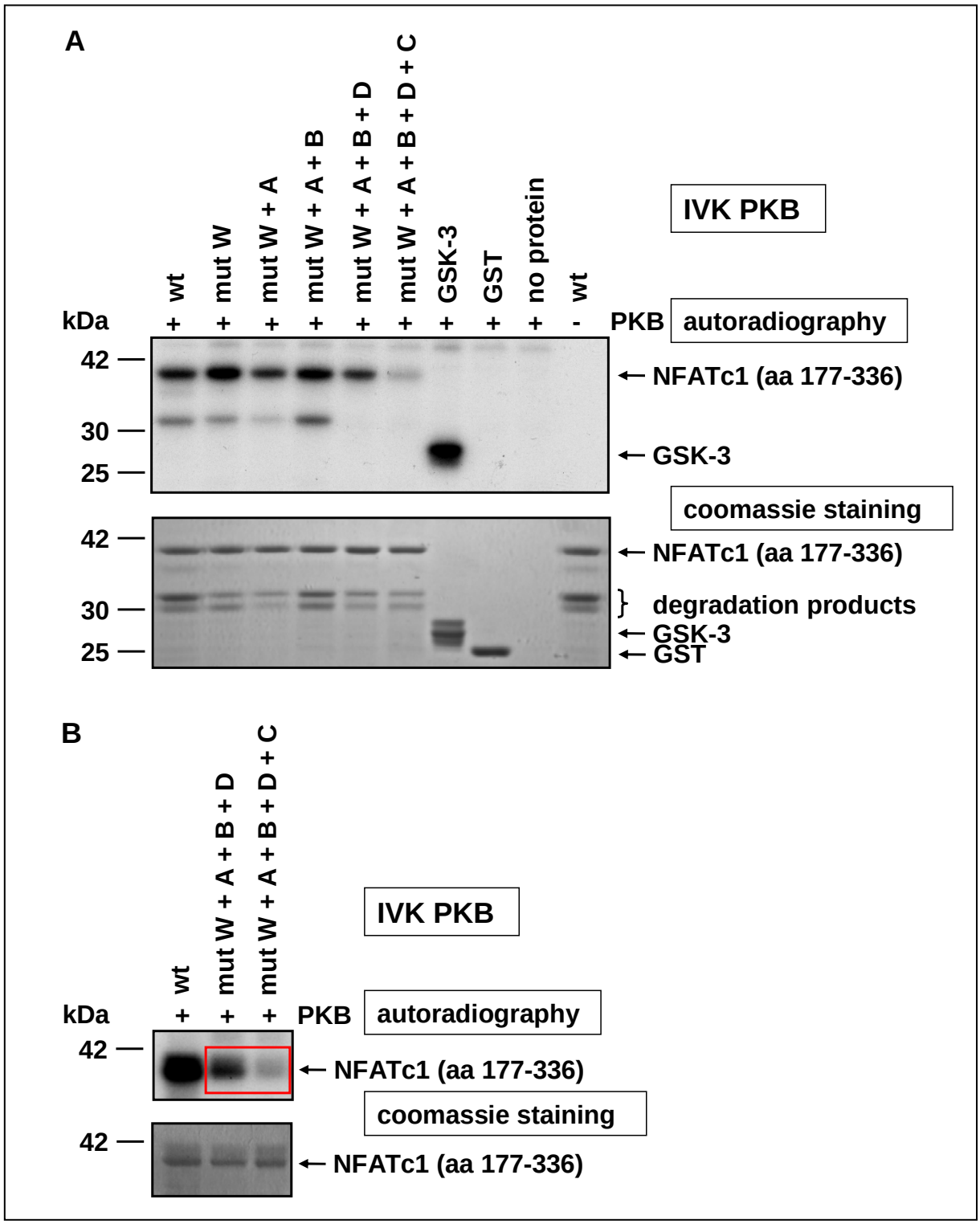

Figure 5.7 The combination of mut W, A and B with mut D or with mut D + C reduces the phosphorylation of the NFATc1A regulatory domain by PKB *in vitro*
A) Wild type (wt) GST-NFATc1A fusion protein (aa 177-336) and the indicated GST-NFATc1A mutants, GSK-3 and GST were used in PKB IVKs. Samples were run on a SDS-PAGE gel and analyzed by autoradiography. The amount of substrate was controlled by coomassie staining of the gel.
B) Wild type (wt) GST-NFATc1A fusion protein (aa 177-336) and the indicated GST-NFATc1A mutants were used in PKB IVKs performed as described under A.

The results shown in Figure 5.7 suggested phosphorylation of NFAT by recombinant PKB at serines/threonines present in the mut D and mut C sequences, although these sequences do

not contain a canonical PKB phosphorylation motif. Since mut D contains 3 mutations, i.e. S245, T247 and S250, and mut C contains mutations to A at S294, T296 and S299, we wanted to identify the exact site(s) of phosphorylation. Therefore, serine and threonine sites in the mut D and mut C regions were mutated one by another to A without the additional mutations in the mut W, A or B regions. However, analysis of these GST-NFAT mutants in IVKs showed similar phosphorylation of all proteins. Neither 3 mutations in the D region alone nor mutations within regions C + D alone abrogated PKB phosphorylation (Figure 5.8). Thus, none of the sites examined seems to be a PKB phosphorylation site *in vitro*. This result was unexpected and the reduction of phosphorylation by insertion of mut D and C in addition to the mutations W, A and B seen in Figure 5.7 seems to be caused by an interplay of all the mutations inserted. Mut C and D could change the folding of the GST-NFAT construct in such a way that mut W, A and/or B would have an impact on the phosphorylation by PKB, or mut W, A and/or B could change the folding that mut C and D would alter phosphorylation by PKB.

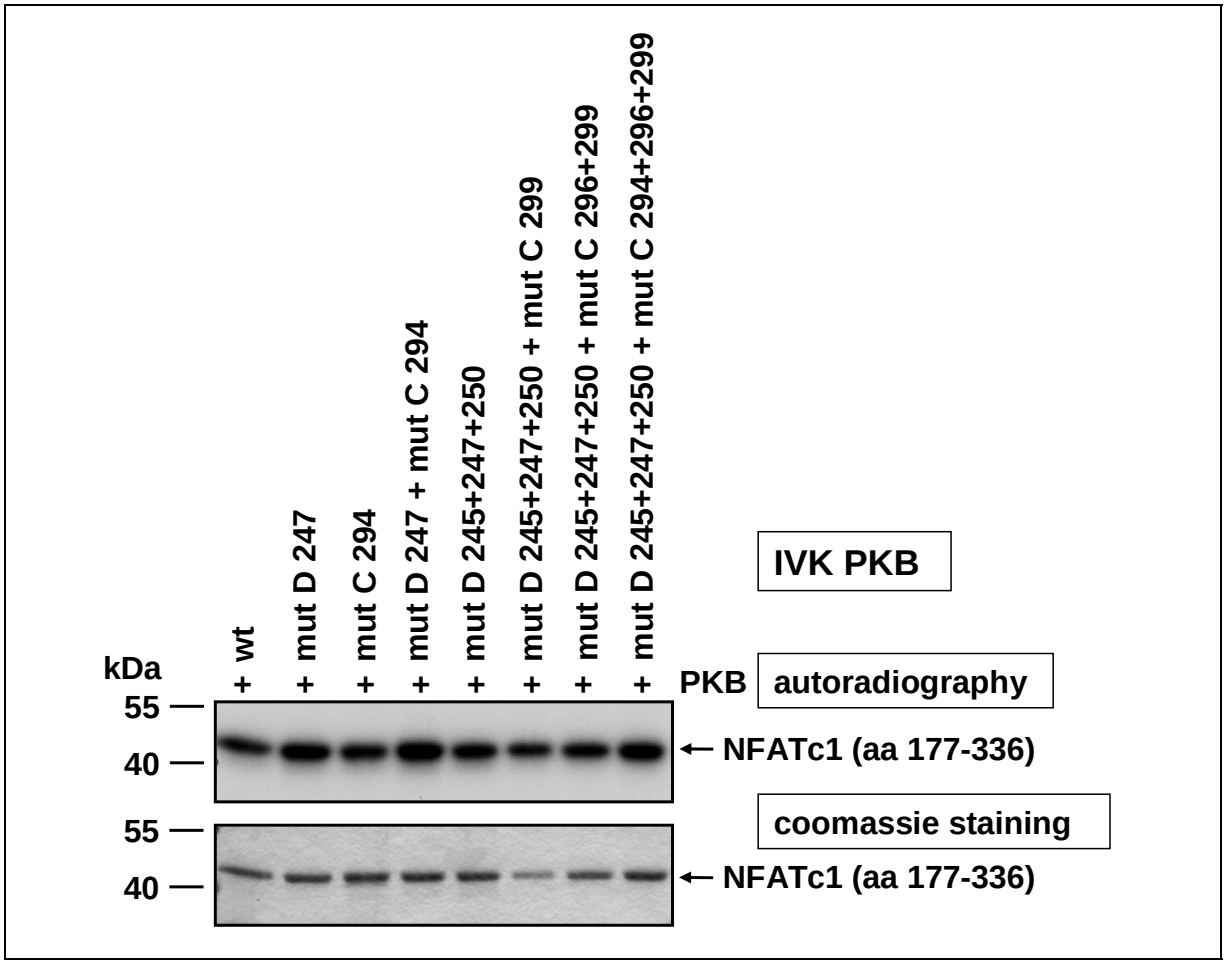

Figure 5.8 S245, T247 and S250 within mut D alone and S294, T296 and S299 within mut C in the NFATc1A regulatory domain are not phosphorylated by PKB *in vitro*
Wild type (wt) GST-NFATc1A fusion protein (aa 177-336) and the indicated GST-NFATc1A mutants were used in PKB IVKs. Samples were run on a SDS-PAGE gel and analyzed by autoradiography. The amount of substrate was controlled by coomassie staining of the gel.

The activity of NFATc1A with mutation of serines and threonines in the regions of mut D and mut C was also analyzed via luciferase assays, but no major difference was detected comparing wt and mutant NFAT proteins (data not shown). Mutations T339 or S403, localized in canonical PKB motifs, also had no effect on NFAT activity.

Taken together, these results suggest that only the complex interplay of mut W, A, B, D and C in the regulatory domain of NFAT can cause a reduction of NFAT phosphorylation by PKB *in vitro*. Modification of NFAT activity *in vivo* by direct phosphorylation of NFAT by PKB may thus be dependent on the interplay and de/phosphorylation status of several residues within the regulatory domain.

5.2 Cross-talk of PKB with the Src kinase Fyn

5.2.1 MyrPKB tg CD4$^+$ T cells are less sensitive to Src kinase and MEK inhibitors

MyrPKB tg thymocytes show enhanced proliferation after TCR/CD3 stimulation and are less sensible to the Src kinase inhibitor PP1 and the MEK inhibitor PD98059 in comparison to wt cells (Na, Patra et al. 2003). Here we analyzed the effect of these inhibitors on the proliferation of peripheral myrPKB tg CD4$^+$ T cells. Wt and myrPKB tg CD4$^+$ T cells were stimulated with immobilized CD3 Ab for 24 h in the presence or absence of the indicated inhibitors and proliferation was measured by [^{3}H]-thymidine incorporation.

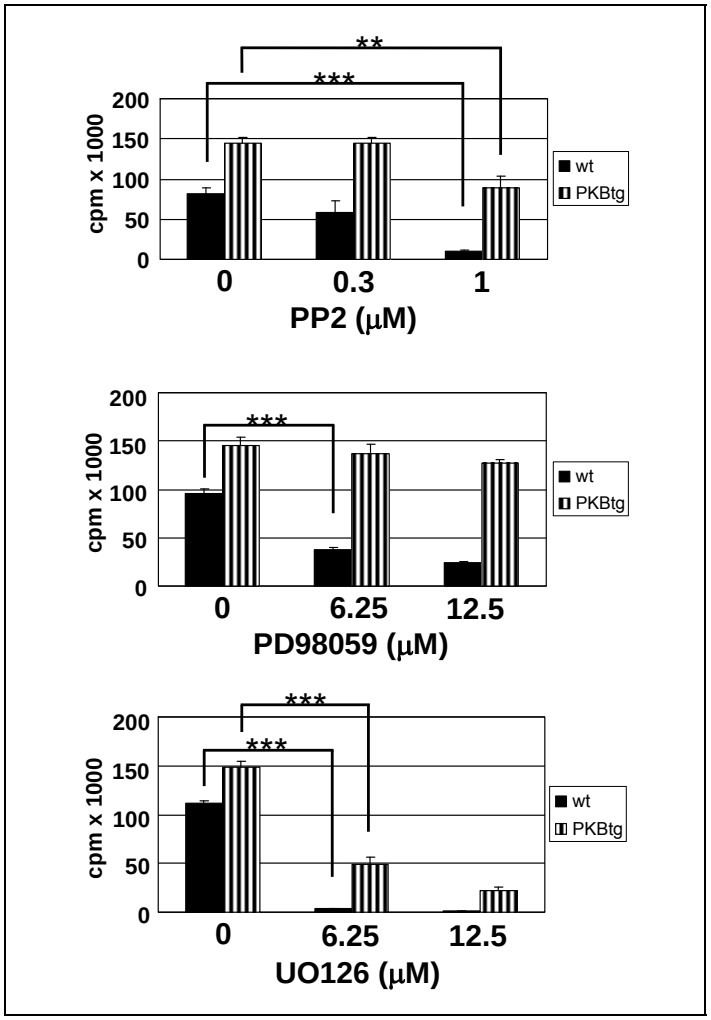

Figure 5.9 Proliferation of myrPKB tg CD4$^+$ T cells is less affected by Src kinase inhibitor PP2 and MEK inhibitors PD98059 and UO126
CD4$^+$ T cells from wt and myrPKB tg mice were stimulated with immobilized CD3 Ab (3 μg/ml) in the presence or absence of PP2, PD98059 and UO126 in concentrations as indicated. Proliferation was measured by [^{3}H]-thymidine incorporation after 24 h and is given as counts per minute (cpm). Error bars show standard deviation of triplicates. Significance was determined by student's t-test (** p<0.01; *** p<0.001).

MyrPKB tg CD4$^+$ T cells showed enhanced proliferation after CD3 Ab stimulation in comparison to wt cells. In this experiment, application of 1 μM PP2 caused a 88% reduction of proliferation of wt CD4$^+$ T cells, whereas proliferation of myrPKB tg cells was only reduced

by 39%. 6.25 μM PD98059 reduced proliferation of wt CD4$^+$ T cells by 61% but of myrPKBtg cells by 6% only. Likewise, treatment with 6.25 μM UO126 almost totally ablated proliferation of wt CD4$^+$ T cells, but proliferation of myrPKB tg cells still occurred quite strongly. Since other experiments showed comparable results, activation of myrPKB tg CD4$^+$ T cells is less affected by Src kinase inhibitor PP2 as well as MEK inhibitors PD98059 and UO126 (Figure 5.9).

5.2.2 Enhanced Erk phosphorylation but similar phosphorylation of activatory tyrosines of Fyn and Lck in activated myrPKB tg CD4$^+$ T cells

The reduced sensibility of myrPKB tg CD4$^+$ T cells to Src kinase inhibitor application indicated that myrPKB could have an impact on Fyn and/or Lck activity. Indeed, enhanced and prolonged Lck activity and Erk phosphorylation were previously detected in myrPKB tg thymocytes (Na, Patra et al. 2003). We, therefore, analyzed the phosphorylation of Fyn at Y417, of Lck at Y394, of Erk1 (p44) at T203/Y205 and of Erk2 (p42) at T183/Y185 (the activatory phosphorylation sites of Fyn, Lck and Erk). For CD3+CD4 Ab-stimulated CD4$^+$ T cells from wt and myrPKB tg mice no major differences in Fyn Y417 and Lck Y394 phosphorylation were detected by western blot analysis. However, enhanced phosphorylation of Fyn and Lck was obvious in unstimulated myrPKB tg CD4$^+$ T cells. In addition, Erk phosphorylation was strongly enhanced in CD3+CD4 Ab-stimulated myrPKB tg cells in comparison to wt CD4$^+$ cells (Figure 5.10).

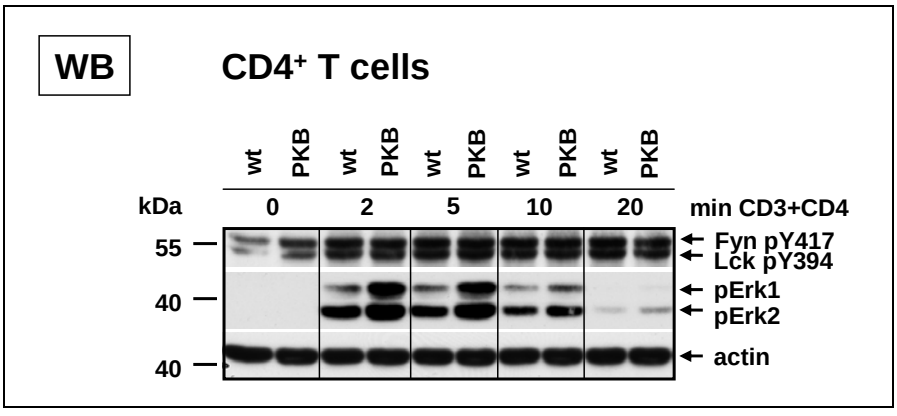

Figure 5.10 Enhanced Erk phosphorylation in myrPKB tg CD4$^+$ T cells
CD4$^+$ T cells from wt and myrPKB tg mice were stimulated with biotin-CD3 Ab (5 μg/ml) and biotin-CD4 Ab (5 μg/ml) plus streptavidin (20 μg/ml) for the indicated time period at 37°C. Expression/phosphorylation of the indicated proteins was analyzed by western blot. Actin expression was used as control for protein loading.

5.2.3 Fyn is hyperactive in myrPKB tg CD4$^+$ T cells and thymocytes

The inhibitor and western blot studies suggested that PKB influences Erk activation, which could be linked to altered Fyn/Lck activity which in a western blot analysis became apparent in unstimulated cells. PKB could either directly act on Fyn and/or Lck or indirectly on Lck via

altered Fyn activity. Since Fyn but not Lck harbors canonical PKB phosphorylation sites, we concentrated on Fyn as a potential novel substrate of PKB. For this, Fyn was immunoprecipitated from unstimulated wt and myrPKB tg CD4$^+$ T cells and IVKs were performed with enolase as a substrate for Fyn.

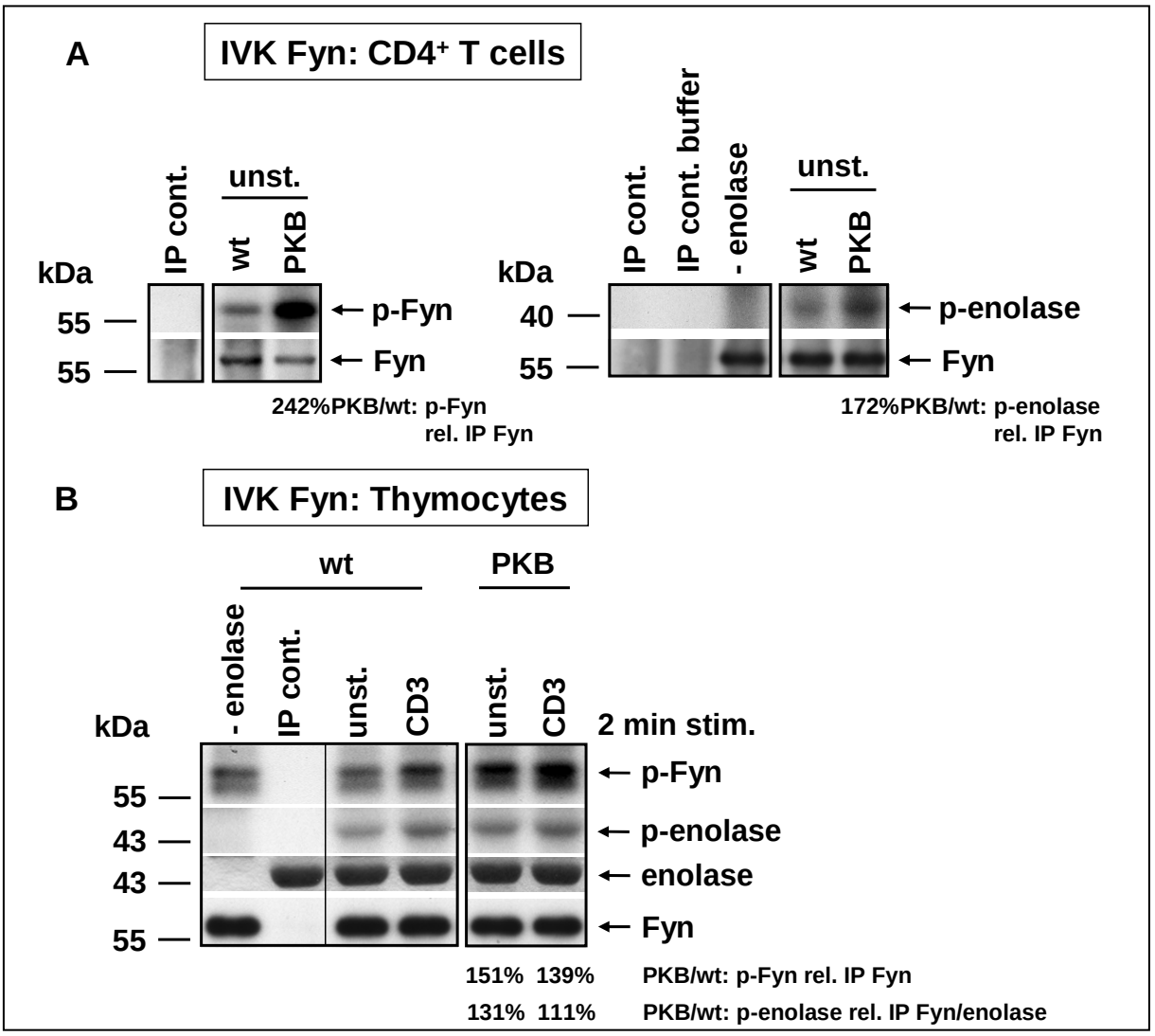

Figure 5.11 Fyn is hyperactive in myrPKB tg CD4$^+$ T cells and thymocytes
A) Unstimulated CD4$^+$ T cells from wt and myrPKB tg mice kept on ice were lysed, Fyn was immunoprecipitated and its activity was assessed by IVK. Fyn autophosphorylation (left figure) and enolase transphosphorylation (right figure) were detected by autoradiography. The amount of Fyn immunoprecipitated was monitored by western blot analysis (bottom-line). IP cont.: specific immunoprecipitation was controlled with mouse anti-rat IgG Ab; IP cont. buffer: mouse anti-rat IgG Ab was incubated with lysis buffer only. Bands were quantified by densitometric analysis and the amounts of phosphorylated Fyn and enolase were normalized to the amounts of Fyn immunoprecipitated (p-Fyn rel. IP Fyn; p-enolase rel. IP Fyn) and are given in percentage for myrPKB tg relative to wt cells.
B) Thymocytes from wt and myrPKB tg mice were left untreated or stimulated with biotin-CD3 Ab (30 μg/ml) plus streptavidin (42 μg/ml) for 2 min at 37°C. Fyn activity was assessed by IVKs. Fyn autophosphorylation and enolase transphosphorylation were detected by autoradiography. The substrate enolase was visualized by coomassie staining and the amount of Fyn immunoprecipitated was monitored by western blot (bottom-line). Specific immunoprecipitation was controlled with mouse anti-rat IgG Ab (IP cont.). Numbers give the amounts of p-Fyn normalized to the amounts of Fyn immunoprecipitated (p-Fyn rel. IP Fyn) and of p-enolase normalized to the amounts of Fyn immunoprecipitated and the total amounts of enolase (p-enolase rel. IP Fyn/enolase) in percentage for myrPKB tg relative to wt cells.

Enhanced Fyn autophosphorylation and enolase transphosphorylation were detected in unstimulated myrPKB tg $CD4^+$ T cells (Figure 5.11 A). Fyn auto- and transphosphorylation activity were also enhanced in unstimulated and CD3 Ab-stimulated myrPKB tg thymocytes in comparison to wt thymocytes (Figure 5.11 B). These experiments show that Fyn is hyperactive in myrPKB tg $CD4^+$ T cells and thymocytes.

5.2.4 Increased Fyn activity in myrPKB tg cells does not lead to increased phosphorylation of PAG at Y314

Tyrosine 314 of PAG is phosphorylated by Fyn and in the phosphorylated state functions as anchor for the recruitment of Csk to PAG (Brdicka, Pavlistova et al. 2000; Yasuda, Nagafuku et al. 2002; Filby, Seddon et al. 2007). We next analyzed whether enhanced Fyn activity in myrPKB tg $CD4^+$ T cells and thymocytes resulted in increased phosphorylation of PAG at Y314. IVKs were performed to assess Fyn activity and western blot analysis to assess PAG phosphorylation at Y314 from the same samples. Wt and myrPKB tg $CD4^+$ T cells were stimulated with immobilized CD3 Ab (2 μg/ml) or CD3+CD28 Abs (2/5 μg/ml). As shown in Figure 5.12 A, Fyn transphosphorylation activity on enolase in myrPKB tg $CD4^+$ T cells was the highest 1 h after stimulation and reduced at 4 h, but still higher than in unstimulated cells. No enhanced Fyn activity was detected in wt $CD4^+$ T cells 1 h after stimulation, and after 4 h Fyn activity was lower than in unstimulated cells. Thus, Fyn activity was increased in myrPKB tg $CD4^+$ T cells in comparison to wt $CD4^+$ T cells. However, despite increased Fyn activity phosphorylation of PAG at Y314 was similar or even reduced in myrPKB tg $CD4^+$ T cells in comparison to wt $CD4^+$ T cells. This effect was most obvious at 4 h CD3 Ab stimulation (indicated by red rectangles in Figure 5.12 A). No major differences were found between CD3 Ab and CD3+CD28 Abs in wt and myrPKB tg cells for these time points.

Western blot analysis of wt and myrPKB tg thymocytes showed similar PAG phosphorylation at Y314 in the unstimulated state (Figure 5.12 B) and CD3 Ab stimulation led to PAG Y314 dephosphorylation with similar kinetics in wt and myrPKB tg thymocytes. Altogether, these data show that myrPKB tg thymocytes and $CD4^+$ T cells reveal similar or even less PAG phosphorylation at Y314 despite increased Fyn activity.

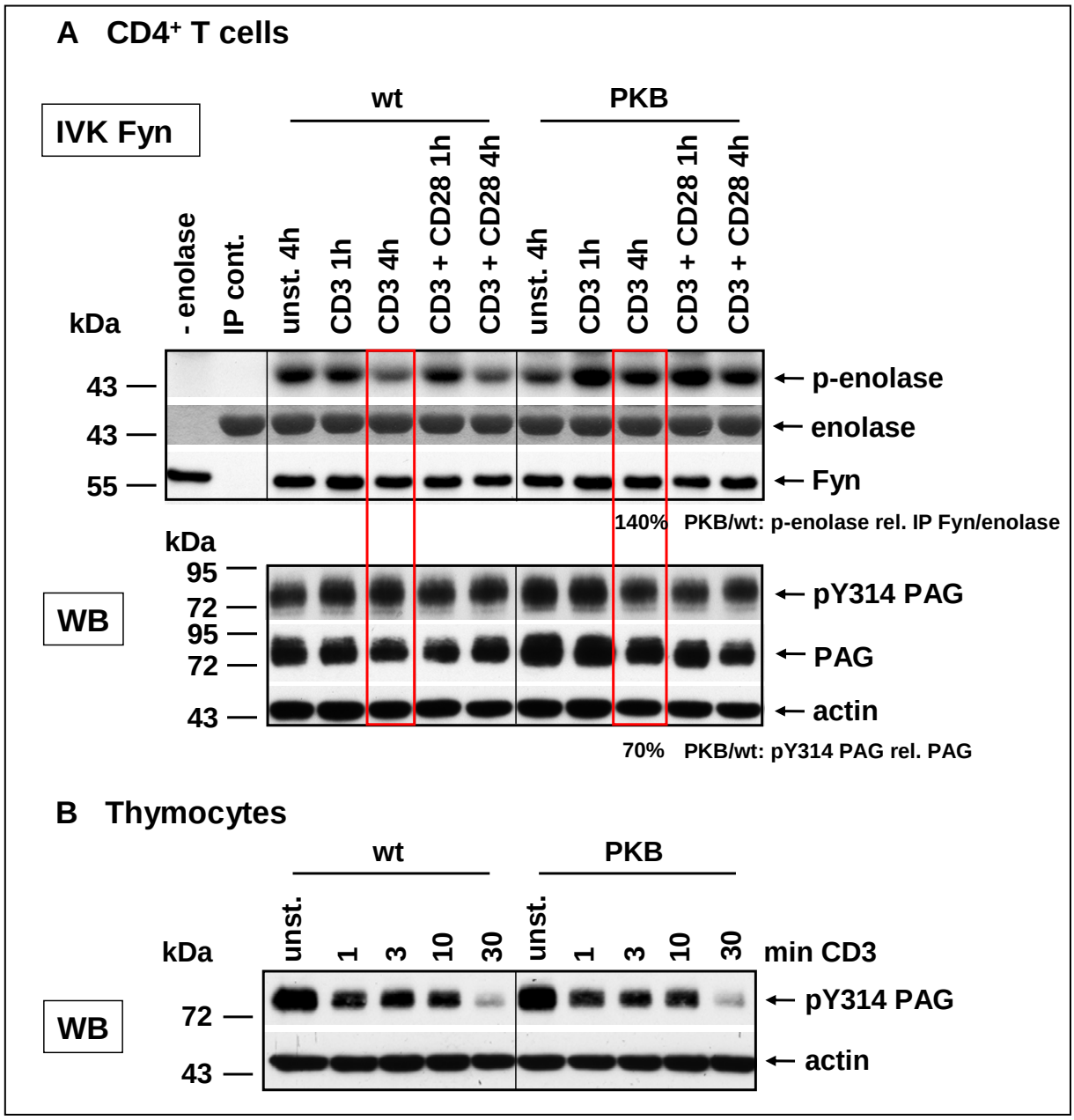

Figure 5.12 PAG phosphorylation at Y314 is not enhanced in myrPKB tg cells despite increased Fyn activity

A) CD4$^+$ T cells from wt and myrPKB tg mice were stimulated with immobilized CD3 Ab (2 μg/ml) or CD3+CD28 Abs (2/5 μg/ml) for the indicated time period at 37°C. Cells were lysed, Fyn was immunoprecipitated and its activity was assessed by IVK. The substrate enolase was visualized by coomassie staining of the gel and the amount of Fyn immunoprecipitated was monitored by western blot analysis (bottom-line). Mouse anti-rat IgG Ab was used for control immunoprecipitation (IP cont.). pY314 PAG and total PAG were determined by western blot and actin was used as protein loading control. The amounts of p-enolase normalized to the amounts of Fyn immunoprecipitated and the total amounts of enolase (p-enolase rel. IP Fyn/enolase) are given in percentage for myrPKB tg cells relative to wt cells as well as the amounts of pY314 PAG normalized to the amounts of total PAG (pY314 PAG rel. PAG) of myrPKB tg relative to wt cells.

B) Thymocytes from wt and myrPKB tg mice were stimulated with biotin-CD3 Ab (30 μg/ml) plus streptavidin (42 μg/ml) for the indicated time period at 37°C. Protein extracts were analyzed by western blot for PAG phosphorylation with an antibody specific for pY314. Actin was used as protein loading control.

5.2.5 Enhanced Fyn activity in myrPKB tg CD4$^+$ T cells does not result in increased binding of Csk to PAG

IVKs of Fyn from wt and myrPKB tg CD4$^+$ T cells showed that Fyn autophosphorylation and activity were increased in unstimulated and CD3 Ab-stimulated myrPKB tg CD4$^+$ T cells (Figure 5.11 A and Figure 5.12 A). Because phosphorylated Y314 of PAG is the anchor, which recruits Csk to PAG, and Y314 phosphorylation of PAG was found to be similar in myrPKB tg CD4$^+$ T cells despite Fyn hyperactivity, the amount of Csk bound to PAG was determined. As shown in Figure 5.13 A, untreated and CD3 Ab-stimulated myrPKB tg CD4$^+$ T cells showed enhanced Fyn auto- and transphosphorylation activity as seen before. The amount of Csk co-immunoprecipitated with PAG was slightly reduced in myrPKB tg in comparison to wt cells (Figure 5.13 B). Therefore, the increased Fyn activity in myrPKB tg cells does not correlate with a proportional increase of Csk association to PAG.

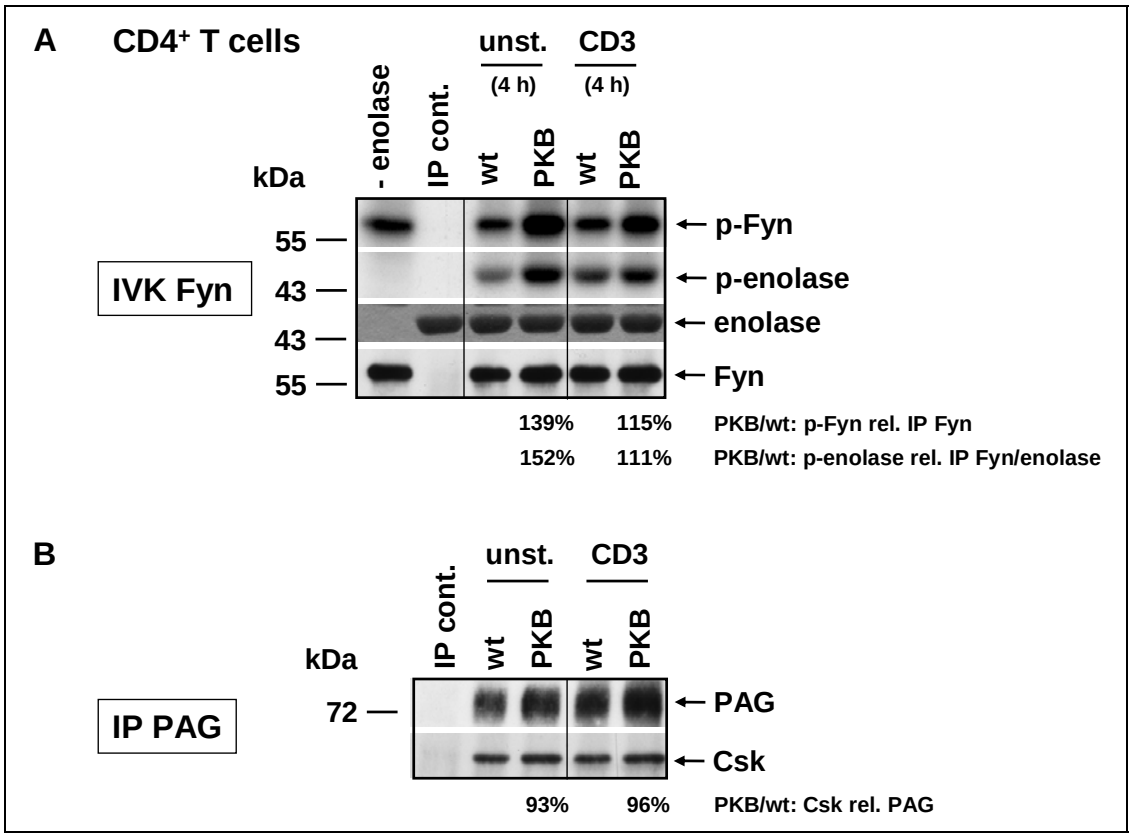

Figure 5.13 Similar amounts of Csk bind to PAG in wt and myrPKB tg CD4$^+$ T cells
A) CD4$^+$ T cells from wt and myrPKB tg mice were left untreated or stimulated with immobilized CD3 Ab (2 μg/ml) for 4 h at 37°C. Cells were lysed, Fyn was immunoprecipitated and its activity was assessed by IVK. The substrate enolase was visualized by coomassie staining and the amount of Fyn immunoprecipitated was monitored by western blot (bottom-line). Mouse anti-rat IgG Ab was used for control immunoprecipitation (IP cont.).The amounts of p-Fyn normalized to the amounts of Fyn immunoprecipitated (p-Fyn rel. IP Fyn) and the amounts of p-enolase normalized to the amounts of Fyn immunoprecipitated and the total amounts of enolase (p-enolase rel. IP Fyn/enolase) are given in percentage for myrPKB tg relative to wt cells.
B) PAG was immunoprecipitated from the same cell lysates and the amount of associated Csk was detected by western blot. Control immunoprecipitation (IP cont.) was performed with rabbit IgG control Ab. PAG and Csk bands were densitometrically analyzed and the amounts of Csk co-immunoprecipitated relative to the amounts of PAG precipitated (Csk rel. PAG) are given in percentage for myrPKB tg relative to wt cells.

5.2.6 Tyrosine phosphatase activity is inhibited at 4°C

The above data raised the question of the mechanism(s) for the discrepancy between Fyn hyperactivity and the lack of a concomitant increase of PAG Y314 phosphorylation and Csk association in myrPKB tg cells. One possibility to consider is PKB mediated increase in tyrosine phosphatase activity, because the phosphorylation status of PAG at Y314 is caused by the reaction equilibrium between Fyn that phosphorylates PAG and a so far unknown phosphatase that dephosphorylates PAG at this site. We, therefore, performed a western blot analysis of thymocytes at 4°C or 37°C. Increased global tyrosine phosphorylation was observed at 4°C compared to 37°C for unstimulated as well as CD3 Ab-stimulated cells (Figure 5.14), indicating that tyrosine phosphatase activity is reduced at 4°C but not so kinase activity.

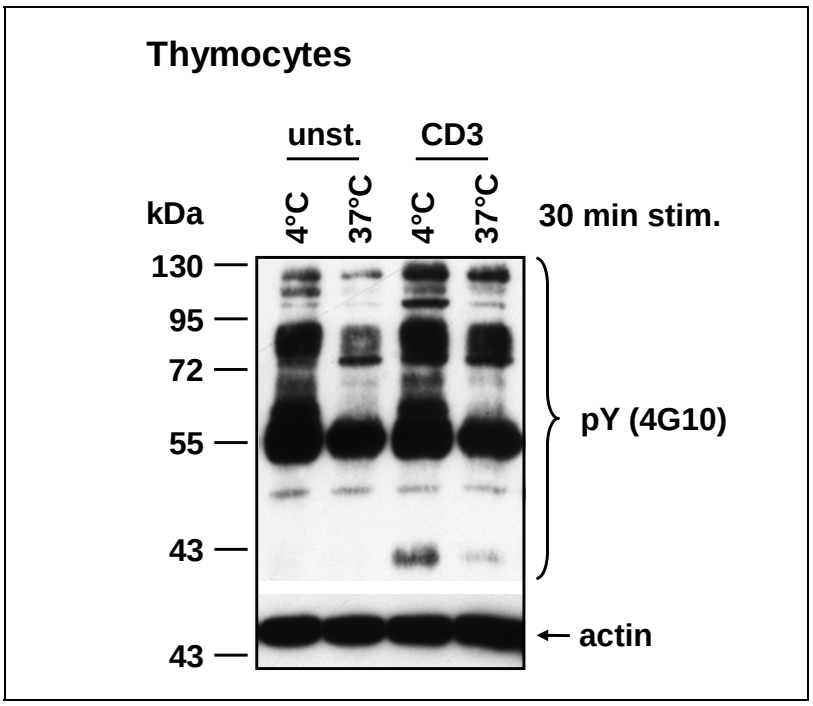

Figure 5.14 Thymocytes show decreased tyrosine phosphatase activity at 4°C
Thymocytes from wt mice were left unstimulated or stimulated with biotin-CD3 Ab (30 μg/ml) plus streptavidin (42 μg/ml) for 30 min at 4°C or 37°C. Cells were lysed and protein extracts were analyzed by western blot for global tyrosine phosphorylation using 4G10 Ab. Actin staining was used as protein loading control.

5.2.7 Fyn is hyperactive but PAG is not hyperphosphorylated at Y314 in myrPKB tg thymocytes stimulated with CD3 Ab at 4°C

We next investigated the dependency of Y314 phosphorylation of PAG in myrPKB tg cells on tyrosine phosphatase activity by performing experiments at 4°C. If the low level of Y314 phosphorylation of PAG in stimulated myrPKB tg cells is caused by hyperactivity of tyrosine phosphatases, inhibition of tyrosine phosphatase activity at 4°C should alter the observed results. Thymocytes from wt and myrPKB tg mice were left unstimulated or stimulated with CD3 Ab at 4°C and Fyn auto- and transphosphorylation activity were analyzed by IVK. Fyn

autophosphorylation and transphosphorylation activity after 120 min CD3 stimulation at 4°C were increased in myrPKB tg in comparison to wt thymocytes. However, increased Fyn activity in myrPKB tg thymocytes did not result in enhanced phosphorylation of PAG at Y314 but was even lower than in wt thymocytes. These results indicate that lack of hyperphosphorylation of Y314 of PAG in myrPKB tg thymocytes with increased Fyn activity is not caused by increased tyrosine phosphatase activity acting on pY314 of PAG. We cannot completely exclude that the reduction of Y314 phosphorylation of PAG despite Fyn hyperactivity in myrPKB tg thymocytes is caused by a tyrosine phosphatase that is temperature insensitive.

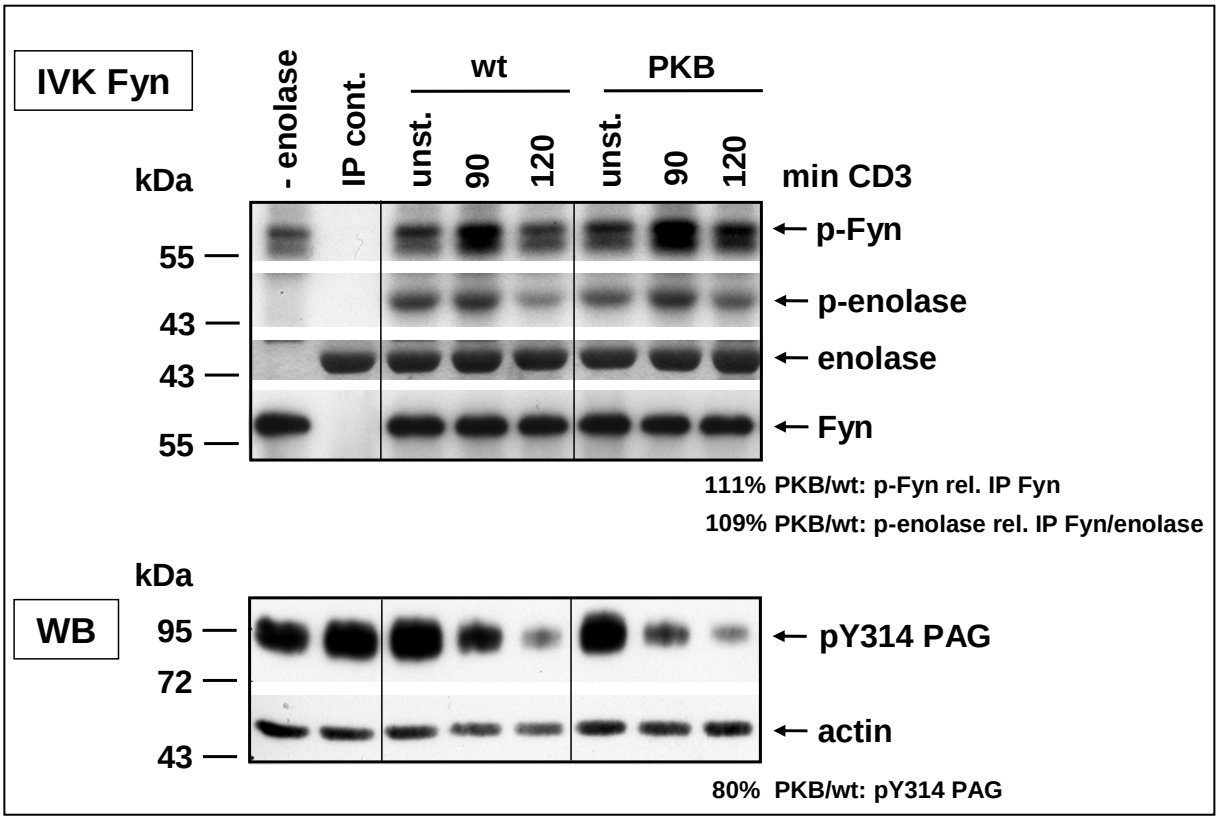

Figure 5.15 Hyperactivity of Fyn in myrPKB tg thymocytes stimulated with CD3 Ab at 4°C does not result in increased phosphorylation of PAG at Y314

Thymocytes from wt and myrPKB tg mice were stimulated with biotin-CD3 Ab (30 μg/ml) plus streptavidin (42 μg/ml) for 90 and 120 min at 4°C. Fyn was immunoprecipitated and its activity was assessed by IVK. Control immunoprecipitation (IP cont.) was performed with mouse anti-rat IgG Ab. The amount of enolase was visualized by coomassie staining and the amount of Fyn immunoprecipitated was visualized by western blot. The amount of p-Fyn normalized to the amount of Fyn immunoprecipitated (p-Fyn rel. IP Fyn) and the amount of p-enolase normalized to the amount of Fyn immunoprecipitated and the total amount of enolase (p-enolase rel. IP Fyn/enolase) are given in percentage for myrPKB tg relative to wt cells.
Phosphorylation of PAG at Y314 was monitored by western blot. Actin levels were used to control for protein loading. The amount of Y314 phosphorylated PAG is given in percentage for myrPKB tg relative to wt cells.

5.2.8 Enhanced Fyn activity in myrPKB tg thymocytes at 4°C does not result in increased binding of Csk to PAG

The experiments performed at 4°C did not reveal increased phosphorylation of PAG at Y314 in myrPKB tg cells despite increased Fyn activity. To analyze to what degree Csk binds to PAG, wt and myrPKB tg thymocytes were stimulated with CD3 Ab for 30, 90 and 120 min at 4°C and phosphorylation of PAG at Y314 was determined. Again, the kinetics of dephosphorylation of PAG at Y314 in CD3 Ab-stimulated wt and myrPKB tg thymocytes was comparable. PAG was immunoprecipitated from the same cell lysates and the co-immunoprecipitated Csk was detected by western blot. The kinetics of Csk dissociation from immunoprecipitated PAG was also similar in wt and myrPKB tg thymocytes and the amount of Csk bound to PAG correlated with the dephosphorylation of PAG at Y314 (Figure 5.16). Thus, increased Fyn activity in myrPKB tg thymocytes does not result in increased binding of Csk to PAG.

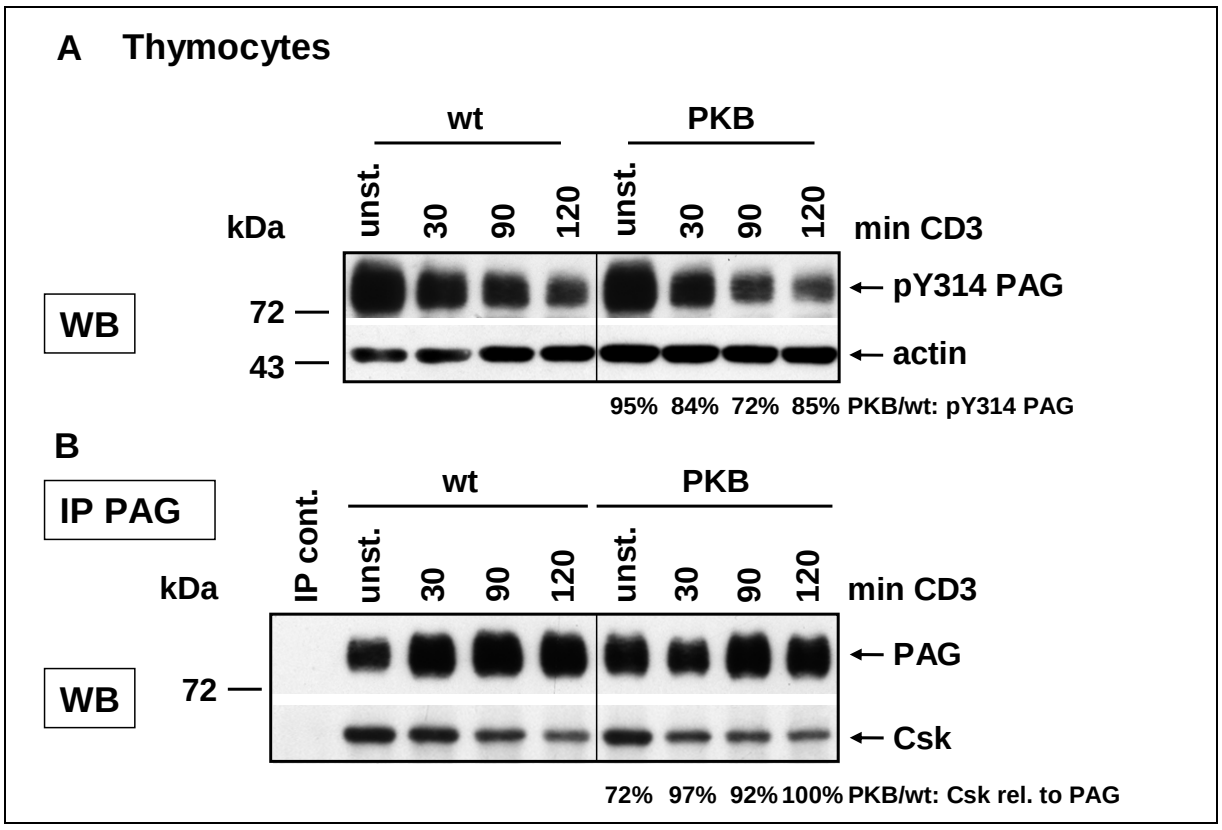

Figure 5.16 Similar binding of Csk to PAG and PAG phosphorylation at Y314 in wt and myrPKB tg thymocytes stimulated with CD3 Ab at 4°C

Thymocytes from wt and myrPKB tg mice were stimulated with biotin-CD3 Ab (30 μg/ml) plus streptavidin (42 μg/ml) for 30, 90 and 120 min at 4°C.

A) PAG phosphorylation was assessed by western blot with an antibody specific for pY314 of PAG, and actin expression was used as control for protein loading. Y314 phosphorylation of PAG was quantified and is given in percentage for myrPKB tg relative to wt cells.

B) PAG was immunoprecipitated from the same cell lysates, which were used in A, and the amount of co-immunoprecipitated Csk was determined by western blot. Control immunoprecipitation (IP cont.) was performed with rabbit IgG control Ab. The relative amounts of co-immunoprecipitated Csk normalized to the amounts of total PAG immunoprecipitated (Csk rel. to PAG) are given in percentage for myrPKB tg relative to wt cells.

5.2.9 Hyperactive Fyn and PAG co-localize in lipid rafts of myrPKB tg thymocytes

The previous experiments showed that Fyn is hyperactive in myrPKB tg $CD4^+$ T cells and thymocytes, but PAG phosphorylation at Y314 and association with Csk are not correspondingly increased. This does not result from increased phosphatase activity in myrPKB tg cells leading to enhanced dephosphorylation of PAG at Y314, since similar results were obtained in experiments performed at 4°C, which blocks phosphatase activity. We next hypothesized that hyperactive Fyn might be sequestered from PAG or PAG might be, at least partially, sequestered from lipid rafts in myrPKB tg cells.

To analyze co-localization of Fyn, PAG and Csk and activation of Fyn in lipid rafts, sucrose density gradient centrifugation was performed with lysates from wt and myrPKB tg thymocytes. A temperature of 4°C was choosen to block phosphatase activity. Thymocytes were stimulated with CD3 Ab for 120 min at 4°C since at this point in time the difference in Fyn activity between wt and myrPKB tg thymocytes stimulated at 4°C was most obvious (Figure 5.15). Insoluble fractions 1-4 were identified as lipid raft fractions by detection of ganglioside GM1 with cholera toxin (GM1-CTX). GM1 was not present in soluble fractions 8 and 9. Ganglioside GM1 (monosialotetrahexosylganglioside) belongs to the ganglio series of gangliosides, which possess one sialic acid residue, bind to CTX (cholera toxin) and have been shown to localize in lipid rafts (Morales-Garcia, Fournie et al. 2008).

Analysis of CD3 stimulated cells (Figure 5.17) revealed an increased amount of total Fyn, pY417 Fyn and total PAG in the lipid raft fractions 1-3 of myrPKB tg thymocytes, especially in fraction 1 (marked by red rectangles in Figure 5.17). Importantly, the higher accumulation of pY417 Fyn in fraction 1 did not correlate with a proportional increase of pY314 PAG, suggesting that ‘hyperactive’ Fyn in this fraction did not lead to a proportional hyperphosphorylation of PAG. Thus, in stimulated myrPKB tg thymocytes Y417 phosphorylated ‘hyperactive’ Fyn and PAG are pesent in the same lipid raft fractions, i.e. Fyn and PAG are not sequestered from each other, but ‘hyperactive’ Fyn does not enhance phosphorylation of PAG at Y314 and recruitment of Csk, under these stimulatory conditions.

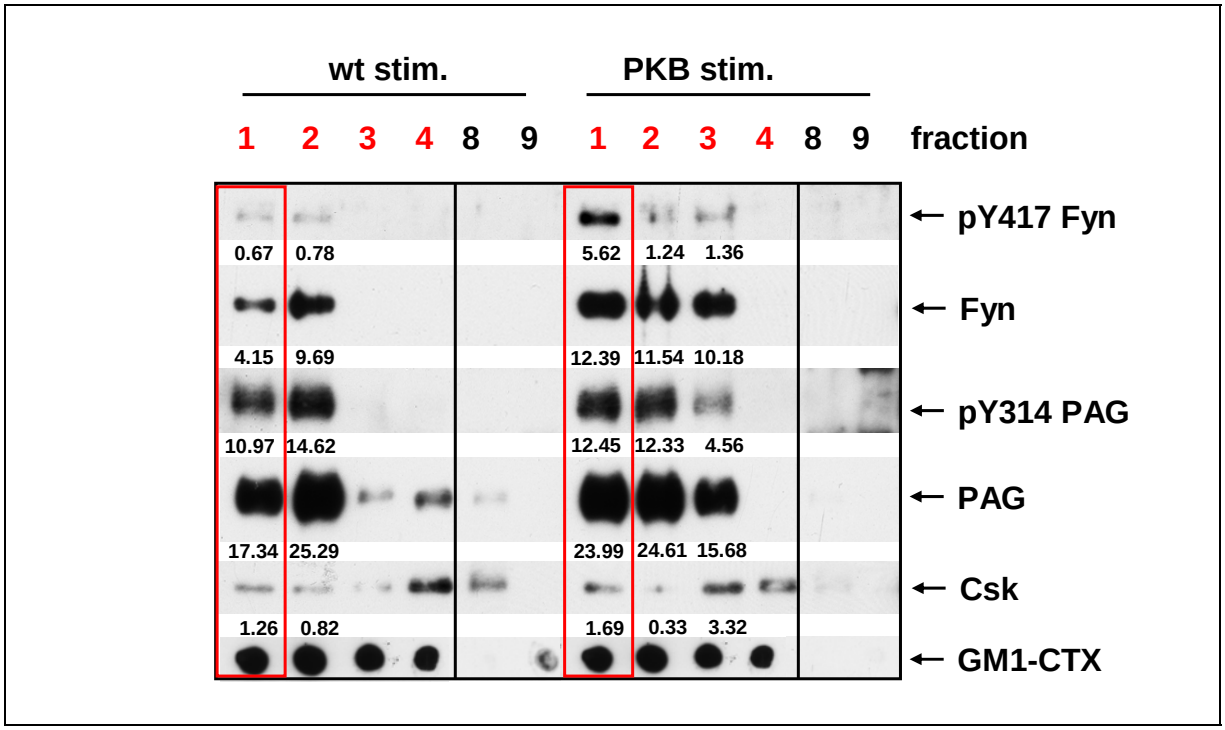

Figure 5.17 'Hyperactive' Fyn and PAG co-localize in lipid rafts of myrPKB tg thymocytes, but this does not lead to hyperphosphorylation of PAG at Y314
Sucrose density gradient centrifugation of protein lysates from wt and myrPKB tg thymocytes, which were stimulated with biotin-CD3 Ab (30 μg/ml) plus streptavidin (42 μg/ml) for 120 min at 4°C, was performed. Protein fractions 1-9 were taken from top to bottom of the gradient and analyzed by western blot for the indicated proteins. Insoluble lipid raft fractions (lanes 1-4) were identified by detection of ganglioside GM1 with cholera toxin (GM1-CTX). Ganglioside GM1 was not detectable in soluble fractions 8 and 9. Numbers give the quantified intensities of signals as indicated on the right.

5.2.10 Fyn and PKB co-immunoprecipitate in HEK 293T cells overexpressing Fyn and myrPKB

The previous data indicated a cross-talk between PKB and Fyn, which could be mediated by a direct interaction of both molecules. To examine whether PKB and Fyn are associated *in vivo*, experiments to co-immunoprecipitate Fyn and PKB from lysates of wt and myrPKB tg thymocytes were performed. However, no association was detectable. We assumed that only small amounts of the total pools of Fyn and PKB interact for a restricted period of time or that the association is very labile. Therefore, transfected HEK 293T cells overexpressing Fyn and myrPKB were analyzed. When PKBα was immunoprecipitated, association of transfected Fyn was detected (Figure 5.18 A). Likewise, immunoprecipitated Fyn associated with PKB (Figure 5.18 B). Thus, under these conditions Fyn and myrPKB associate *in vivo*.

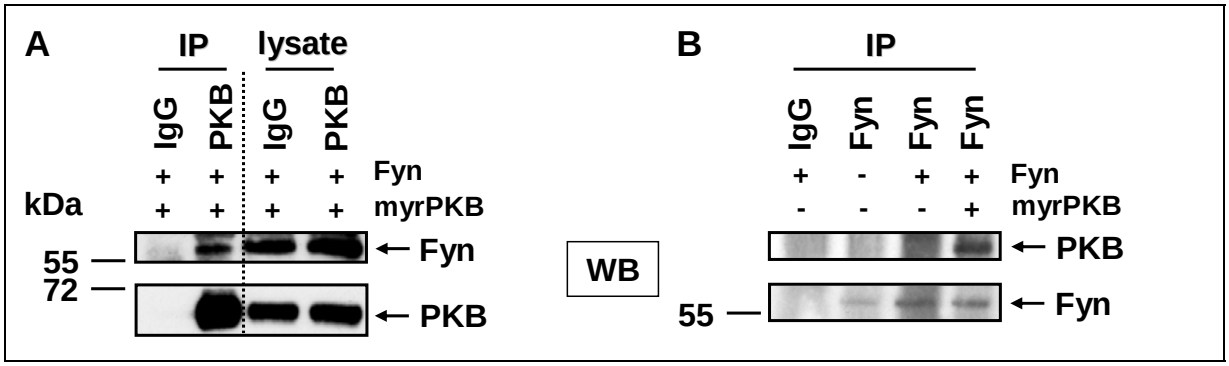

Figure 5.18 Fyn and myrPKB co-immunoprecipitate *in vivo*
HEK 293T cells were transfected with Fyn and myrPKB. Cells were lysed and IPs were performed:
A) IP of PKBα and detection of associated Fyn by western blot (lane 2). Analysis with mouse anti-rat IgG Ab served as isotype control for PKBα IP (lane 1). The two right lanes depict Fyn and myrPKB expression in the cell lysates used for IPs.
B) IP of Fyn and detection of associated PKB by western blot. IP with mouse anti-rat IgG Ab (lane 1) served as isotype control for Fyn IPs.

5.2.11 MyrPKB reduces PAG phosphorylation at Y314 in HEK 293T cells overexpressing Fyn, PAG and myrPKB

Since myrPKB tg thymocytes and $CD4^+$ T cells showed enhanced Fyn activity, we analyzed the impact of myrPKB on the activatory phosphorylation of Fyn at Y417 and phosphorylation of PAG at Y314 in HEK 293T cells transfected with Fyn, Flag-tagged PAG and myrPKB. Protein expression of the transfected DNA constructs was controlled by detection of Flag-tagged PAG, total Fyn and pS473 PKB via western blot. PAG Y314 phosphorylation was not observed in the absence of Fyn co-transfection, whereas Fyn overexpression resulted in strong phosphorylation of PAG at Y314 (Figure 5.19). Co-transfection of myrPKB resulted in a reduction of the activatory phosphorylation of Fyn at Y417 and an almost complete loss of PAG phosphorylation at Y314. If Y314 phosphorylation of PAG is considered as an indicator of Fyn activity, co-transfection of myrPKB led to decreased Fyn activity, resulting in reduced phosphorylation of PAG at Y314. Thus, PKB clearly affects Fyn activity in HEK 293T cells, however, opposite to the effects seen in $CD4^+$ T cells and thymocytes from myrPKB tg mice, where myrPKB led to increased Fyn activity. This is most likely due to the different cell types used and the different expression levels of Fyn and myrPKB in these cells.

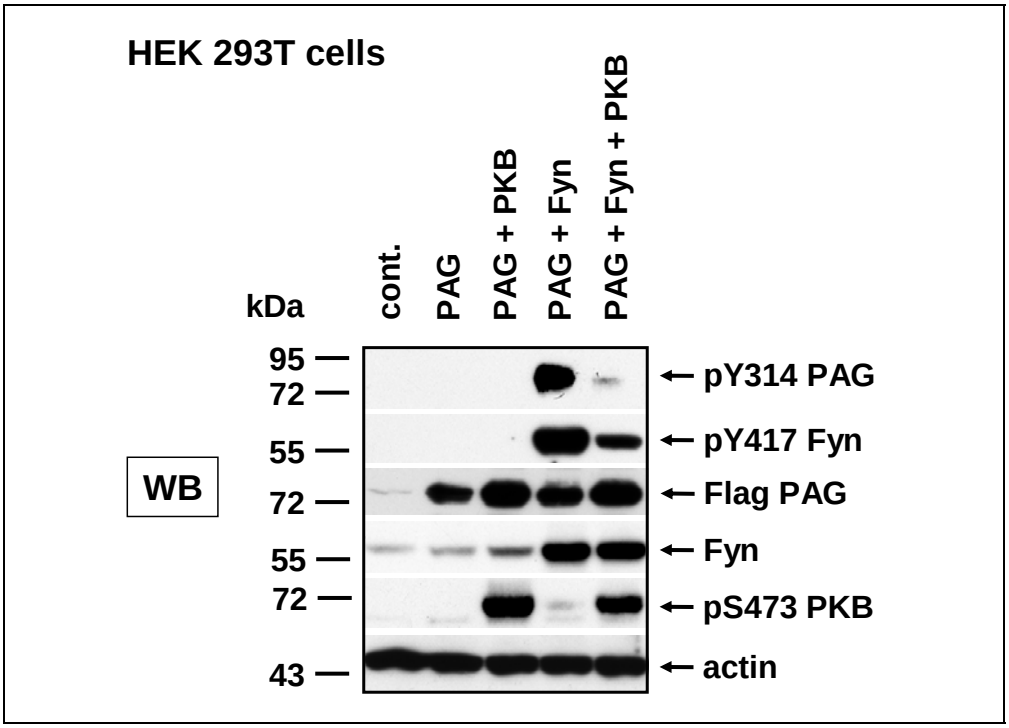

Figure 5.19 MyrPKB reduces the phosphorylation of Fyn at Y417 and of PAG at Y314 in HEK 293T cells overexpressing Fyn, PAG and myrPKB
HEK 293T cells were transfected with Fyn (4000 ng), Flag-tagged PAG (950 ng) and myrPKB (PKB, 50 ng). Cells were lysed and western blot analysis for expression and phosphorylation of the indicated proteins was performed. Control cells (cont.) were transfected with empty vector only. Actin expression was used as control for protein loading. Data are representative of 3 independent experiments.

5.2.12 Generation of GST-Fyn and GST-Csk fusion constructs

The increased Fyn activity in myrPKB tg cells and the co-immunoprecipitation of PKB and Fyn in HEK 293T cells suggested that Fyn could be a direct target of PKB, the more as Fyn possesses canonical PKB phosphorylation sites at T12 and T82. T82 is conserved in mouse and human Fyn and T12 is present in human, but not mouse Fyn. In addition, the sequences at T181, T223, S444 and S448 of Fyn show similarity to the PKB consensus motif and thus could also be PKB target sites. To examine whether PKB phosphorylates Fyn at these sites, GST-Fyn fusion proteins were generated as illustrated in Figure 5.20 A. The GST-tag was fused to the N-terminus. Fyn1/2 consists of the N-terminal, unique and SH3 domain of Fyn, whereas Fyn1/3 additonally includes major parts of the SH2 domain. Fyn4/5 contains the major part of the Fyn kinase domain and the C-terminal negative regulatory domain of Fyn.

A possible cross-talk of PKB with Fyn could be mediated via Csk. Csk is known to phosphorylate Fyn at Y528, which is an inhibitory phosphorylation in the C-terminal regulatory domain of Fyn (Takeuchi, Kuramochi et al. 1993). Csk could also be a target of PKB, because it possesses a canonical PKB phosphorylation site at S284 in its catalytic domain. We, therefore, also generated GST-Csk fusion proteins with the GST-tag fused to the N-terminus (Figure 5.20 B). Csk1/2 consists of the N-terminal amino acids 1-177 of Csk,

which include the SH3 and SH2 domains. Csk3/4 contains the C-termial amino acids 178-450 and harbors the kinase domain. S364 of Csk, which is phosphorylated by PKA and leads to increased Csk activity, is also indicated (Vang, Torgersen et al. 2001).

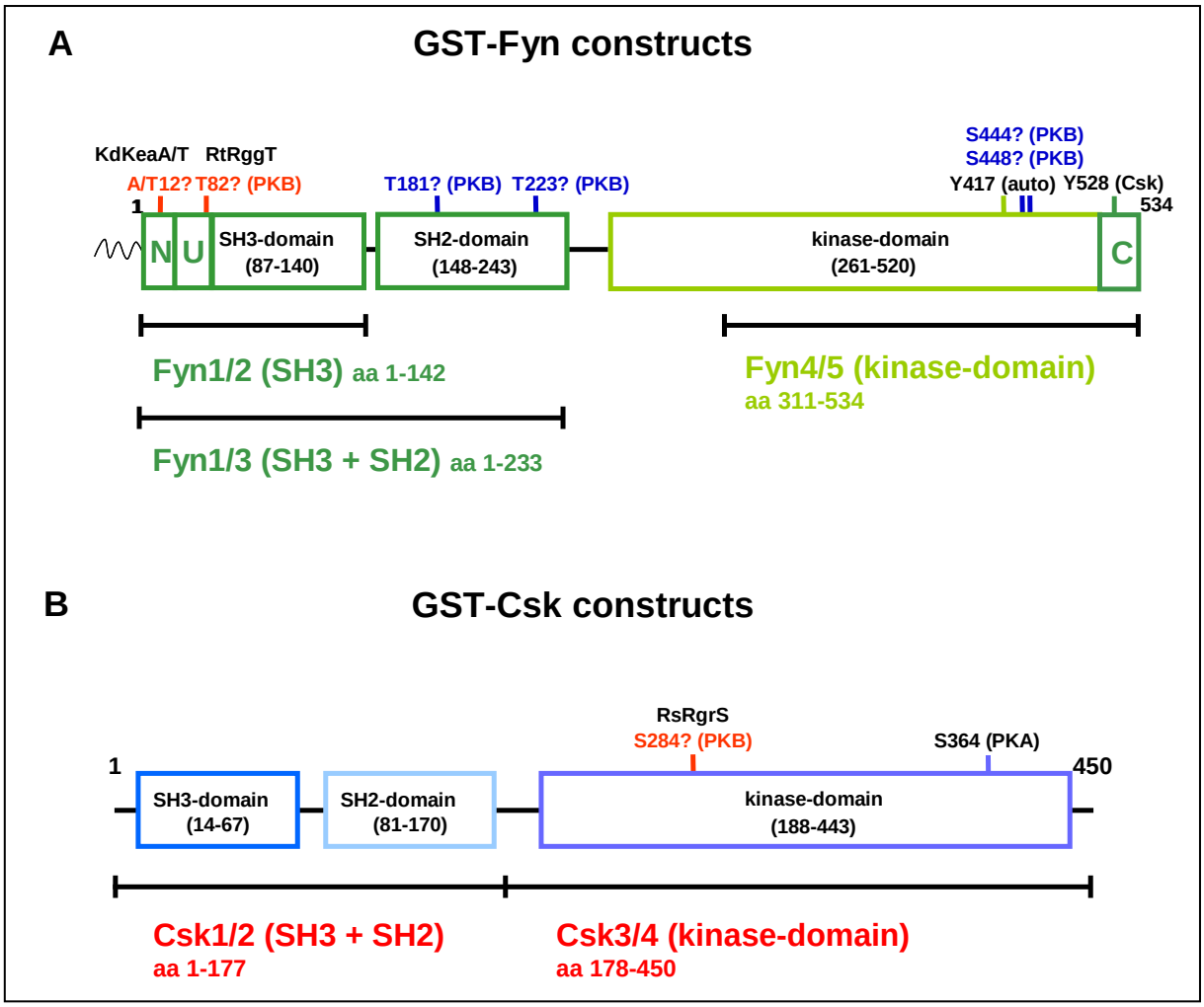

Figure 5.20 Schematic representation of GST-Fyn and GST-Csk fusion constructs
A) GST-Fyn constructs: the canonical PKB phosphorylation motifs at T12 and T82 are indicated as well as possible non-canonical PKB phosphorylation sites at T181, T223, S444 and S448. The Fyn autophosphorylation site at Y417 and the Csk phosphorylation site at Y528 are also indicated.
B) GST-Csk constructs: the canonical PKB phosphorylation site at S284 and the PKA phosphorylation site at S364 are indicated.

5.2.13 PKB phosphorylates Fyn at T82 *in vitro*

The GST-fusion constructs represented in Figure 5.20 were expressed in E. coli BL21, GST-fusion proteins were isolated via glutathione columns and examined in IVKs for phosphorylation by PKB. Figure 5.21 shows the analysis of GST-Fyn fusion proteins. The amount of GST-Fyn present in each reaction was monitored by coomassie staining of the gel (lower panel). The GST-NFAT fusion protein hNFATc1A (aa 177-336) was used as positive control for PKB activity (lanes 1-3). PKB was active in the presence of DMSO (lane 2) or the Src kinase inhibitor PP2 (lane 3), which were used as vehicle control and to inhibit possible

autophosphorylation of the GST-Fyn4/5 fusion protein harboring parts of the kinase domain (lanes 8-11). No phosphorylation of GST-NFAT was detected without PKB (lane 14). The background phosphorylation caused by PKB and reaction mixture, i.e. without any substrate, was also monitored (lane 13). The bands appearing in this lane (and all other lanes) thus represent unspecific phosphorylation resulting from contaminating proteins in the commercial PKB enzyme sample. To exclude that signals obtained from GST-Fyn proteins resulted from phosphorylation of the GST part by PKB, the phosphorylation of GST was also tested. GST has a molecular mass of about 26 kDa and was detected by coomassie staining (lane 12). Phosphorylation of GST by PKB was not detectable.

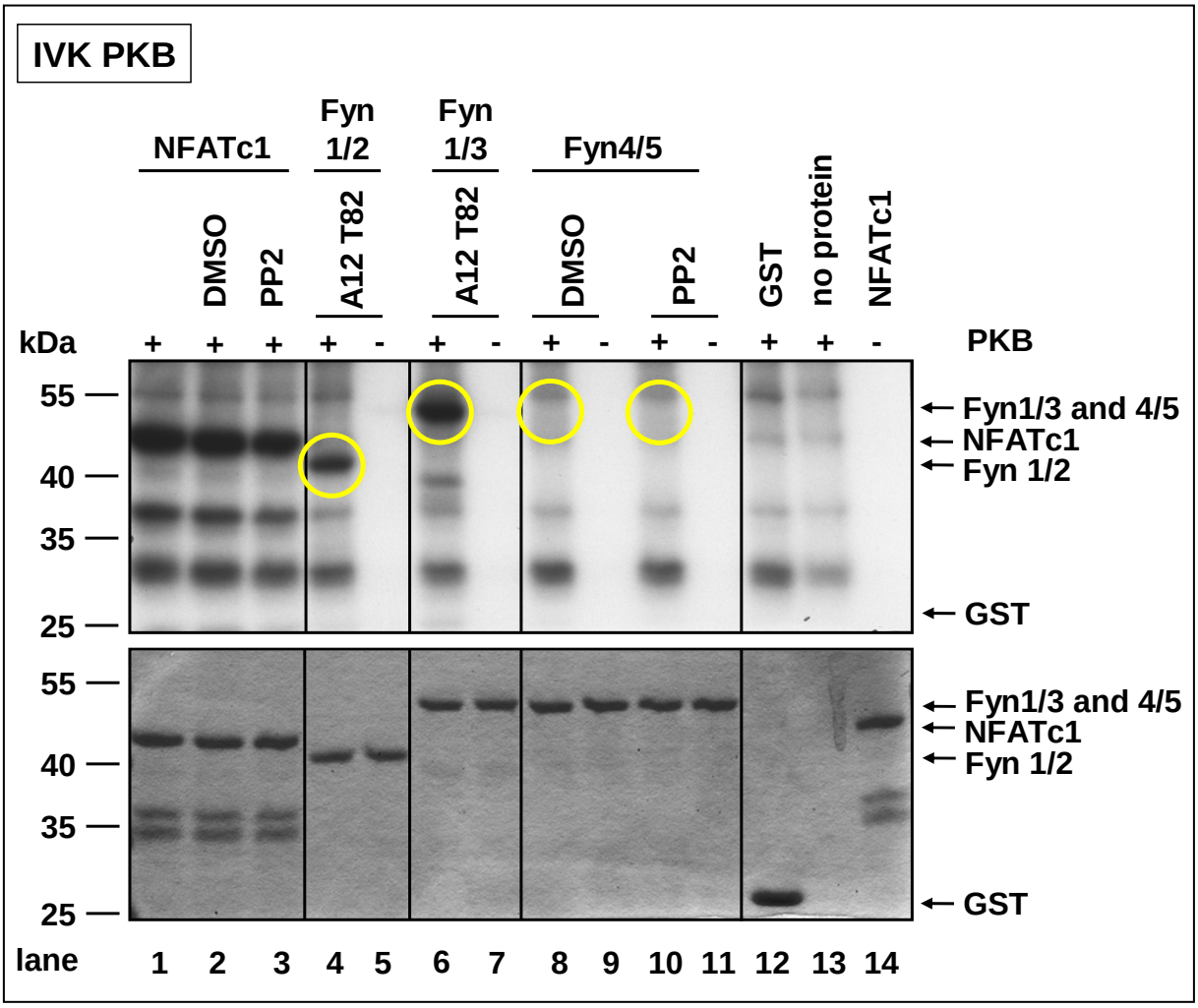

Figure 5.21 PKB phosphorylates Fyn *in vitro*
GST-Fyn1/2, GST-Fyn1/3 and GST-Fyn4/5 fusion proteins were analyzed for phosphorylation by PKB by IVKs. The analyzed proteins were incubated with IVK reaction mixture without or with PKB. hNFATc1A (aa 177-336) was used as positive control for PKB kinase activity. Phosphorylation of substrates was detected by autoradiography (upper panel). The amount of substrate protein in each reaction was visualized by coomassie staining (lower panel).

GST-Fyn1/2 (lanes 4, 5) as well as GST-Fyn1/3 (lanes 6, 7) harboring A12 and T82 were phosphorylated by PKB. The signal of GST-Fyn1/3 was slightly stronger in comparison to the phosphorylation intensity of GST-Fyn1/2. Additional phosphorylation could occur in the SH2

domain present in GST-Fyn1/3, which could be T181 or T223, or combination of the SH2, SH3, unique and N-terminal domain might increase PKB phosphorylation efficiency. To exclude possible autophosphorylation of GST-Fyn4/5, the Src kinase inhibitor PP2, dissolved in DMSO, was included. However, GST-Fyn4/5 was not phosphorylated by PKB and autophosphorylation was also not detectable.

To identify the PKB phosphorylation site(s) in N-terminal Fyn, constructs were generated with mutations at position A12 and/or T82. Mutation T−>A82 in combination with A12 resulted in complete abolishment of GST-Fyn1/2 phosphorylation (Figure 5.22). Since GST-FynT12/A82 was not phosphorylated but GST-FynA12/T82 was phosphorylated, T82 is a PKB site in Fyn. Analysis of GST-Fyn1/3 harboring A82 and A12 led to a strong decrease in phosphorylation in comparison to GST-Fyn1/3 possessing T82. The low level of phosphorylation left despite the elimination of T82 could result from additional PKB sites present in GST-Fyn1/3, which are absent in GST-Fyn1/2. Altogether, the IVKs clearly showed that the conserved T82, but not T12, is a PKB phosphorylation site *in vitro*.

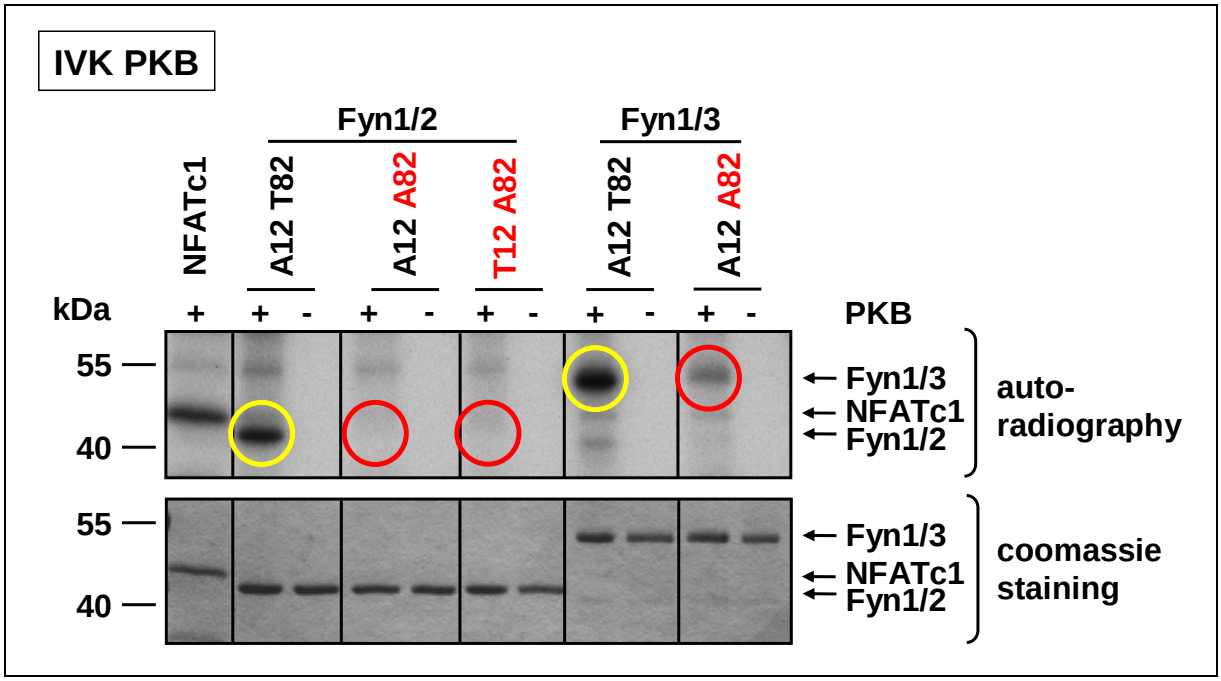

Figure 5.22 PKB phosphorylates Fyn at T82 *in vitro*
GST-Fyn1/2 and GST-Fyn1/3 fusion proteins with the indicated mutations were analyzed for phosphorylation by PKB by IVKs. The analyzed proteins were incubated with IVK reaction mixture without or with PKB. hNFATc1A (aa 177-336) was used as positive control for PKB kinase activity. Phosphorylation of substrates was detected by autoradiography (upper panel). The amount of substrate protein in each reaction was visualized by coomassie staining (lower panel).

IVK analysis of GST-Csk1/2, GST-Csk3/4 and GST-Csk3/4 with S264 mutated to A showed that Csk is not phosphorylated by PKB *in vitro* (Figure 5.23).

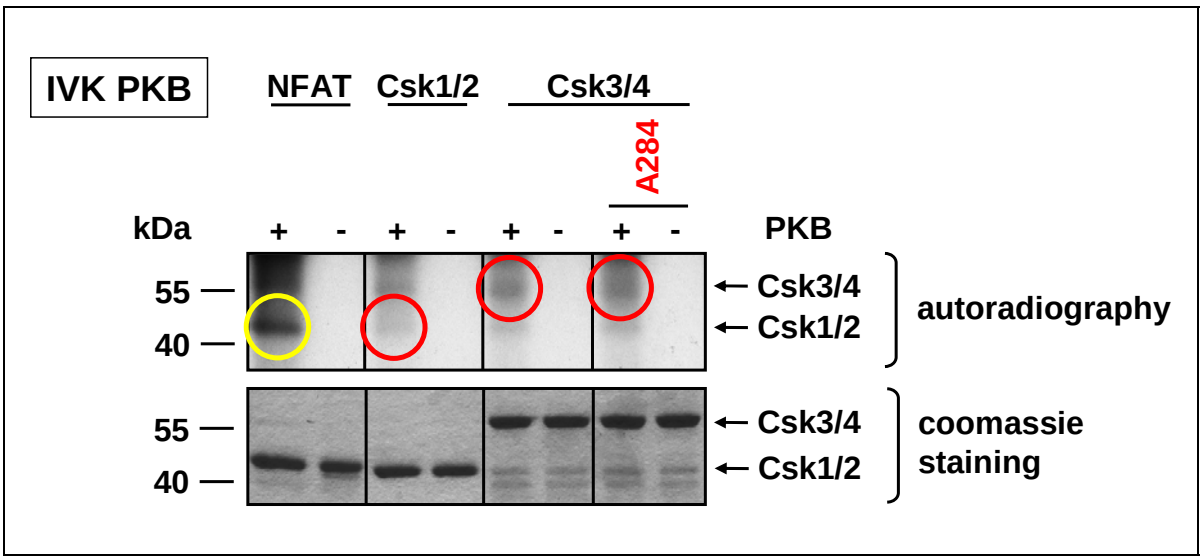

Figure 5.23 Csk is not phosphorylated by PKB *in vitro*
GST-Csk1/2, GST-Csk3/4 and GST-Csk3/4 fusion proteins with the indicated mutation (S−>A284) were analyzed for phosphorylation by PKB by IVKs. The analyzed proteins were incubated with IVK reaction mixture without or with PKB. GST-NFATc1A (aa 177-336) was used as positive control for PKB kinase activity. Phosphorylation of substrates was detected by autoradiography (upper panel). The amount of substrate protein in each reaction was visualized by coomassie staining (lower panel).

5.3 Ionomycin induced anergy

5.3.1 Ionomycin induced anergy is reduced in myrPKB tg CD4$^+$ T cells

Previous publication showed an increased amount of Fyn associated with PAG in CD4$^+$ T cells anergized by ionomycin treatment (Davidson, Schraven et al. 2007). These and other data (Smida, Posevitz-Fejfar et al. 2007) suggest that Fyn plays an important role in anergy. We, therefore, examined the impact of hyperactive Fyn in myrPKB tg CD4$^+$ T cells on ionomycin induced anergy. Wt and myrPKB tg CD4$^+$ T cells were stimulated with CD3+CD28 Abs for 2 days, expanded in IL-2 for 3 days and then treated for 16 h with ionomycin to induce anergy or with the vehicle DMSO. After ionomycin treatment, cells were restimulated for 48 h with immobilized CD3 Ab, CD3+CD28 Abs or PMA+Ionomycin and proliferation was determined. As shown in Figure 5.24 A, ionomycin treatment reduced the proliferation of CD3 Ab-stimulated wt CD4$^+$ T cells by 84% in comparison to DMSO treated cells, indicating that ionomycin induced anergy in wt cells. However, ionomycin treatment of myrPKB tg CD4$^+$ T cells reduced their proliferation only by 44%. When assessing proliferation after stimulation with CD3+CD28 Abs, hyporesponsiveness was no longer detectable in ionomycin treated myrPKB tg CD4$^+$ T cells, whereas ionomycin treated wt cells still showed a 79% reduction in proliferation. Anergy was overcome by restimulation of cells with PMA+ionomycin, which resulted in intensive proliferation of wt and myrPKB tg cells. Taken together, these results

show that myrPKB delivers signals that counteract or ameliorate anergy induction by ionomycin.

Figure 5.24 B shows the reduction of CD3 Ab induced proliferation after ionomycin treatment relative to the DMSO control of wt and myrPKB tg $CD4^+$ T cells for 2 experiments, demonstrating that ionomycin induced anergy was 'stronger' in wt than myrPKB tg cells.

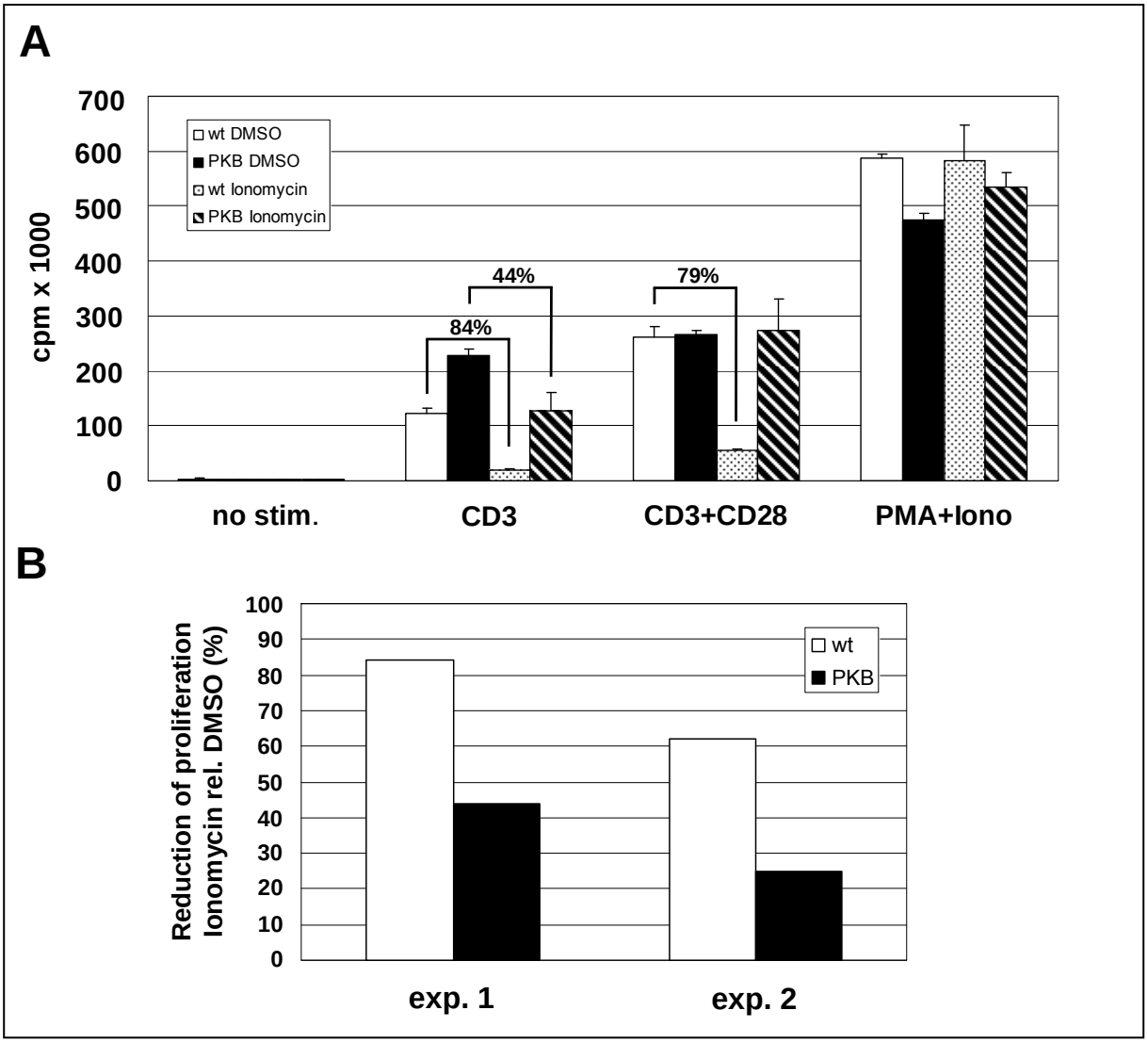

Figure 5.24 Ionomycin induced anergy is reduced in myrPKB tg $CD4^+$ T cells
A) $CD4^+$ T cells from wt and myrPKB tg mice were activated for 48 h with immobilized CD3 Ab (3 µg/ml) and soluble CD28 Ab (1 µg/ml) followed by expansion in IL-2 for 3 days. Subsequently, cells were treated with ionomycin (1 µM) for 16 h. Control cultures were treated with DMSO. Cells were then restimulated for 48 h with immobilized CD3 Ab (1 µg/ml), immobilized CD3+CD28 Abs (1/2.5 µg/ml) or with PMA plus ionomycin (50/747 ng/ml) and proliferation was measured by [^{3}H]-thymidine incorporation (cpm). Standard deviations from triplicates are shown.
B) Bars represent percent reduction of proliferation induced by ionomycin treatment relative to DMSO control of wt and myrPKB tg $CD4^+$ T cells for 2 independent experiments. $CD4^+$ T cells were expanded and anergized as described under A and thereafter restimulated for 48 h with immobilized CD3 Ab (1 µg/ml). Proliferation of DMSO treated control cells was set as 100%.

Above data raised the question, whether anergized wt and more 'resistant' myrPKB tg T cells would show altered Fyn activity. Therefore, wt and myrPKB tg $CD4^+$ T cells were anergized with ionomycin, Fyn was immunoprecipitated and Fyn activity determined by IVK. Ionomycin treated wt $CD4^+$ T cells showed increased Fyn auto- and transphosphorylation activity in comparison to DMSO treated cells (black numbers in Figure 5.25). In contrast, ionomycin treated myrPKB tg $CD4^+$ T cells showed a slight reduction in Fyn autophosphorylation and stronger reduction of enolase phosphorylation (red numbers in Figure 5.25). Thus, ionomycin induced anergy in wt $CD4^+$ T cells is associated with an increase in Fyn activity, whereas ionomycin treatment of myrPKB tg T cells does not lead to enhanced Fyn activity, which correlates with an increased proliferation after restimulation.

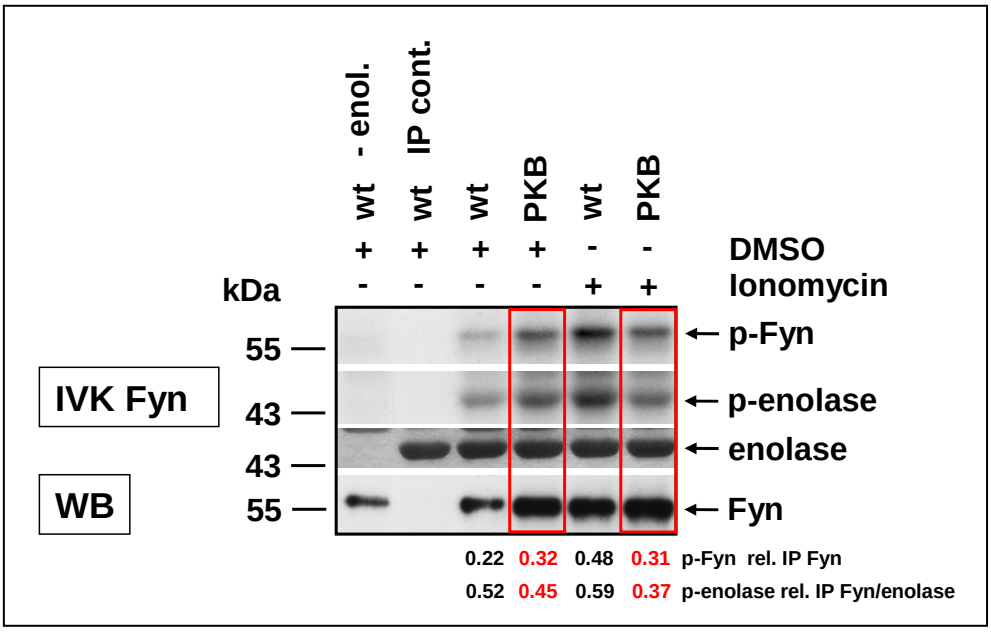

Figure 5.25 Analysis of Fyn activity in ionomycin treated $CD4^+$ T cells
$CD4^+$ T cells were activated for 48 h with immobilized CD3 Ab (3 µg/ml) and soluble CD28 Ab (1 µg/ml). After that, cells were expanded in IL-2 (50 units/ml) for 3 days and treated with ionomycin (1 µM) for 16 h for anergy induction. Control cultures were treated with DMSO instead. Fyn was immunoprecipitated from 1 x 10^7 cells per sample and IVKs were performed to assess Fyn activity. Fyn autophosphorylation and enolase transphosphorylation were detected by autoradiography. The substrate enolase was visualized by coomassie staining and the amount of Fyn immunoprecipitated was monitored by western blot (bottom-line). Control immunoprecipitation (IP cont.) was performed with mouse anti-rat IgG Ab. Numbers give the amounts of p-Fyn normalized to the amounts of Fyn immunoprecipitated (p-Fyn rel. IP Fyn) and the amounts of p-enolase normalized to the amounts of Fyn immunoprecipitated and the total amounts of enolase (p-enolase rel. IP Fyn/enolase).

6 Discussion

6.1 Cross-talk of PKB with NFAT

Thymocytes from ΔCam tg mice, expressing a constitutively active form of the phosphatase calcineurin, show strongly increased nuclear NFAT and a DN3 block in differentiation. This block is linked to a failure of Rag expression and TCR β-chain rearrangement. Simultaneous expression of myrPKB reduces this DN3 block by allowing Rag and pre-TCR formation. Since nuclear NFAT levels are strongly downregulated in myrPKB ΔCam tg thymocytes, the question arose whether NFAT factors are involved in Rag gene expression. To answer this question, EL4 cells were transfected with a Rag2 promoter luciferase reporter construct and Rag2 promoter activity was detected in these cells. Co-transfection of either NFATc1 or NFATc2 led to a shut down of Rag2 promoter activity. These and CHIP studies (Patra, Drewes et al. 2006) revealed that NFAT binds to the Rag promoter/enhancer elements, and thus we identified NFAT as a novel and one of the few transcription factors so far known to be involved in the regulation of Rag expression in T cells (Kuo and Schlissel 2009).

Previous studies showed that active PKB also regulates NFAT activation in peripheral T cells: myrPKB tg T cells showed reduced NFAT activation after TCR stimulation, although they proliferated better than wt T cells and produced more cytokines. An interaction of NFAT and PKB *in vivo* was shown by co-immunoprecipitation of both proteins in peripheral T cells (Patra, Na et al. 2004). The latter suggested that NFAT could be a direct phosphorylation target of PKB. Therefore, several GST-NFATc1A fusion proteins, which harbor parts of the NFATc1 regulatory domain, were generated to analyze whether PKB phosphorylates NFAT *in vitro*. Indeed, in IVKs recombinant PKB phosphorylated the NFATc1 regulatory domain in the N-terminal (aa 177-261) and C-terminal (aa 262-336) segment *in vitro* (Figure 5.6). Analysis of mutants, in which possible PKB phosphorylation sites were mutated one by another, indicated that PKB phosphorylates NFATc1 within the motifs SPRVSVTDDS and SPRASVTEES, named mut C and mut D, respectively. However, several single mutations in the regions of mut C and mut D did not cause a reduction of NFATc1 phosphorylation (Figure 5.8). Only additive mutations, mut W, mut A, mut B in combination with mut D or mut C and mut D, led to a reduction of NFATc1 phosphorylation (Figure 5.7). Thus, the complex interplay of all mutations seems to be a prerequisite for the impact on phosphorylation of the NFATc1 regulatory domain by PKB *in vitro*. We can only speculate that mut C and D would change the conformation of the NFAT regulatory domain in a way that mut W, mut A and/or mut B lead to a reduction of phosphorylation. A modification of protein conformation by mutations W, A and/or B leading to reduced phosphorylation by insertion of mut C and D is also possible. Transfection experiments to analyze the *in vivo* effect of PKB on NFAT activity

clearly showed that myrPKB reduces NFAT-induced IL-2 promoter activity (Figure 5.2). However, mutation of serines and threonines present in the sequences of mut C and D in NFATc1A did not change its activity as analyzed by IL-2 promoter luciferase assays (data not shown). Thus, so far it was impossible to identify the definite PKB site(s) in NFAT.

PKA phosphorylates NFAT at S245, S269 and S294, priming NFAT for further phosphorylation by GSK-3 at the GSK-3 consensus sites (S/TXXXpS) at S241 and S290, leading to cytoplasmic accumulation and inactivation of NFAT (Sheridan, Heist et al. 2002). Thus, we tested whether PKA, GSK-3 and PKB alone or in combination revealed differences in inhibiting NFAT activation. PKB, GSK-3 and PKA alone inhibited NFAT activity and PKB in combination with GSK-3 or PKA enhanced NFAT inhibition induced by the NFAT kinases alone. PKA and GSK-3 in combination caused stronger inhibition of NFAT than each protein alone confirming that both kinases cooperate in causing cytoplasmic accumulation of NFAT. The strongest reduction of NFAT activity was obtained by co-transfection of PKB, PKA and GSK-3 (Figure 5.3). Thus, PKB, PKA and GSK-3 additively inhibit NFAT activity. It is, however, unclear, whether PKB inhibits NFAT by a mechanism independent from PKA and GSK-3 and the single mechanisms sum up to the total effect or whether PKB affects GSK-3 and PKA activity or other proteins.

NFAT and Foxp3 were shown to interact in co-transfected HEK293 T cells, and retroviral expression of Foxp3 in naive peripheral mouse $CD4^+$ T cells causes a reduction of IL-2 and IL-4 expression (Bettelli, Dastrange et al. 2005). Foxp3 is a definitive marker of murine regulatory T cells and was shown to downmodulate the activation of NFAT in Jurkat transfection assays. The crystallographic structure of the NFATp-Foxp2-DNA complex has been unravelled and disruption of the NFAT-Foxp3 interaction by mutating the NFAT-binding sites in Foxp3 had an impact on several cellular processes: it reduced the ability of Foxp3 to repress IL-2 gene expression, interfered with the ability of Foxp3 to upregulate expression of the Treg markers CD25 and CTLA4 and diminished Treg suppressor function in a model of autoimmune diabetes in mice (Wu, Borde et al. 2006).

In tansfection experiments with HEK 293T cells, we analyzed the impact of Foxp3 alone or in combination with myrPKB on NFAT-induced IL-2 production. MyrPKB as well as Foxp3 reduced NFAT activity, and co-transfection of Foxp3 and myrPKB caused stronger inhibition of NFAT activity than either factor alone (Figure 5.4). Thus, Foxp3 and myrPKB additively inhibit NFAT activity, similar to the above results with PKA and GSK-3. Transfection of NFATc1 with mutations in mut C and mut D yielded results similar to wt NFATc1.

Mass spectrometry analysis of NFATc2 extracted from resting D5 and Cl.7W2 mouse T cell lines revealed phosphorylation at 21 serine residues. Eighteen of these serine residues were localized in the N-terminal regulatory domain and three phosphoserines were present within

the C-teminal domain. Fourteen of the eighteen phosphoserines in the N-terminal regulatory domain of NFAT were localized in the conserved serine-rich regions (SRR) and serine-proline boxes (SP), SRR-1, SP-2, SRR-2 and SP-3. It was shown that concerted dephosphorylation of 13 serine residues in the conserved sequences of the regulatory domain of NFAT is required for masking of the nuclear export signal (NES) and for full unmasking of the nuclear localization signal (NLS), resulting in nuclear translocation and full transcriptional activity of NFAT (Okamura, Aramburu et al. 2000). Two models have been used to describe the activation of NFAT: the conformational switch model is based on the assumption that only 2 conformations of NFAT exist: an active and an inactive conformation. When NFAT proteins are phosphorylated, many NFAT molecules are in the inactive conformation at any time and only a small number is in the active conformation. This conformational preference is reversed by dephosphorylation of NFAT. Thus, progressive dephosphorylation of NFAT increases the probability that a single NFAT molecule will fold into the active conformation. The model of progressive conformational changes is based on the assumption that each phosphorylation state of NFAT defines a distinct conformation. Sequential changes in NFAT phosphorylation would lead to sequential changes of conformation. Thus, all fully phosphorylated NFAT proteins would exclusively exist in an inactive conformation, and all completely dephosphorylated proteins would assume an active conformation.

Our IVKs with wt and mutant GST-NFAT fusion proteins revealed that the complex interplay of all mutations analyzed in the regulatory NFAT domain seems to be a prerequisite for the reduction of NFAT phosphorylation by PKB *in vitro*. In view of the model of progressive conformational changes, a specific protein conformation could be caused by each mutation inserted. Only the interplay of mut W, A, B with mut D or with mut C plus mut D could lead to a protein conformation, which inhibits NFAT phosphorylation by PKB. With regard to the conformational switch model, only the interplay of all mutations would increase the probability of a conformation, which causes a reduction of NFAT phosphorylation.

In conclusion, in various transfection assays and in ΔCam tg mice PKB was shown to downregulate NFAT activity. The *in vitro* kinase assays showed that PKB phosphorylates NFAT in the regulatory domain, suggesting that PKB could directly act on NFAT. Since inhibition of NFAT by GSK3 and PKA was enhanced by PKB, one could speculate that *in vivo* PKB could act as a priming kinase for PKA and/or GSK3 or vice versa. A single site for PKB phosphorylation, however, could not be identified, suggesting that special conformations and several phosphorylations by PKB might be involved. Recent publication showed that PKB activates NFAT via Homer proteins. The interaction of the cytoplasmic scaffolding proteins Homer2 and Homer3 with NFAT diminishes binding of CN to NFAT and thus reduces dephosphorylation of NFAT by CN, leading to reduced NFAT activity. Thus,

Homer molecules act as negative regulators of TCR signaling. Active PKB reduces the binding of Homer2 and Homer3 to NFAT, which results in enhancement of NFAT activity and thus TCR signaling (Huang, Huso et al. 2008).

6.2 Cross-talk of PKB with Fyn

Protein modifications by phosphorylation and acetylation in response to extracellular stimuli provide a mechanism to induce rapid changes in protein function (Karin and Hunter 1995; Berger 1999). Protein modifications influence protein function by generating or eliminating binding sites for the recruitment of other proteins or by modification of the conformation of a protein. Phosphorylation and dephosphorylation are ubiquitous modes for regulation of protein function (Cohen 2000). As outlined before, NFAT family transcription factors are a good example for regulation of protein activity by phosphorylation and dephosphorylation (Okamura, Aramburu et al. 2000). Phosphate groups can also modify the local environment of a functional structure and thereby determine the affinity of a protein for other interaction partners. Examples for this modus of changing protein function are plenty when looking at TCR signaling. For instance, docking sites for other proteins (e.g. ZAP-70, GRB2 and Csk) are provided by phosphorylation of the TCR-associated ITAMs after TCR triggering or by phosphorlyation of the transmembrane adapter proteins LAT and PAG, respectively (Horejsi, Zhang et al. 2004; Smith-Garvin, Koretzky et al. 2009) The activity of a protein can be modified by phosphorylation of sites distant from the functional motifs by induction of global conformational changes (Volkman, Lipson et al. 2001). A striking example for changes in global protein conformation induced by phosphorylation leading to catalytic activation of enzymes is the activation of the Src kinases Fyn and Lck after TCR stimulation (Palacios and Weiss 2004).

This study showed that activated myrPKB tg $CD4^+$ T cells are more resistant to Src kinase inhibitor PP2 and to MEK inhibitors PD98059 and UO126 (Figure 5.9), since the proliferation of myrPKB tg cells was clearly less inhibited in the presence of the inhibitors in comparison to wt $CD4^+$ T cells. In western blot analysis of CD3/CD4 stimulated $CD4^+$ T cells enhanced Erk phosphorylation was detected in myrPKB tg $CD4^+$ T cells (Figure 5.10), but increased phosphorylation of the activatory tyrosines 394 and 417 of Lck and Fyn was not obvious, except for unstimulated myrPKB tg cells. However, assessment of Fyn activity by IVKs revealed Fyn hyperactivity in unstimulated and stimulated myrPKB tg $CD4^+$ T cells and thymocytes (Figure 5.11, Figure 5.13). Increased Fyn activity could contribute to increased inhibitor resistance and increased downstream Erk phosphorylation. Both, PKB and Fyn, are proto-oncogenes. Membrane targeting of PKB was shown to be the mechanism for the oncogenic potential of v-Akt. A mutation in the PH domain of PKB has impact on its oncogenic potential: a glutamic acid to lysine substitution at position 17 in the PH domain led

to increased membrane translocation and thus activation of PKB, and this was associated with the induction of leukemia in mice (Carpten, Faber et al. 2007). In PKB tg mice, hyperactivity of PKB was induced by its constitutive membrane targeting via an N-terminal myristoylation sequence. Thus, the mechanism of hyperactivation of PKB in tg mice used here is similar to hyperactivation of PKB causing cancer. Indeed, myrPKB tg mice develop lymphoma on a homozygous background (data not shown). Our data suggest that a cross-talk of PKB with Fyn, resulting in enhanced Fyn activity, could be an important mechanism by which aberrant PKB signaling fosters tumorigenesis. Enhanced Fyn activity could result from a direct interaction of PKB with Fyn or from indirect mechanisms like phosphorylation and inactivation of Csk. Both, Fyn and Csk harbor canonical PKB phosphorylation sites and inhibition of Csk by PKB phosphorylation could therefore enhance Fyn activity.

Phosphorylation of Src in the N-terminal region at S12 in PMA stimulated SH-SY5Y cells (an adrenergic clone of the human neuroblastoma cell line SK-N-SH) coincided with increased Src activity and neuronal cell differentiation (Bjelfman, Meyerson et al. 1990), and PKC was shown to phosphorylate S12 of Src *in vitro* (Gould, Woodgett et al. 1985). Phosphorylation of Src at S17 mediated by PKA (Schmitt and Stork 2002; Abrahamsen, Vang et al. 2003; Obara, Labudda et al. 2004) and at S75 mediated by Cdk5 kinase (Kato and Maeda 1995; Kato and Maeda 1997; Kato and Maeda 1999) have been reported, and phosphorylation of S75 is associated with spherical cell morphology. Chicken Src is also phosphorylated in the N-terminal region at T34, T46 and S72 during mitosis of fibroblasts and the catalytic component of metaphase promoting factor (MPF) from Xenopus eggs phosphorylates these sites *in vitro* (Chackalaparampil and Shalloway 1988; Shenoy, Choi et al. 1989). The phosphorylations at T34 and S72 increase the kinase activity of Src in mitotic cells (Shenoy, Chackalaparampil et al. 1992). However, the exact functions of these phosphorylations and whether they occur in T cells are not clear.

PKA phosphorylates S364 of Csk leading to enhanced Csk activity thereby causing reduced Lck activity and thus reduced TCR ζ-chain phosphorylation (Vang, Torgersen et al. 2001). PKA and PKC phosphorylate Lck at S42 and Erk phosphorylates Lck at S59 *in vitro* (Watts, Sanghera et al. 1993; Winkler, Park et al. 1993). Lck S59 phosphorylation by Erk is considered as a mechanism, which inhibits dephosphorylation and inactivation of Lck by the SH2 domain-containing phosphatase 1 (SHP-1) (Stefanova, Hemmer et al. 2003). Altogether, these data suggest that S/T phosphorylations of Src kinases in T cells have a central impact on their function.

In this work, Fyn was identified as a novel potential substrate of PKB, and T82 of Fyn was identified as the critical PKB phosphorylation site *in vitro*. T82 is conserved in mouse and human Fyn. T12, which is present in human Fyn but missing in mouse Fyn, was not

phosphorylated by PKB (Figure 5.22). Phosphorylation of Csk by PKB *in vitro* was not detected under the experimental conditions used (Figure 5.23). However, it cannot be excluded that the canonical PKB site in the kinase domain of Csk, nevertheless, could be a PKB target *in vivo*, for instance, after priming of Csk by other kinases. The PKB phosphorylation site, T82, is positioned in the unique region of Fyn in close proximity to its SH3 domain. Thus, phosphorylation of T82 could modify the local conformation of Fyn and thereby influence the conformation of the SH3 domain. This could reduce its binding to the SH2-kinase linker region of Fyn, which stabilizes the inactive conformation. Therefore, a modification of the local conformation of Fyn by phosphorylation of T82 could modify its global conformation and thereby increase Fyn activity. Binding of PKB to Fyn, which was detected in HEK 293T cells overexpressing both molecules (Figure 5.18), could also change the conformation of Fyn and thus enhance its activity or the interaction with specific binding partners.

Besides increased Fyn activity, Erk phosphorylation was enhanced in myrPKB tg $CD4^+$ T cells (Figure 5.10). Interaction of PKB and Erk was found in mouse kidney proximal tubular epithelial (MK-PT) cells. Erk and PKB were shown to co-immunoprecipitate as parts of a multimolecular complex additionally containing PDK1 and ribosomal S6 kinase (Rsk) (Sinha, Bannergee et al. 2004). Enhanced Erk activity could have an impact on Lck by reduced binding of the phosphatase SHP-1 due to enhanced phosphorylation of Lck at S59 by Erk. Since SHP-1 dephosphorylates the activatory Y394 of Lck (Chiang and Sefton 2001), decreased SHP-1 binding to Lck should result in enhanced Lck activity. Lck is positioned upsream of Erk signaling, and hyperactivity of Lck should result in enhanced Erk phosphorylation, constituting a positive feedback loop. Indeed, Lck was shown to be hyperactive in thymocytes from myrPKB tg mice (Na, Patra et al. 2003). The activation of Fyn in $CD4^+$ T cells stimulated by co-aggregation of TCR and CD4 was shown to be dependent on Lck in lipid raft fractions (Filipp, Zhang et al. 2003). The dependency of Fyn activation on the presence of active Lck was also found in NIH 3T3 cells overexpressing these two enzymes (Filipp, Moemeni et al. 2008). Thus, hyperactivity of Fyn in myrPKB tg thymocytes could also be caused by enhanced activity of Lck. Both, hyperactive Fyn and Lck, could contribute to hyperphosphorylation of Erk in myrPKB tg cells.

Fyn and Lck were shown to contribute to Erk phosphorylation but via different mechanisms. $Lck^{-/-}$ $CD4^+$ T cells display reduced activity of ZAP-70, reduced phosphorylation of LAT at Y136, which is important for recruitment of PLCγ, reduced recruitment of Ras GRP to the plasma membrane and diminished phosphorylation of PKCθ at T538. The RasGRP pathway is mainly responsible for the activation of Erk in Jurkat cells (Roose, Mollenauer et al. 2005). Although this pathway is switched off in $Lck^{-/-}$ $CD4^+$ T cells, Erk phosphorylation was still

induced after stimulation with CD3 Ab or CD3+CD4 Abs. Since pErk levels were only moderately reduced in $Lck^{-/-}$ in comparison to wt $CD4^+$ T cells, it seems that Lck contributes to Erk activation but does not represent the only pathway mediating Erk phosphorylation. On the other hand, co-elimination of Fyn in $Lck^{-/-}$ $CD4^+$ T cells nearly completely abrogated Erk activation after stimulation, indicating that Fyn mediates phosphorylation of Erk by another pathway than Lck (Lovatt, Filby et al. 2006). The detected increased Fyn activity in myrPKB tg cells in combination with enhanced Lck activity, as previously shown for thymocytes, thus could lead to enhanced Erk activation, decreased sensitivity to Src/MEK inhibitors and enhanced proliferation.

It is important to note that Fyn does not exclusively act as a positive regulator of TCR signaling, but can also function as a negative regulator. A positive regulatory function of Fyn was deduced from slightly reduced proliferative responses of $Fyn^{-/-}$ splenic T cells after stimulation with CD3 Ab and PMA and their low level of IL-2 secretion. A stronger proliferative defect was found in $Fyn^{-/-}$ thymocytes after stimulation with CD3 Abs and PMA (Appleby, Gross et al. 1992; Stein, Lee et al. 1992). On the contrary, $Fyn^{-/-}$ T cells were shown to be hyperproliferative and to produce more IL-2 after peptide/MHC stimulation. Enhanced proliferation of $Fyn^{-/-}$ T cells was blocked by IL-2 Abs, indicating that the hyperproliferation was driven by IL-2. Furthermore, $Fyn^{-/-}$ T cells required shorter peptide/MHC stimulation for the induction of IL-2 production than their wt counterparts. Under these conditions, Fyn functions as a negative regulator of TCR signaling and has an impact on the response of primary T cells to antigens (Filby, Seddon et al. 2007).

Fyn is implicated in another negative regulatory mechanism of TCR signaling as it phosphorylates Y314 of PAG, the site for recruitment of Csk to PAG (Brdicka, Pavlistova et al. 2000; Yasuda, Nagafuku et al. 2002; Filby, Seddon et al. 2007). Thereby, Csk is localized in the proximity of its substrates Lck and Fyn and can catalyze the inhibitory phosphorylations at Y505 and Y528, respectively. Interestingly, we detected increased Fyn activity in myrPKB tg T cells and thymocytes, but this did not lead to a proportional increase of Y314 phosphorylation of PAG (Figure 5.12). The amount of Csk associated with PAG was also not increased (Figure 5.13). This could be caused by hyperactivity of so far unknown phosphatases mediating dephosphorylation of PAG. Reduction of the temperature from 37°C to 4°C shifted the reaction equilibrium between kinases and phosphatases towards kinases resulting in increased tyrosine phosphorylation (Figure 5.14). Even when experiments were performed at 4°C, phosphorylation of Y314 of PAG in myrPKB tg cells showing Fyn hyperactivity was not enhanced (Figure 5.15). Thus, it can be excluded to a great extent that the lack of increased phosphorylation of PAG at Y314 in PKB tg cells is caused by increased activity of phosphatases that dephosphorylate PAG at pY314. Likewise, PAG was associated with similar amounts of Csk in wt and myrPKB tg cells, even at 4°C (Figure 5.16).

We also considered that the discrepancy between Fyn hyperactivity and PAG Y314 phosphorylation could result from sequestration of PAG from hyperactive Fyn in myrPKB tg cells. We, therefore, performed sucrose density gradient centrifugation to analyze the distribution of Fyn and PAG in lipid rafts and cytosolic fractions of wt and myrPKB tg thymocytes. Fyn and PAG were present in the same lipid raft fractions, i.e. in PKB tg thymocytes PAG and Fyn were not sequestered from each other. In CD3 Ab-stimulated cells (120 min at 4°C), increased amounts of Y417 phosphorylated Fyn were found in lipid raft fraction 1 of myrPKB tg cells. However, there was no proportional increase in phosphorylation of PAG at Y314 (Figure 5.17). Thus, hyperactive Fyn is present in the same lipid raft fraction as PAG, but does not enhance PAG phosphorylation. So far, we can only speculate on the mechanism for this intriguing result. Physical interaction of Fyn with myrPKB or phosphorylation of Fyn by myrPKB, which is also localized in lipid rafts, could recruit other molecules into the proximity of Fyn and prevent PAG phosphorylation by this phosphorylated form of Fyn. Indeed, Fyn and myrPKB co-immunoprecipitated when overexpressed in HEK 293T cells (Figure 5.18), showing that Fyn and myrPKB can associate *in vivo*. Whether Fyn and myrPKB interact directly or via additional proteins functioning as adapters is still open. So far, we could not detect myrPKB association with Fyn in thymocytes or T cells. Perhaps only small amounts of the total pools of Fyn and myrPKB interact which each other for a restricted period of time or the association is very labile. Immunoprecipitations of PKB/Fyn/PAG from lipid rafts should shed light on this. Fyn and myrPKB do not only associate when overexpressed in HEK 293T cells, but transfection of myrPKB resulted in reduced phosphorylation of Fyn at its activatory tyrosine 417 and reduced phosphorylation of PAG at Y314. Thus, it seems that PKB reduces Fyn activity when overexpressed in HEK 293T cells, an opposite effect as seen in thymocytes and $CD4^+$ T cells where myrPKB enhanced Fyn activity. These results confirm a definite cross-talk between PKB and Fyn. However, we can only speculate that the opposite effects of PKB on Fyn activity in T cells and HEK 293T cells result from the different cell types and different expression levels of Fyn and myrPKB.

Taken together, Fyn is a novel substrate of PKB, whereby active myrPKB can influence proximal TCR signaling and T cell activation.

We also analyzed whether myrPKB tg cells respond differentially to signals inducing anergy in T cells. Anergy is a pivotal mechanism to limit ‘unwanted’ T cell activation, e.g. of cells reacting to self-antigens outside the thymus or T cells activated without proper co-stimulation. Human T cells anergized by CD3 stimulation in the absence of CD28 co-stimulation display enhanced Fyn activity correlating with increased phosphorylation of PAG at Y317 and increased Csk association to PAG. This demonstrates that hightened Fyn activity is involved in anergy (Smida, Posevitz-Fejfar et al. 2007). Also, induction of anergy in

mouse T cells by prolonged ionomycin treatment resulted in enhanced binding of FynT to PAG, indicating that Fyn also has a function in the model of ionomycin induced anergy (Davidson, Schraven et al. 2007).

In view of increased Fyn activity in myrPKB tg T cells, we stimulated wt and myrPKB tg $CD4^+$ T cells with CD3+CD28 Abs, expanded them for 3 days in IL-2 and then induced anergy by treatment of cells for 16 h with ionomycin. Thereafter, cells were restimulated to measure their proliferative response and Fyn activity was determined by IVKs. Our experiments showed that CD3 Ab induced proliferation of ionomycin treated wt $CD4^+$ T cells was reduced by 84% in comparison to wt control cells, whereas proliferation of ionomycin treated myrPKB tg $CD4^+$ T cells was only reduced by 44% (Figure 5.24). Thus, induction of anergy is less efficient in myrPKB tg cells.

Analysis of Fyn activity after anergy induction showed increased Fyn activity in wt cells but not myrPKB tg cells. Thus, lower Fyn activity in ionomycin treated myrPKB tg $CD4^+$ T cells coincided with weak induction of anergy and strong proliferation, whereas ionomycin treatment of wt $CD4^+$ T cells resulted in enhanced Fyn activity and strong hyporesponsiveness to TCR/CD3 signals (Figure 5.24, Figure 5.25). Weaker Fyn activity in PKB tg cells should lead to less efficient PAG phosphorylation and recruitment of Csk and other factors that inhibit Ras-Erk signaling (Smida, Posevitz-Fejfar et al. 2007). In addition, hyperactivity of Fyn in non-anergized PKB tg cells was not associated with increased PAG Y314 phosphorylation. Thus, other Fyn dependent and also Fyn independent mechanisms regulated by PKB may contribute to the relative resistance of myrPKB tg cells to anergy induction by ionomycin.

In summary, this study demonstrates that elevated PKB signals critically affect thymocyte differentiation processes, T cell activation and anergy induction, involving a cross-talk with a novel substrate Fyn and NFAT. Since Fyn and other Src kinases are proto-oncogenes involved in cancer progression, which is also valid for PKB, regulation of Fyn activity by PKB may represent a novel and important mechanism, whereby PKB promotes tumor formation in T cells.

7 References

Abraham, N., M. C. Miceli, et al. (1991). "Enhancement of T-cell responsiveness by the lymphocyte-specific tyrosine protein kinase p56lck." Nature **350**(6313): 62-6.

Abrahamsen, H., T. Vang, et al. (2003). "Protein kinase A intersects SRC signaling in membrane microdomains." J Biol Chem **278**(19): 17170-7.

Adler, A. J., C. T. Huang, et al. (2000). "In vivo CD4+ T cell tolerance induction versus priming is independent of the rate and number of cell divisions." J Immunol **164**(2): 649-55.

Ahmed, N. N., T. F. Franke, et al. (1993). "The proteins encoded by c-akt and v-akt differ in post-translational modification, subcellular localization and oncogenic potential." Oncogene **8**(7): 1957-63.

Akiba, H., K. Takeda, et al. (2005). "The role of ICOS in the CXCR5+ follicular B helper T cell maintenance in vivo." J Immunol **175**(4): 2340-8.

Alessi, D. R., M. Andjelkovic, et al. (1996). "Mechanism of activation of protein kinase B by insulin and IGF-1." Embo J **15**(23): 6541-51.

Altomare, D. A., K. Guo, et al. (1995). "Cloning, chromosomal localization and expression analysis of the mouse Akt2 oncogene." Oncogene **11**(6): 1055-60.

Andjelkovic, M., T. Jakubowicz, et al. (1996). "Activation and phosphorylation of a pleckstrin homology domain containing protein kinase (RAC-PK/PKB) promoted by serum and protein phosphatase inhibitors." Proc Natl Acad Sci U S A **93**(12): 5699-704.

Appleby, M. W., J. A. Gross, et al. (1992). "Defective T cell receptor signaling in mice lacking the thymic isoform of p59fyn." Cell **70**(5): 751-63.

Aramburu, J., F. Garcia-Cozar, et al. (1998). "Selective inhibition of NFAT activation by a peptide spanning the calcineurin targeting site of NFAT." Mol Cell **1**(5): 627-37.

Asai, K., S. Hachimura, et al. (2002). "T cell hyporesponsiveness induced by oral administration of ovalbumin is associated with impaired NFAT nuclear translocation and p27kip1 degradation." J Immunol **169**(9): 4723-31.

Atkinson, E. A., H. Ostergaard, et al. (1996). "A physical interaction between the cell death protein Fas and the tyrosine kinase p59fynT." J Biol Chem **271**(11): 5968-71.

Avni, O., D. Lee, et al. (2002). "T(H) cell differentiation is accompanied by dynamic changes in histone acetylation of cytokine genes." Nat Immunol **3**(7): 643-51.

Avota, E., A. Avots, et al. (2001). "Disruption of Akt kinase activation is important for immunosuppression induced by measles virus." Nat Med **7**(6): 725-31.

Avots, A., M. Buttmann, et al. (1999). "CBP/p300 integrates Raf/Rac-signaling pathways in the transcriptional induction of NF-ATc during T cell activation." Immunity **10**(5): 515-24.

Badour, K., J. Zhang, et al. (2004). "Fyn and PTP-PEST-mediated regulation of Wiskott-Aldrich syndrome protein (WASp) tyrosine phosphorylation is required for coupling T cell antigen receptor engagement to WASp effector function and T cell activation." J Exp Med **199**(1): 99-112.

Bassing, C. H., W. Swat, et al. (2002). "The mechanism and regulation of chromosomal V(D)J recombination." Cell **109 Suppl**: S45-55.

Beals, C. R., C. M. Sheridan, et al. (1997). "Nuclear export of NF-ATc enhanced by glycogen synthase kinase-3." Science **275**(5308): 1930-4.

Bellacosa, A., J. R. Testa, et al. (1991). "A retroviral oncogene, akt, encoding a serine-threonine kinase containing an SH2-like region." Science **254**(5029): 274-7.

Ben-Amor, A., M. C. Leite-De-Moraes, et al. (1996). "In vitro T cell unresponsiveness following low-dose injection of anti-CD3 MoAb." Clin Exp Immunol **103**(3): 491-8.

Berg, L. J., L. D. Finkelstein, et al. (2005). "Tec family kinases in T lymphocyte development and function." Annu Rev Immunol **23**: 549-600.

Berger, S. L. (1999). "Gene activation by histone and factor acetyltransferases." Curr Opin Cell Biol **11**(3): 336-41.

Bettelli, E., M. Dastrange, et al. (2005). "Foxp3 interacts with nuclear factor of activated T cells and NF-kappa B to repress cytokine gene expression and effector functions of T helper cells." Proc Natl Acad Sci U S A **102**(14): 5138-43.

Beverly, B., S. M. Kang, et al. (1992). "Reversal of in vitro T cell clonal anergy by IL-2 stimulation." Int Immunol **4**(6): 661-71.

Beyers, A. D., L. L. Spruyt, et al. (1992). "Molecular associations between the T-lymphocyte antigen receptor complex and the surface antigens CD2, CD4, or CD8 and CD5." Proc Natl Acad Sci U S A **89**(7): 2945-9.

Bjelfman, C., G. Meyerson, et al. (1990). "Early activation of endogenous pp60src kinase activity during neuronal differentiation of cultured human neuroblastoma cells." Mol Cell Biol **10**(1): 361-70.

Bodor, J. and J. F. Habener (1998). "Role of transcriptional repressor ICER in cyclic AMP-mediated attenuation of cytokine gene expression in human thymocytes." J Biol Chem **273**(16): 9544-51.

Boggon, T. J. and M. J. Eck (2004). "Structure and regulation of Src family kinases." Oncogene **23**(48): 7918-27.

Bommhardt, U., K. C. Chang, et al. (2004). "Akt decreases lymphocyte apoptosis and improves survival in sepsis." J Immunol **172**(12): 7583-91.

Boussiotis, V. A., G. J. Freeman, et al. (1997). "Maintenance of human T cell anergy: blocking of IL-2 gene transcription by activated Rap1." Science **278**(5335): 124-8.

Boussiotis, V. A., G. J. Freeman, et al. (1993). "B7 but not intercellular adhesion molecule-1 costimulation prevents the induction of human alloantigen-specific tolerance." J Exp Med **178**(5): 1753-63.

Brazil, D. P. and B. A. Hemmings (2001). "Ten years of protein kinase B signalling: a hard Akt to follow." Trends Biochem Sci **26**(11): 657-64.

Brdicka, T., D. Pavlistova, et al. (2000). "Phosphoprotein associated with glycosphingolipid-enriched microdomains (PAG), a novel ubiquitously expressed transmembrane adaptor protein, binds the protein tyrosine kinase csk and is involved in regulation of T cell activation." J Exp Med **191**(9): 1591-604.

Brodbeck, D., P. Cron, et al. (1999). "A human protein kinase Bgamma with regulatory phosphorylation sites in the activation loop and in the C-terminal hydrophobic domain." J Biol Chem **274**(14): 9133-6.

Brunkow, M. E., E. W. Jeffery, et al. (2001). "Disruption of a new forkhead/winged-helix protein, scurfin, results in the fatal lymphoproliferative disorder of the scurfy mouse." Nat Genet **27**(1): 68-73.

Bubeck Wardenburg, J., C. Fu, et al. (1996). "Phosphorylation of SLP-76 by the ZAP-70 protein-tyrosine kinase is required for T-cell receptor function." J Biol Chem **271**(33): 19641-4.

Calera, M. R., C. Martinez, et al. (1998). "Insulin increases the association of Akt-2 with Glut4-containing vesicles." J Biol Chem **273**(13): 7201-4.

Cantrell, D. A. (2003). "GTPases and T cell activation." Immunol Rev **192**: 122-30.

Cardone, M. H., N. Roy, et al. (1998). "Regulation of cell death protease caspase-9 by phosphorylation." Science **282**(5392): 1318-21.

Carpten, J. D., A. L. Faber, et al. (2007). "A transforming mutation in the pleckstrin homology domain of AKT1 in cancer." Nature **448**(7152): 439-44.

Chackalaparampil, I. and D. Shalloway (1988). "Altered phosphorylation and activation of pp60c-src during fibroblast mitosis." Cell **52**(6): 801-10.

Chakraborty, A. K., J. Das, et al. (2009). "Molecular origin and functional consequences of digital signaling and hysteresis during Ras activation in lymphocytes." Sci Signal **2**(66): pt2.

Chan, A. C., M. Dalton, et al. (1995). "Activation of ZAP-70 kinase activity by phosphorylation of tyrosine 493 is required for lymphocyte antigen receptor function." Embo J **14**(11): 2499-508.

Chan, B., A. Lanyi, et al. (2003). "SAP couples Fyn to SLAM immune receptors." Nat Cell Biol **5**(2): 155-60.

Chen, L., J. N. Glover, et al. (1998). "Structure of the DNA-binding domains from NFAT, Fos and Jun bound specifically to DNA." Nature **392**(6671): 42-8.
Chen, W. S., P. Z. Xu, et al. (2001). "Growth retardation and increased apoptosis in mice with homozygous disruption of the Akt1 gene." Genes Dev **15**(17): 2203-8.
Chiang, G. G. and B. M. Sefton (2001). "Specific dephosphorylation of the Lck tyrosine protein kinase at Tyr-394 by the SHP-1 protein-tyrosine phosphatase." J Biol Chem **276**(25): 23173-8.
Chiodetti, L., S. Choi, et al. (2006). "Adaptive tolerance and clonal anergy are distinct biochemical states." J Immunol **176**(4): 2279-91.
Cho, H., J. Mu, et al. (2001). "Insulin resistance and a diabetes mellitus-like syndrome in mice lacking the protein kinase Akt2 (PKB beta)." Science **292**(5522): 1728-31.
Cho, H., J. L. Thorvaldsen, et al. (2001). "Akt1/PKBalpha is required for normal growth but dispensable for maintenance of glucose homeostasis in mice." J Biol Chem **276**(42): 38349-52.
Chow, C. W., C. Dong, et al. (2000). "c-Jun NH(2)-terminal kinase inhibits targeting of the protein phosphatase calcineurin to NFATc1." Mol Cell Biol **20**(14): 5227-34.
Chuvpilo, S., E. Jankevics, et al. (2002). "Autoregulation of NFATc1/A expression facilitates effector T cells to escape from rapid apoptosis." Immunity **16**(6): 881-95.
Chuvpilo, S., M. Zimmer, et al. (1999). "Alternative polyadenylation events contribute to the induction of NF-ATc in effector T cells." Immunity **10**(2): 261-9.
Clevers, H., B. Alarcon, et al. (1988). "The T cell receptor/CD3 complex: a dynamic protein ensemble." Annu Rev Immunol **6**: 629-62.
Cloutier, J. F. and A. Veillette (1996). "Association of inhibitory tyrosine protein kinase p50csk with protein tyrosine phosphatase PEP in T cells and other hemopoietic cells." Embo J **15**(18): 4909-18.
Cloutier, J. F. and A. Veillette (1999). "Cooperative inhibition of T-cell antigen receptor signaling by a complex between a kinase and a phosphatase." J Exp Med **189**(1): 111-21.
Coffer, P. J. and J. R. Woodgett (1991). "Molecular cloning and characterisation of a novel putative protein-serine kinase related to the cAMP-dependent and protein kinase C families." Eur J Biochem **201**(2): 475-81.
Coffey, A. J., R. A. Brooksbank, et al. (1998). "Host response to EBV infection in X-linked lymphoproliferative disease results from mutations in an SH2-domain encoding gene." Nat Genet **20**(2): 129-35.
Cohen, P. (2000). "The regulation of protein function by multisite phosphorylation--a 25 year update." Trends Biochem Sci **25**(12): 596-601.
Cooke, M. P., K. M. Abraham, et al. (1991). "Regulation of T cell receptor signaling by a src family protein-tyrosine kinase (p59fyn)." Cell **65**(2): 281-91.
Cooke, M. P. and R. M. Perlmutter (1989). "Expression of a novel form of the fyn proto-oncogene in hematopoietic cells." New Biol **1**(1): 66-74.
Cross, D. A., D. R. Alessi, et al. (1995). "Inhibition of glycogen synthase kinase-3 by insulin mediated by protein kinase B." Nature **378**(6559): 785-9.
da Silva, A. J., Z. Li, et al. (1997). "Cloning of a novel T-cell protein FYB that binds FYN and SH2-domain-containing leukocyte protein 76 and modulates interleukin 2 production." Proc Natl Acad Sci U S A **94**(14): 7493-8.
Das, J., M. Ho, et al. (2009). "Digital signaling and hysteresis characterize ras activation in lymphoid cells." Cell **136**(2): 337-51.
Datta, S. R., H. Dudek, et al. (1997). "Akt phosphorylation of BAD couples survival signals to the cell-intrinsic death machinery." Cell **91**(2): 231-41.
Datta, S. R., A. Katsov, et al. (2000). "14-3-3 proteins and survival kinases cooperate to inactivate BAD by BH3 domain phosphorylation." Mol Cell **6**(1): 41-51.
Davidson, D., M. Bakinowski, et al. (2003). "Phosphorylation-dependent regulation of T-cell activation by PAG/Cbp, a lipid raft-associated transmembrane adaptor." Mol Cell Biol **23**(6): 2017-28.
Davidson, D., B. Schraven, et al. (2007). "PAG-associated FynT regulates calcium signaling and promotes anergy in T lymphocytes." Mol Cell Biol **27**(5): 1960-73.

Decker, E. L., N. Nehmann, et al. (2003). "Early growth response proteins (EGR) and nuclear factors of activated T cells (NFAT) form heterodimers and regulate proinflammatory cytokine gene expression." Nucleic Acids Res **31**(3): 911-21.

Diehl, J. A., M. Cheng, et al. (1998). "Glycogen synthase kinase-3beta regulates cyclin D1 proteolysis and subcellular localization." Genes Dev **12**(22): 3499-511.

Diehn, M., A. A. Alizadeh, et al. (2002). "Genomic expression programs and the integration of the CD28 costimulatory signal in T cell activation." Proc Natl Acad Sci U S A **99**(18): 11796-801.

Dobenecker, M. W., C. Schmedt, et al. (2005). "The ubiquitously expressed Csk adaptor protein Cbp is dispensable for embryogenesis and T-cell development and function." Mol Cell Biol **25**(23): 10533-42.

Dong, C. (2008). "TH17 cells in development: an updated view of their molecular identity and genetic programming." Nat Rev Immunol **8**(5): 337-48.

Dummler, B., O. Tschopp, et al. (2006). "Life with a single isoform of Akt: mice lacking Akt2 and Akt3 are viable but display impaired glucose homeostasis and growth deficiencies." Mol Cell Biol **26**(21): 8042-51.

Duncliffe, K. N., A. G. Bert, et al. (1997). "A T cell-specific enhancer in the interleukin-3 locus is activated cooperatively by Oct and NFAT elements within a DNase I-hypersensitive site." Immunity **6**(2): 175-85.

Eberl, G., B. Lowin-Kropf, et al. (1999). "Cutting edge: NKT cell development is selectively impaired in Fyn- deficient mice." J Immunol **163**(8): 4091-4.

Ebinu, J. O., D. A. Bottorff, et al. (1998). "RasGRP, a Ras guanyl nucleotide- releasing protein with calcium- and diacylglycerol-binding motifs." Science **280**(5366): 1082-6.

Eck, M. J., S. E. Shoelson, et al. (1993). "Recognition of a high-affinity phosphotyrosyl peptide by the Src homology-2 domain of p56lck." Nature **362**(6415): 87-91.

Eguez, L., A. Lee, et al. (2005). "Full intracellular retention of GLUT4 requires AS160 Rab GTPase activating protein." Cell Metab **2**(4): 263-72.

Ehrhardt, Schmolke, et al. (2006). "Polyethylenimine, a cost-effective transfection reagent." Signal Transduction **6**: 179-184.

Elly, C., S. Witte, et al. (1999). "Tyrosine phosphorylation and complex formation of Cbl-b upon T cell receptor stimulation." Oncogene **18**(5): 1147-56.

Elstrom, R. L., D. E. Bauer, et al. (2004). "Akt stimulates aerobic glycolysis in cancer cells." Cancer Res **64**(11): 3892-9.

Emmel, E. A., C. L. Verweij, et al. (1989). "Cyclosporin A specifically inhibits function of nuclear proteins involved in T cell activation." Science **246**(4937): 1617-20.

Ezekowitz, R. A. B., and Hoffman, J (1998). "Innate immunity: The blossoming of innate immunity." Curr. Opin. Immunol. **10**: 9-11.

Feske, S., R. Draeger, et al. (2000). "The duration of nuclear residence of NFAT determines the pattern of cytokine expression in human SCID T cells." J Immunol **165**(1): 297-305.

Fields, P. E., T. F. Gajewski, et al. (1996). "Blocked Ras activation in anergic CD4+ T cells." Science **271**(5253): 1276-8.

Filby, A., B. Seddon, et al. (2007). "Fyn regulates the duration of TCR engagement needed for commitment to effector function." J Immunol **179**(7): 4635-44.

Filipp, D., B. Moemeni, et al. (2008). "Lck-dependent Fyn activation requires C terminus-dependent targeting of kinase-active Lck to lipid rafts." J Biol Chem **283**(39): 26409-22.

Filipp, D., J. Zhang, et al. (2003). "Regulation of Fyn through translocation of activated Lck into lipid rafts." J Exp Med **197**(9): 1221-7.

Flajnik, M. F. and L. Du Pasquier (2004). "Evolution of innate and adaptive immunity: can we draw a line?" Trends Immunol **25**(12): 640-4.

Fontenot, J. D., J. P. Rasmussen, et al. (2005). "Regulatory T cell lineage specification by the forkhead transcription factor foxp3." Immunity **22**(3): 329-41.

Frauwirth, K. A., M. L. Alegre, et al. (2001). "CTLA-4 is not required for induction of CD8(+) T cell anergy in vivo." J Immunol **167**(9): 4936-41.

Furstenau, U., M. Schwaninger, et al. (1999). "Characterization of a novel calcium response element in the glucagon gene." J Biol Chem **274**(9): 5851-60.
Fusaki, N., A. Iwamatsu, et al. (1997). "Interaction between Sam68 and Src family tyrosine kinases, Fyn and Lck, in T cell receptor signaling." J Biol Chem **272**(10): 6214-9.
Fusaki, N., S. Matsuda, et al. (1996). "Physical and functional interactions of protein tyrosine kinases, p59fyn and ZAP-70, in T cell signaling." J Immunol **156**(4): 1369-77.
Gajewski, T. F., P. Fields, et al. (1995). "Induction of the increased Fyn kinase activity in anergic T helper type 1 clones requires calcium and protein synthesis and is sensitive to cyclosporin A." Eur J Immunol **25**(7): 1836-42.
Gajewski, T. F., D. Qian, et al. (1994). "Anergic T-lymphocyte clones have altered inositol phosphate, calcium, and tyrosine kinase signaling pathways." Proc Natl Acad Sci U S A **91**(1): 38-42.
Gao, T., F. Furnari, et al. (2005). "PHLPP: a phosphatase that directly dephosphorylates Akt, promotes apoptosis, and suppresses tumor growth." Mol Cell **18**(1): 13-24.
Garcia-Cozar, F. J., H. Okamura, et al. (1998). "Two-site interaction of nuclear factor of activated T cells with activated calcineurin." J Biol Chem **273**(37): 23877-83.
Garcon, F., D. T. Patton, et al. (2008). "CD28 provides T-cell costimulation and enhances PI3K activity at the immune synapse independently of its capacity to interact with the p85/p110 heterodimer." Blood **111**(3): 1464-71.
Garofalo, R. S., S. J. Orena, et al. (2003). "Severe diabetes, age-dependent loss of adipose tissue, and mild growth deficiency in mice lacking Akt2/PKB beta." J Clin Invest **112**(2): 197-208.
Geng, L., M. Raab, et al. (1999). "Cutting edge: SLP-76 cooperativity with FYB/FYN-T in the Up-regulation of TCR-driven IL-2 transcription requires SLP-76 binding to FYB at Tyr595 and Tyr651." J Immunol **163**(11): 5753-7.
Germain, R. N. (1994). "MHC-dependent antigen processing and peptide presentation: providing ligands for T lymphocyte activation." Cell **76**(2): 287-99.
Gjorloff-Wingren, A., M. Saxena, et al. (1999). "Characterization of TCR-induced receptor-proximal signaling events negatively regulated by the protein tyrosine phosphatase PEP." Eur J Immunol **29**(12): 3845-54.
Gomez del Arco, P., S. Martinez-Martinez, et al. (2000). "A role for the p38 MAP kinase pathway in the nuclear shuttling of NFATp." J Biol Chem **275**(18): 13872-8.
Gorska, M. M., S. J. Stafford, et al. (2004). "Unc119, a novel activator of Lck/Fyn, is essential for T cell activation." J Exp Med **199**(3): 369-79.
Gould, K. L., J. R. Woodgett, et al. (1985). "Protein kinase C phosphorylates pp60src at a novel site." Cell **42**(3): 849-57.
Griffiths, E. K., C. Krawczyk, et al. (2001). "Positive regulation of T cell activation and integrin adhesion by the adapter Fyb/Slap." Science **293**(5538): 2260-3.
Gwack, Y., S. Sharma, et al. (2006). "A genome-wide Drosophila RNAi screen identifies DYRK-family kinases as regulators of NFAT." Nature **441**(7093): 646-50.
Hanada, M., J. Feng, et al. (2004). "Structure, regulation and function of PKB/AKT--a major therapeutic target." Biochim Biophys Acta **1697**(1-2): 3-16.
Harrington, L. E., R. D. Hatton, et al. (2005). "Interleukin 17-producing CD4+ effector T cells develop via a lineage distinct from the T helper type 1 and 2 lineages." Nat Immunol **6**(11): 1123-32.
He, Z., Y. Y. Cho, et al. (2005). "Regulation of ultraviolet B-induced phosphorylation of histone H3 at serine 10 by Fyn kinase." J Biol Chem **280**(4): 2446-54.
Heissmeyer, V., F. Macian, et al. (2004). "Calcineurin imposes T cell unresponsiveness through targeted proteolysis of signaling proteins." Nat Immunol **5**(3): 255-65.
Hermiston, M. L., Z. Xu, et al. (2003). "CD45: a critical regulator of signaling thresholds in immune cells." Annu Rev Immunol **21**: 107-37.
Hickman, S. P., J. Yang, et al. (2006). "Defective activation of protein kinase C and Ras-ERK pathways limits IL-2 production and proliferation by CD4+CD25+ regulatory T cells." J Immunol **177**(4): 2186-94.

Hirsch, R., M. Eckhaus, et al. (1988). "Effects of in vivo administration of anti-T3 monoclonal antibody on T cell function in mice. I. Immunosuppression of transplantation responses." J Immunol **140**(11): 3766-72.
Ho, I. C., M. R. Hodge, et al. (1996). "The proto-oncogene c-maf is responsible for tissue-specific expression of interleukin-4." Cell **85**(7): 973-83.
Hodge, M. R., A. M. Ranger, et al. (1996). "Hyperproliferation and dysregulation of IL-4 expression in NF-ATp-deficient mice." Immunity **4**(4): 397-405.
Hogan, P. G., L. Chen, et al. (2003). "Transcriptional regulation by calcium, calcineurin, and NFAT." Genes Dev **17**(18): 2205-32.
Horejsi, V., W. Zhang, et al. (2004). "Transmembrane adaptor proteins: organizers of immunoreceptor signalling." Nat Rev Immunol **4**(8): 603-16.
Huang, G. N., D. L. Huso, et al. (2008). "NFAT binding and regulation of T cell activation by the cytoplasmic scaffolding Homer proteins." Science **319**(5862): 476-81.
Huang, J., D. Tilly, et al. (2000). "T-cell receptor antagonists induce Vav phosphorylation by selective activation of Fyn kinase." Proc Natl Acad Sci U S A **97**(20): 10923-9.
Hunter, S., E. A. Burton, et al. (1999). "Fyn associates with Cbl and phosphorylates tyrosine 731 in Cbl, a binding site for phosphatidylinositol 3-kinase." J Biol Chem **274**(4): 2097-106.
Iacobelli, M., W. Wachsman, et al. (2000). "Repression of IL-2 promoter activity by the novel basic leucine zipper p21SNFT protein." J Immunol **165**(2): 860-8.
Irving, B. A., A. C. Chan, et al. (1993). "Functional characterization of a signal transducing motif present in the T cell antigen receptor zeta chain." J Exp Med **177**(4): 1093-103.
Jacinto, E., V. Facchinetti, et al. (2006). "SIN1/MIP1 maintains rictor-mTOR complex integrity and regulates Akt phosphorylation and substrate specificity." Cell **127**(1): 125-37.
Jacobs, S. R., C. E. Herman, et al. (2008). "Glucose uptake is limiting in T cell activation and requires CD28-mediated Akt-dependent and independent pathways." J Immunol **180**(7): 4476-86.
Jain, J., P. G. McCaffrey, et al. (1992). "Nuclear factor of activated T cells contains Fos and Jun." Nature **356**(6372): 801-4.
James, S. R., C. P. Downes, et al. (1996). "Specific binding of the Akt-1 protein kinase to phosphatidylinositol 3,4,5-trisphosphate without subsequent activation." Biochem J **315 (Pt 3)**: 709-13.
Janeway, C. A., Jr. and R. Medzhitov (2002). "Innate immune recognition." Annu Rev Immunol **20**: 197-216.
Jenkins, M. K., C. A. Chen, et al. (1990). "Inhibition of antigen-specific proliferation of type 1 murine T cell clones after stimulation with immobilized anti-CD3 monoclonal antibody." J Immunol **144**(1): 16-22.
Jenkins, M. K., D. M. Pardoll, et al. (1987). "Molecular events in the induction of a nonresponsive state in interleukin 2-producing helper T-lymphocyte clones." Proc Natl Acad Sci U S A **84**(15): 5409-13.
Jenkins, M. K. and R. H. Schwartz (1987). "Antigen presentation by chemically modified splenocytes induces antigen-specific T cell unresponsiveness in vitro and in vivo." J Exp Med **165**(2): 302-19.
Jo, E. K., H. Wang, et al. (2005). "An essential role for SKAP-55 in LFA-1 clustering on T cells that cannot be substituted by SKAP-55R." J Exp Med **201**(11): 1733-9.
Johnson, D. R., R. S. Bhatnagar, et al. (1994). "Genetic and biochemical studies of protein N-myristoylation." Annu Rev Biochem **63**: 869-914.
Jones, P. F., T. Jakubowicz, et al. (1991). "Molecular cloning of a second form of rac protein kinase." Cell Regul **2**(12): 1001-9.
Jones, P. F., T. Jakubowicz, et al. (1991). "Molecular cloning and identification of a serine/threonine protein kinase of the second-messenger subfamily." Proc Natl Acad Sci U S A **88**(10): 4171-5.
Jones, R. G., A. R. Elford, et al. (2002). "CD28-dependent activation of protein kinase B/Akt blocks Fas-mediated apoptosis by preventing death-inducing signaling complex assembly." J Exp Med **196**(3): 335-48.

Jones, R. G., M. Parsons, et al. (2000). "Protein kinase B regulates T lymphocyte survival, nuclear factor kappaB activation, and Bcl-X(L) levels in vivo." J Exp Med **191**(10): 1721-34.

Jones, R. G., S. D. Saibil, et al. (2005). "NF-kappaB couples protein kinase B/Akt signaling to distinct survival pathways and the regulation of lymphocyte homeostasis in vivo." J Immunol **175**(6): 3790-9.

Juntilla, M. M., J. A. Wofford, et al. (2007). "Akt1 and Akt2 are required for alphabeta thymocyte survival and differentiation." Proc Natl Acad Sci U S A **104**(29): 12105-10.

Kagi, D., F. Vignaux, et al. (1994). "Fas and perforin pathways as major mechanisms of T cell-mediated cytotoxicity." Science **265**(5171): 528-30.

Kaminuma, O. (2008). "Selective inhibitors of nuclear factor of activated T cells: potential therapeutic drugs for the treatment of immunological and inflammatory diseases." Inflamm Allergy Drug Targets **7**(1): 35-40.

Kandel, E. S. and N. Hay (1999). "The regulation and activities of the multifunctional serine/threonine kinase Akt/PKB." Exp Cell Res **253**(1): 210-29.

Kandel, E. S., J. Skeen, et al. (2002). "Activation of Akt/protein kinase B overcomes a G(2)/m cell cycle checkpoint induced by DNA damage." Mol Cell Biol **22**(22): 7831-41.

Kang, H., C. Freund, et al. (2000). "SH3 domain recognition of a proline-independent tyrosine-based RKxxYxxY motif in immune cell adaptor SKAP55." Embo J **19**(12): 2889-99.

Karin, M. and T. Hunter (1995). "Transcriptional control by protein phosphorylation: signal transmission from the cell surface to the nucleus." Curr Biol **5**(7): 747-57.

Kato, G. and S. Maeda (1995). "Novel phosphorylation at a mitotic site, serine 75, in human pp60c-src from unsynchronized human tumor cells having a spherical morphology." Biochem Biophys Res Commun **216**(2): 619-29.

Kato, G. and S. Maeda (1997). "High-level expression of human c-Src can cause a spherical morphology without loss of anchorage-dependent growth of NIH 3T3 cells." FEBS Lett **411**(2-3): 317-21.

Kato, G. and S. Maeda (1999). "Neuron-specific Cdk5 kinase is responsible for mitosis-independent phosphorylation of c-Src at Ser75 in human Y79 retinoblastoma cells." J Biochem **126**(5): 957-61.

Kawabuchi, M., Y. Satomi, et al. (2000). "Transmembrane phosphoprotein Cbp regulates the activities of Src-family tyrosine kinases." Nature **404**(6781): 999-1003.

Kearney, E. R., K. A. Pape, et al. (1994). "Visualization of peptide-specific T cell immunity and peripheral tolerance induction in vivo." Immunity **1**(4): 327-39.

Kel, A., O. Kel-Margoulis, et al. (1999). "Recognition of NFATp/AP-1 composite elements within genes induced upon the activation of immune cells." J Mol Biol **288**(3): 353-76.

Kiani, A., F. J. Garcia-Cozar, et al. (2001). "Regulation of interferon-gamma gene expression by nuclear factor of activated T cells." Blood **98**(5): 1480-8.

Kiani, A., J. P. Viola, et al. (1997). "Down-regulation of IL-4 gene transcription and control of Th2 cell differentiation by a mechanism involving NFAT1." Immunity **7**(6): 849-60.

King, C. G., J. L. Buckler, et al. (2008). "Cutting edge: requirement for TRAF6 in the induction of T cell anergy." J Immunol **180**(1): 34-8.

King, F. W., J. Skeen, et al. (2004). "Inhibition of Chk1 by activated PKB/Akt." Cell Cycle **3**(5): 634-7.

Kishi, H., X. C. Wei, et al. (2000). "Lineage-specific regulation of the murine RAG-2 promoter: GATA-3 in T cells and Pax-5 in B cells." Blood **95**(12): 3845-52.

Kliche, S., D. Breitling, et al. (2006). "The ADAP/SKAP55 signaling module regulates T-cell receptor-mediated integrin activation through plasma membrane targeting of Rap1." Mol Cell Biol **26**(19): 7130-44.

Knighton, D. R., J. H. Zheng, et al. (1991). "Crystal structure of the catalytic subunit of cyclic adenosine monophosphate-dependent protein kinase." Science **253**(5018): 407-14.

Kobayashi, N., T. Kono, et al. (1993). "Functional coupling of the src-family protein tyrosine kinases p59fyn and p53/56lyn with the interleukin 2 receptor: implications for redundancy and pleiotropism in cytokine signal transduction." Proc Natl Acad Sci U S A **90**(9): 4201-5.

Koegl, M., P. Zlatkine, et al. (1994). "Palmitoylation of multiple Src-family kinases at a homologous N-terminal motif." Biochem J **303 (Pt 3)**: 749-53.
Kohn, A. D., S. A. Summers, et al. (1996). "Expression of a constitutively active Akt Ser/Thr kinase in 3T3-L1 adipocytes stimulates glucose uptake and glucose transporter 4 translocation." J Biol Chem **271**(49): 31372-8.
Konishi, H., S. Kuroda, et al. (1995). "Molecular cloning and characterization of a new member of the RAC protein kinase family: association of the pleckstrin homology domain of three types of RAC protein kinase with protein kinase C subspecies and beta gamma subunits of G proteins." Biochem Biophys Res Commun **216**(2): 526-34.
Konishi, H., H. Matsuzaki, et al. (1996). "Activation of RAC-protein kinase by heat shock and hyperosmolarity stress through a pathway independent of phosphatidylinositol 3-kinase." Proc Natl Acad Sci U S A **93**(15): 7639-43.
Koretzky, G. A., J. Picus, et al. (1991). "Tyrosine phosphatase CD45 is required for T-cell antigen receptor and CD2-mediated activation of a protein tyrosine kinase and interleukin 2 production." Proc Natl Acad Sci U S A **88**(6): 2037-41.
Kovacina, K. S., G. Y. Park, et al. (2003). "Identification of a proline-rich Akt substrate as a 14-3-3 binding partner." J Biol Chem **278**(12): 10189-94.
Kuo, T. C. and M. S. Schlissel (2009). "Mechanisms controlling expression of the RAG locus during lymphocyte development." Curr Opin Immunol **21**(2): 173-8.
Lafont, V., E. Astoul, et al. (2000). "The T cell antigen receptor activates phosphatidylinositol 3-kinase-regulated serine kinases protein kinase B and ribosomal S6 kinase 1." FEBS Lett **486**(1): 38-42.
Lamb, J. R., B. J. Skidmore, et al. (1983). "Induction of tolerance in influenza virus-immune T lymphocyte clones with synthetic peptides of influenza hemagglutinin." J Exp Med **157**(5): 1434-47.
Lanoue, A., C. Bona, et al. (1997). "Conditions that induce tolerance in mature CD4+ T cells." J Exp Med **185**(3): 405-14.
Latour, S., G. Gish, et al. (2001). "Regulation of SLAM-mediated signal transduction by SAP, the X-linked lymphoproliferative gene product." Nat Immunol **2**(8): 681-90.
Latour, S., R. Roncagalli, et al. (2003). "Binding of SAP SH2 domain to FynT SH3 domain reveals a novel mechanism of receptor signalling in immune regulation." Nat Cell Biol **5**(2): 149-54.
Latour, S. and A. Veillette (2001). "Proximal protein tyrosine kinases in immunoreceptor signaling." Curr Opin Immunol **13**(3): 299-306.
Lee, M. and J. Park (2006). "Regulation of NFAT activation: a potential therapeutic target for immunosuppression." Mol Cells **22**(1): 1-7.
Legname, G., B. Seddon, et al. (2000). "Inducible expression of a p56Lck transgene reveals a central role for Lck in the differentiation of CD4 SP thymocytes." Immunity **12**(5): 537-46.
Letourneur, F. and R. D. Klausner (1992). "Activation of T cells by a tyrosine kinase activation domain in the cytoplasmic tail of CD3 epsilon." Science **255**(5040): 79-82.
Li, W., C. D. Whaley, et al. (1996). "Blocked signal transduction to the ERK and JNK protein kinases in anergic CD4+ T cells." Science **271**(5253): 1272-6.
Liang, J., J. Zubovitz, et al. (2002). "PKB/Akt phosphorylates p27, impairs nuclear import of p27 and opposes p27-mediated G1 arrest." Nat Med **8**(10): 1153-60.
Liu, J., H. Kang, et al. (1998). "FYB (FYN binding protein) serves as a binding partner for lymphoid protein and FYN kinase substrate SKAP55 and a SKAP55-related protein in T cells." Proc Natl Acad Sci U S A **95**(15): 8779-84.
Lopez-Rodriguez, C., J. Aramburu, et al. (1999). "NFAT5, a constitutively nuclear NFAT protein that does not cooperate with Fos and Jun." Proc Natl Acad Sci U S A **96**(13): 7214-9.
Lovatt, M., A. Filby, et al. (2006). "Lck regulates the threshold of activation in primary T cells, while both Lck and Fyn contribute to the magnitude of the extracellular signal-related kinase response." Mol Cell Biol **26**(22): 8655-65.

Luo, C., E. Burgeon, et al. (1996). "Recombinant NFAT1 (NFATp) is regulated by calcineurin in T cells and mediates transcription of several cytokine genes." Mol Cell Biol **16**(7): 3955-66.

Luo, C., E. Burgeon, et al. (1996). "Mechanisms of transactivation by nuclear factor of activated T cells-1." J Exp Med **184**(1): 141-7.

Macian, F. (2005). "NFAT proteins: key regulators of T-cell development and function." Nat Rev Immunol **5**(6): 472-84.

Macian, F., F. Garcia-Cozar, et al. (2002). "Transcriptional mechanisms underlying lymphocyte tolerance." Cell **109**(6): 719-31.

Macian, F., C. Lopez-Rodriguez, et al. (2001). "Partners in transcription: NFAT and AP-1." Oncogene **20**(19): 2476-89.

Maehama, T. and J. E. Dixon (1998). "The tumor suppressor, PTEN/MMAC1, dephosphorylates the lipid second messenger, phosphatidylinositol 3,4,5-trisphosphate." J Biol Chem **273**(22): 13375-8.

Maksumova, L., H. T. Le, et al. (2005). "Protein tyrosine phosphatase alpha regulates Fyn activity and Cbp/PAG phosphorylation in thymocyte lipid rafts." J Immunol **175**(12): 7947-56.

Manel, N., D. Unutmaz, et al. (2008). "The differentiation of human T(H)-17 cells requires transforming growth factor-beta and induction of the nuclear receptor RORgammat." Nat Immunol **9**(6): 641-9.

Mao, C., E. G. Tili, et al. (2007). "Unequal contribution of Akt isoforms in the double-negative to double-positive thymocyte transition." J Immunol **178**(9): 5443-53.

Marie-Cardine, A., E. Bruyns, et al. (1997). "Molecular cloning of SKAP55, a novel protein that associates with the protein tyrosine kinase p59fyn in human T-lymphocytes." J Biol Chem **272**(26): 16077-80.

Marie-Cardine, A., L. R. Hendricks-Taylor, et al. (1998). "Molecular interaction between the Fyn-associated protein SKAP55 and the SLP-76-associated phosphoprotein SLAP-130." J Biol Chem **273**(40): 25789-95.

Marie-Cardine, A., H. Kirchgessner, et al. (1995). "Human T lymphocyte activation induces tyrosine phosphorylation of alpha-tubulin and its association with the SH2 domain of the p59fyn protein tyrosine kinase." Eur J Immunol **25**(12): 3290-7.

Martin-Cofreces, N. B., D. Sancho, et al. (2006). "Role of Fyn in the Rearrangement of Tubulin Cytoskeleton Induced through TCR." J Immunol **176**(7): 4201-7.

Martin-Orozco, N., Y. H. Wang, et al. (2006). "Cutting Edge: Programmed death (PD) ligand-1/PD-1 interaction is required for CD8+ T cell tolerance to tissue antigens." J Immunol **177**(12): 8291-5.

Martinez-Martinez, S., A. Rodriguez, et al. (2006). "Blockade of NFAT activation by the second calcineurin binding site." J Biol Chem **281**(10): 6227-35.

McKinsey, T. A., C. L. Zhang, et al. (2002). "MEF2: a calcium-dependent regulator of cell division, differentiation and death." Trends Biochem Sci **27**(1): 40-7.

Meier, R., M. Thelen, et al. (1998). "Inactivation and dephosphorylation of protein kinase Balpha (PKBalpha) promoted by hyperosmotic stress." Embo J **17**(24): 7294-303.

Miyakawa, H., S. K. Woo, et al. (1999). "Tonicity-responsive enhancer binding protein, a rel-like protein that stimulates transcription in response to hypertonicity." Proc Natl Acad Sci U S A **96**(5): 2538-42.

Monticelli, S. and A. Rao (2002). "NFAT1 and NFAT2 are positive regulators of IL-4 gene transcription." Eur J Immunol **32**(10): 2971-8.

Morales-Garcia, M. G., J. J. Fournie, et al. (2008). "A flow-cytometry method for analyzing the composition of membrane rafts." Cytometry A **73**(10): 918-25.

Mustelin, T., T. Pessa-Morikawa, et al. (1992). "Regulation of the p59fyn protein tyrosine kinase by the CD45 phosphotyrosine phosphatase." Eur J Immunol **22**(5): 1173-8.

Na, S. Y., A. Patra, et al. (2003). "Constitutively active protein kinase B enhances Lck and Erk activities and influences thymocyte selection and activation." J Immunol **171**(3): 1285-96.

Nakatani, K., H. Sakaue, et al. (1999). "Identification of a human Akt3 (protein kinase B gamma) which contains the regulatory serine phosphorylation site." Biochem Biophys Res Commun **257**(3): 906-10.

Nayak, A., J. Glockner-Pagel, et al. (2009). "Sumoylation of the transcription factor NFATc1 leads to its subnuclear relocalization and interleukin-2 repression by histone deacetylase." J Biol Chem **284**(16): 10935-46.

Nichols, K. E., D. P. Harkin, et al. (1998). "Inactivating mutations in an SH2 domain-encoding gene in X-linked lymphoproliferative syndrome." Proc Natl Acad Sci U S A **95**(23): 13765-70.

Obara, Y., K. Labudda, et al. (2004). "PKA phosphorylation of Src mediates Rap1 activation in NGF and cAMP signaling in PC12 cells." J Cell Sci **117**(Pt 25): 6085-94.

Oh-hora, M. and A. Rao (2008). "Calcium signaling in lymphocytes." Curr Opin Immunol **20**(3): 250-8.

Ohteki, T., M. Parsons, et al. (2000). "Negative regulation of T cell proliferation and interleukin 2 production by the serine threonine kinase GSK-3." J Exp Med **192**(1): 99-104.

Okada, M., S. Nada, et al. (1991). "CSK: a protein-tyrosine kinase involved in regulation of src family kinases." J Biol Chem **266**(36): 24249-52.

Okamura, H., J. Aramburu, et al. (2000). "Concerted dephosphorylation of the transcription factor NFAT1 induces a conformational switch that regulates transcriptional activity." Mol Cell **6**(3): 539-50.

Okazaki, T. and T. Honjo (2006). "The PD-1-PD-L pathway in immunological tolerance." Trends Immunol **27**(4): 195-201.

Ostergaard, H. L., D. A. Shackelford, et al. (1989). "Expression of CD45 alters phosphorylation of the lck-encoded tyrosine protein kinase in murine lymphoma T-cell lines." Proc Natl Acad Sci U S A **86**(22): 8959-63.

Palacios, E. H. and A. Weiss (2004). "Function of the Src-family kinases, Lck and Fyn, in T-cell development and activation." Oncogene **23**(48): 7990-8000.

Pancer, Z. and M. D. Cooper (2006). "The evolution of adaptive immunity." Annu Rev Immunol **24**: 497-518.

Parravicini, V., M. Gadina, et al. (2002). "Fyn kinase initiates complementary signals required for IgE-dependent mast cell degranulation." Nat Immunol **3**(8): 741-8.

Parsons, J. N., G. J. Wiederrecht, et al. (1994). "Regulation of calcineurin phosphatase activity and interaction with the FK-506.FK-506 binding protein complex." J Biol Chem **269**(30): 19610-6.

Parsons, M. J., R. G. Jones, et al. (2001). "Expression of active protein kinase B in T cells perturbs both T and B cell homeostasis and promotes inflammation." J Immunol **167**(1): 42-8.

Patra, A. K., T. Drewes, et al. (2006). "PKB rescues calcineurin/NFAT-induced arrest of Rag expression and pre-T cell differentiation." J Immunol **177**(7): 4567-76.

Patra, A. K., S. Y. Na, et al. (2004). "Active protein kinase B regulates TCR responsiveness by modulating cytoplasmic-nuclear localization of NFAT and NF-kappa B proteins." J Immunol **172**(8): 4812-20.

Peng, S. L., A. J. Gerth, et al. (2001). "NFATc1 and NFATc2 together control both T and B cell activation and differentiation." Immunity **14**(1): 13-20.

Peng, X. D., P. Z. Xu, et al. (2003). "Dwarfism, impaired skin development, skeletal muscle atrophy, delayed bone development, and impeded adipogenesis in mice lacking Akt1 and Akt2." Genes Dev **17**(11): 1352-65.

Peterson, E. J., M. L. Woods, et al. (2001). "Coupling of the TCR to integrin activation by Slap-130/Fyb." Science **293**(5538): 2263-5.

Peterson, R. T. and S. L. Schreiber (1999). "Kinase phosphorylation: Keeping it all in the family." Curr Biol **9**(14): R521-4.

Porter, C. M. and N. A. Clipstone (2002). "Sustained NFAT signaling promotes a Th1-like pattern of gene expression in primary murine CD4+ T cells." J Immunol **168**(10): 4936-45.

Potter, C. J., L. G. Pedraza, et al. (2002). "Akt regulates growth by directly phosphorylating Tsc2." Nat Cell Biol **4**(9): 658-65.
Prasad, K. V., O. Janssen, et al. (1993). "Src-homology 3 domain of protein kinase p59fyn mediates binding to phosphatidylinositol 3-kinase in T cells." Proc Natl Acad Sci U S A **90**(15): 7366-70.
Puc, J., M. Keniry, et al. (2005). "Lack of PTEN sequesters CHK1 and initiates genetic instability." Cancer Cell **7**(2): 193-204.
Qian, D., S. Lev, et al. (1997). "Tyrosine phosphorylation of Pyk2 is selectively regulated by Fyn during TCR signaling." J Exp Med **185**(7): 1253-9.
Quill, H., M. P. Riley, et al. (1992). "Anergic Th1 cells express altered levels of the protein tyrosine kinases p56lck and p59fyn." J Immunol **149**(9): 2887-93.
Quill, H. and R. H. Schwartz (1987). "Stimulation of normal inducer T cell clones with antigen presented by purified Ia molecules in planar lipid membranes: specific induction of a long-lived state of proliferative nonresponsiveness." J Immunol **138**(11): 3704-12.
Raab, M., Y. C. Cai, et al. (1995). "p56Lck and p59Fyn regulate CD28 binding to phosphatidylinositol 3-kinase, growth factor receptor-bound protein GRB-2, and T cell-specific protein-tyrosine kinase ITK: implications for T-cell costimulation." Proc Natl Acad Sci U S A **92**(19): 8891-5.
Randak, C., T. Brabletz, et al. (1990). "Cyclosporin A suppresses the expression of the interleukin 2 gene by inhibiting the binding of lymphocyte-specific factors to the IL-2 enhancer." Embo J **9**(8): 2529-36.
Ranger, A. M., M. R. Hodge, et al. (1998). "Delayed lymphoid repopulation with defects in IL-4-driven responses produced by inactivation of NF-ATc." Immunity **8**(1): 125-34.
Rathmell, J. C., R. L. Elstrom, et al. (2003). "Activated Akt promotes increased resting T cell size, CD28-independent T cell growth, and development of autoimmunity and lymphoma." Eur J Immunol **33**(8): 2223-32.
Rellahan, B. L., L. A. Jones, et al. (1990). "In vivo induction of anergy in peripheral V beta 8+ T cells by staphylococcal enterotoxin B." J Exp Med **172**(4): 1091-100.
Rengarajan, J., K. A. Mowen, et al. (2002). "Interferon regulatory factor 4 (IRF4) interacts with NFATc2 to modulate interleukin 4 gene expression." J Exp Med **195**(8): 1003-12.
Rengarajan, J., B. Tang, et al. (2002). "NFATc2 and NFATc3 regulate T(H)2 differentiation and modulate TCR-responsiveness of naive T(H)cells." Nat Immunol **3**(1): 48-54.
Resh, M. D. (1998). "Fyn, a Src family tyrosine kinase." Int J Biochem Cell Biol **30**(11): 1159-62.
Reth, M. (1989). "Antigen receptor tail clue." Nature **338**(6214): 383-4.
Rocha, B. and H. von Boehmer (1991). "Peripheral selection of the T cell repertoire." Science **251**(4998): 1225-8.
Roose, J. P., M. Mollenauer, et al. (2005). "A diacylglycerol-protein kinase C-RasGRP1 pathway directs Ras activation upon antigen receptor stimulation of T cells." Mol Cell Biol **25**(11): 4426-41.
Roose, J. P., M. Mollenauer, et al. (2007). "Unusual interplay of two types of Ras activators, RasGRP and SOS, establishes sensitive and robust Ras activation in lymphocytes." Mol Cell Biol **27**(7): 2732-45.
Saez-Rodriguez, J., L. Simeoni, et al. (2007). "A logical model provides insights into T cell receptor signaling." PLoS Comput Biol **3**(8): e163.
Saibil, S. D., R. G. Jones, et al. (2007). "CD4+ and CD8+ T cell survival is regulated differentially by protein kinase Ctheta, c-Rel, and protein kinase B." J Immunol **178**(5): 2932-9.
Salmond, R. J., A. Filby, et al. (2009). "T-cell receptor proximal signaling via the Src-family kinases, Lck and Fyn, influences T-cell activation, differentiation, and tolerance." Immunol Rev **228**(1): 9-22.
Samelson, L. E. (2002). "Signal transduction mediated by the T cell antigen receptor: the role of adapter proteins." Annu Rev Immunol **20**: 371-94.
Samelson, L. E., J. B. Harford, et al. (1985). "Identification of the components of the murine T cell antigen receptor complex." Cell **43**(1): 223-31.

Samelson, L. E., A. F. Phillips, et al. (1990). "Association of the fyn protein-tyrosine kinase with the T-cell antigen receptor." Proc Natl Acad Sci U S A **87**(11): 4358-62.
Sancak, Y., C. C. Thoreen, et al. (2007). "PRAS40 is an insulin-regulated inhibitor of the mTORC1 protein kinase." Mol Cell **25**(6): 903-15.
Sano, H., S. Kane, et al. (2003). "Insulin-stimulated phosphorylation of a Rab GTPase-activating protein regulates GLUT4 translocation." J Biol Chem **278**(17): 14599-602.
Sarbassov, D. D., D. A. Guertin, et al. (2005). "Phosphorylation and regulation of Akt/PKB by the rictor-mTOR complex." Science **307**(5712): 1098-101.
Sayos, J., C. Wu, et al. (1998). "The X-linked lymphoproliferative-disease gene product SAP regulates signals induced through the co-receptor SLAM." Nature **395**(6701): 462-9.
Schmitt, J. M. and P. J. Stork (2002). "PKA phosphorylation of Src mediates cAMP's inhibition of cell growth via Rap1." Mol Cell **9**(1): 85-94.
Schwartz, R. H. (1996). "Models of T cell anergy: is there a common molecular mechanism?" J Exp Med **184**(1): 1-8.
Schwartz, R. H. (2003). "T cell anergy." Annu Rev Immunol **21**: 305-34.
Sekimoto, T., M. Fukumoto, et al. (2004). "14-3-3 suppresses the nuclear localization of threonine 157-phosphorylated p27(Kip1)." Embo J **23**(9): 1934-42.
Serfling, E., A. Avots, et al. (1995). "The architecture of the interleukin-2 promoter: a reflection of T lymphocyte activation." Biochim Biophys Acta **1263**(3): 181-200.
Serfling, E., F. Berberich-Siebelt, et al. (2000). "The role of NF-AT transcription factors in T cell activation and differentiation." Biochim Biophys Acta **1498**(1): 1-18.
Serfling, E., S. Chuvpilo, et al. (2006). "NFATc1 autoregulation: a crucial step for cell-fate determination." Trends Immunol **27**(10): 461-9.
Shaw, J. P., P. J. Utz, et al. (1988). "Identification of a putative regulator of early T cell activation genes." Science **241**(4862): 202-5.
Shaw, K. T., A. M. Ho, et al. (1995). "Immunosuppressive drugs prevent a rapid dephosphorylation of transcription factor NFAT1 in stimulated immune cells." Proc Natl Acad Sci U S A **92**(24): 11205-9.
Shenoy, S., I. Chackalaparampil, et al. (1992). "Role of p34cdc2-mediated phosphorylations in two-step activation of pp60c-src during mitosis." Proc Natl Acad Sci U S A **89**(15): 7237-41.
Shenoy, S., J. K. Choi, et al. (1989). "Purified maturation promoting factor phosphorylates pp60c-src at the sites phosphorylated during fibroblast mitosis." Cell **57**(5): 763-74.
Sheridan, C. M., E. K. Heist, et al. (2002). "Protein kinase A negatively modulates the nuclear accumulation of NF-ATc1 by priming for subsequent phosphorylation by glycogen synthase kinase-3." J Biol Chem **277**(50): 48664-76.
Shtivelman, E., J. Sussman, et al. (2002). "A role for PI 3-kinase and PKB activity in the G2/M phase of the cell cycle." Curr Biol **12**(11): 919-24.
Sicheri, F. and J. Kuriyan (1997). "Structures of Src-family tyrosine kinases." Curr Opin Struct Biol **7**(6): 777-85.
Siefken, R., S. Klein-Hessling, et al. (1998). "A CD28-associated signaling pathway leading to cytokine gene transcription and T cell proliferation without TCR engagement." J Immunol **161**(4): 1645-51.
Simarro, M., A. Lanyi, et al. (2004). "SAP increases FynT kinase activity and is required for phosphorylation of SLAM and Ly9." Int Immunol **16**(5): 727-36.
Simeoni, L., S. Kliche, et al. (2004). "Adaptors and linkers in T and B cells." Curr Opin Immunol **16**(3): 304-13.
Singh, N. J. and R. H. Schwartz (2003). "The strength of persistent antigenic stimulation modulates adaptive tolerance in peripheral CD4+ T cells." J Exp Med **198**(7): 1107-17.
Sinha, D., S. Bannergee, et al. (2004). "Inhibition of ligand-independent ERK1/2 activity in kidney proximal tubular cells deprived of soluble survival factors up-regulates Akt and prevents apoptosis." J Biol Chem **279**(12): 10962-72.
Sloan-Lancaster, J., B. D. Evavold, et al. (1993). "Induction of T-cell anergy by altered T-cell-receptor ligand on live antigen-presenting cells." Nature **363**(6425): 156-9.

Smida, M., A. Posevitz-Fejfar, et al. (2007). "A novel negative regulatory function of the phosphoprotein associated with glycosphingolipid-enriched microdomains: blocking Ras activation." Blood **110**(2): 596-615.

Smith-Garvin, J. E., G. A. Koretzky, et al. (2009). "T cell activation." Annu Rev Immunol **27**: 591-619.

Staal, S. P. (1987). "Molecular cloning of the akt oncogene and its human homologues AKT1 and AKT2: amplification of AKT1 in a primary human gastric adenocarcinoma." Proc Natl Acad Sci U S A **84**(14): 5034-7.

Staal, S. P. and J. W. Hartley (1988). "Thymic lymphoma induction by the AKT8 murine retrovirus." J Exp Med **167**(3): 1259-64.

Staal, S. P., J. W. Hartley, et al. (1977). "Isolation of transforming murine leukemia viruses from mice with a high incidence of spontaneous lymphoma." Proc Natl Acad Sci U S A **74**(7): 3065-7.

Stefanova, I., B. Hemmer, et al. (2003). "TCR ligand discrimination is enforced by competing ERK positive and SHP-1 negative feedback pathways." Nat Immunol **4**(3): 248-54.

Stein, P. L., H. M. Lee, et al. (1992). "pp59fyn mutant mice display differential signaling in thymocytes and peripheral T cells." Cell **70**(5): 741-50.

Stockinger, B. and M. Veldhoen (2007). "Differentiation and function of Th17 T cells." Curr Opin Immunol **19**(3): 281-6.

Stone, J. D., L. A. Conroy, et al. (1997). "Aberrant TCR-mediated signaling in CD45-null thymocytes involves dysfunctional regulation of Lck, Fyn, TCR-zeta, and ZAP-70." J Immunol **158**(12): 5773-82.

Stover, D. R., P. Furet, et al. (1996). "Modulation of the SH2 binding specificity and kinase activity of Src by tyrosine phosphorylation within its SH2 domain." J Biol Chem **271**(21): 12481-7.

Straus, D. B. and A. Weiss (1992). "Genetic evidence for the involvement of the lck tyrosine kinase in signal transduction through the T cell antigen receptor." Cell **70**(4): 585-93.

Sugie, K., M. S. Jeon, et al. (2004). "Activation of naive CD4 T cells by anti-CD3 reveals an important role for Fyn in Lck-mediated signaling." Proc Natl Acad Sci U S A **101**(41): 14859-64.

Taha, C., Z. Liu, et al. (1999). "Opposite translational control of GLUT1 and GLUT4 glucose transporter mRNAs in response to insulin. Role of mammalian target of rapamycin, protein kinase b, and phosphatidylinositol 3-kinase in GLUT1 mRNA translation." J Biol Chem **274**(46): 33085-91.

Takeuchi, M., S. Kuramochi, et al. (1993). "Functional and physical interaction of protein-tyrosine kinases Fyn and Csk in the T-cell signaling system." J Biol Chem **268**(36): 27413-9.

Tanchot, C., D. L. Barber, et al. (2001). "Adaptive tolerance of CD4+ T cells in vivo: multiple thresholds in response to a constant level of antigen presentation." J Immunol **167**(4): 2030-9.

Tang, X., Y. Feng, et al. (2007). "Src-family tyrosine kinase fyn phosphorylates phosphatidylinositol 3-kinase enhancer-activating Akt, preventing its apoptotic cleavage and promoting cell survival." Cell Death Differ **14**(2): 368-77.

Terui, Y., N. Saad, et al. (2004). "Dual role of sumoylation in the nuclear localization and transcriptional activation of NFAT1." J Biol Chem **279**(27): 28257-65.

Timson Gauen, L. K., A. N. Kong, et al. (1992). "p59fyn tyrosine kinase associates with multiple T-cell receptor subunits through its unique amino-terminal domain." Mol Cell Biol **12**(12): 5438-46.

Tokunaga, E., E. Oki, et al. (2008). "Deregulation of the Akt pathway in human cancer." Curr Cancer Drug Targets **8**(1): 27-36.

Torgersen, K. M., T. Vang, et al. (2001). "Release from tonic inhibition of T cell activation through transient displacement of C-terminal Src kinase (Csk) from lipid rafts." J Biol Chem **276**(31): 29313-8.

Tran, H., A. Brunet, et al. (2003). "The many forks in FOXO's road." Sci STKE **2003**(172): RE5.

Tschopp, O., Z. Z. Yang, et al. (2005). "Essential role of protein kinase B gamma (PKB gamma/Akt3) in postnatal brain development but not in glucose homeostasis." Development **132**(13): 2943-54.

Tsushima, F., S. Yao, et al. (2007). "Interaction between B7-H1 and PD-1 determines initiation and reversal of T-cell anergy." Blood **110**(1): 180-5.

Tsygankov, A. Y., S. Mahajan, et al. (1996). "Specific association of tyrosine-phosphorylated c-Cbl with Fyn tyrosine kinase in T cells." J Biol Chem **271**(43): 27130-7.

Turner, J. M., M. H. Brodsky, et al. (1990). "Interaction of the unique N-terminal region of tyrosine kinase p56lck with cytoplasmic domains of CD4 and CD8 is mediated by cysteine motifs." Cell **60**(5): 755-65.

Utting, O., J. J. Priatel, et al. (2001). "p59fyn (Fyn) promotes the survival of anergic CD4-CD8- alpha beta TCR+ cells but negatively regulates their proliferative response to antigen stimulation." J Immunol **166**(3): 1540-6.

Utting, O., S. J. Teh, et al. (1998). "T cells expressing receptors of different affinity for antigen ligands reveal a unique role for p59fyn in T cell development and optimal stimulation of T cells by antigen." J Immunol **160**(11): 5410-9.

Utting, O., S. J. Teh, et al. (2000). "A population of in vivo anergized T cells with a lower activation threshold for the induction of CD25 exhibit differential requirements in mobilization of intracellular calcium and mitogen-activated protein kinase activation." J Immunol **164**(6): 2881-9.

Vadlamudi, R. K., A. A. Sahin, et al. (2003). "Heregulin and HER2 signaling selectively activates c-Src phosphorylation at tyrosine 215." FEBS Lett **543**(1-3): 76-80.

van Oers, N. S., N. Killeen, et al. (1996). "Lck regulates the tyrosine phosphorylation of the T cell receptor subunits and ZAP-70 in murine thymocytes." J Exp Med **183**(3): 1053-62.

Vang, T., K. M. Torgersen, et al. (2001). "Activation of the COOH-terminal Src kinase (Csk) by cAMP-dependent protein kinase inhibits signaling through the T cell receptor." J Exp Med **193**(4): 497-507.

Volkman, B. F., D. Lipson, et al. (2001). "Two-state allosteric behavior in a single-domain signaling protein." Science **291**(5512): 2429-33.

Waksman, G., S. E. Shoelson, et al. (1993). "Binding of a high affinity phosphotyrosyl peptide to the Src SH2 domain: crystal structures of the complexed and peptide-free forms." Cell **72**(5): 779-90.

Wary, K. K., A. Mariotti, et al. (1998). "A requirement for caveolin-1 and associated kinase Fyn in integrin signaling and anchorage-dependent cell growth." Cell **94**(5): 625-34.

Watts, J. D., J. S. Sanghera, et al. (1993). "Phosphorylation of serine 59 of p56lck in activated T cells." J Biol Chem **268**(31): 23275-82.

Wei, W., J. Jin, et al. (2005). "The v-Jun point mutation allows c-Jun to escape GSK3-dependent recognition and destruction by the Fbw7 ubiquitin ligase." Cancer Cell **8**(1): 25-33.

Weiss, A. and D. R. Littman (1994). "Signal transduction by lymphocyte antigen receptors." Cell **76**(2): 263-74.

Welcker, M., J. Singer, et al. (2003). "Multisite phosphorylation by Cdk2 and GSK3 controls cyclin E degradation." Mol Cell **12**(2): 381-92.

Welke, J. and N. Zavazava (2002). "P59(fyn) is upregulated in anergic CD8+ T cells." Hum Immunol **63**(10): 834-43.

Wilson, A., W. Held, et al. (1994). "Two waves of recombinase gene expression in developing thymocytes." J Exp Med **179**(4): 1355-60.

Winkler, D. G., I. Park, et al. (1993). "Phosphorylation of Ser-42 and Ser-59 in the N-terminal region of the tyrosine kinase p56lck." Proc Natl Acad Sci U S A **90**(11): 5176-80.

Wofford, J. A., H. L. Wieman, et al. (2008). "IL-7 promotes Glut1 trafficking and glucose uptake via STAT5-mediated activation of Akt to support T-cell survival." Blood **111**(4): 2101-11.

Wu, Y., M. Borde, et al. (2006). "FOXP3 controls regulatory T cell function through cooperation with NFAT." Cell **126**(2): 375-87.

Xu, S., J. Huo, et al. (2005). "Cbp deficiency alters Csk localization in lipid rafts but does not affect T-cell development." Mol Cell Biol **25**(19): 8486-95.

Yang, X. Y., L. H. Wang, et al. (2000). "Activation of human T lymphocytes is inhibited by peroxisome proliferator-activated receptor gamma (PPARgamma) agonists. PPARgamma co-association with transcription factor NFAT." J Biol Chem **275**(7): 4541-4.

Yang, Z. Z., O. Tschopp, et al. (2005). "Dosage-dependent effects of Akt1/protein kinase Balpha (PKBalpha) and Akt3/PKBgamma on thymus, skin, and cardiovascular and nervous system development in mice." Mol Cell Biol **25**(23): 10407-18.

Yasuda, K., M. Nagafuku, et al. (2002). "Cutting edge: Fyn is essential for tyrosine phosphorylation of Csk-binding protein/phosphoprotein associated with glycolipid-enriched microdomains in lipid rafts in resting T cells." J Immunol **169**(6): 2813-7.

Yeh, E., M. Cunningham, et al. (2004). "A signalling pathway controlling c-Myc degradation that impacts oncogenic transformation of human cells." Nat Cell Biol **6**(4): 308-18.

York, I. A. and K. L. Rock (1996). "Antigen processing and presentation by the class I major histocompatibility complex." Annu Rev Immunol **14**: 369-96.

Zha, Y., R. Marks, et al. (2006). "T cell anergy is reversed by active Ras and is regulated by diacylglycerol kinase-alpha." Nat Immunol **7**(11): 1166-73.

Zhang, W., J. Sloan-Lancaster, et al. (1998). "LAT: the ZAP-70 tyrosine kinase substrate that links T cell receptor to cellular activation." Cell **92**(1): 83-92.

Zhou, B., R. Q. Cron, et al. (2002). "Regulation of the murine Nfatc1 gene by NFATc2." J Biol Chem **277**(12): 10704-11.

Zhou, B. P., Y. Liao, et al. (2001). "Cytoplasmic localization of p21Cip1/WAF1 by Akt-induced phosphorylation in HER-2/neu-overexpressing cells." Nat Cell Biol **3**(3): 245-52.

Zhu, J., F. Shibasaki, et al. (1998). "Intramolecular masking of nuclear import signal on NF-AT4 by casein kinase I and MEKK1." Cell **93**(5): 851-61.

8 Abbreviations

Ab	antibody
ADAP	adhesion and degranulation promoting adapter protein
AP-1	activator protein-1
APC	antigen presenting cell
APS	ammoniumperoxodisulfate
ATP	adenosine 5'-triphosphate
BCR	B cell receptor
BH3	Bcl-2 homology domain 3
bZIP	basic region-leucine zipper
Cbl	casitas B-lineage lymphoma proto-oncogene
CD	cluster of differentiation
CK1	casein kinase 1
CN	calcineurin
CRAC channel	calcium-release-activated calcium channel
CsA	cyclosporin A
Csk	C-terminal Src kinase
CTL	cytotoxic T cell
CTLA4	cytotoxic T-lymphocyte antigen 4
CTX	cholera toxin
DAG	diacylglycerol
DGK-α	diacylglycerol kinase alpha
DISC	death-inducing signaling complex
DMSO	dimethylsulfoxide
DN	double negative
DP	double positive
DTT	dithiothreitol
DYRK	dual-specificity tyrosine-phosphorylation regulated kinase
E. coli	Escherichia coli
EDTA	ethylenediaminetetraacetic acid
ER	endoplasmatic reticulum
Erk	extracellular signal-regulated kinase
FasL	Fas ligand
FCS	fetal calf serum
FYB	Fyn binding protein
Gab2	GRB2-associated binding protein 2

GADS	Grb2-related adapter downstream of Shc
GEF	guanine nucleotide exchange factor
Glut	glucose transporter
GM-CSF	granulocyte macrophage colony-stimulating factor
Grail	gene related to anergy in lymphocytes
GRB2	growth-factor-receptor-bound protein 2
GSK-3	glycogen synthase kinase-3
GST	glutathione *S*-transferase
h	hour
HSC	hematopoietic stem cell
ic	intracellular
IFN-γ	interferon gamma
Ig	immunoglobulin
IL	interleukin
IP	immunoprecipitation
IP_3	inositol-1,4,5-trisphosphate
IPTG	isopropyl-β-D-thiogalactopyranoside
ITAM	immunoreceptor tyrosine based activation motif
Itk	IL-2 inducible T cell kinase
IVK	*in vitro* kinase assay
JNK	JUN N-terminal kinase
ko	knockout
LAT	linker for activation of T cells
Lck	lymphocyte-specific protein tyrosine kinase
LCR	locus control region
LM	n-Dodecyl-β-D-maltoside
MAPK	mitogen-activated protein kinase
MEK	MAPK/Erk kinase
MES	2-[N-Morpholino] ethanesulfonic acid
MHC	major histocompatibility complex
min	minute
MK-PT cells	mouse kidney proximal tubular epithelial cells
MPF	metaphase promoting factor
mTOR	mammalian target of rapamycin
mTORC1	mTOR complex 1
Nedd4	neural precursor cell expressed developmentally down-regulated protein 4

NES	nuclear export signal
NFAT	nuclear factor of activated T cells
NFκB	nuclear factor kappa-light-chain-enhancer of activated B cells
NHR	NFAT-homology region
NK cell	natural killer cell
NLS	nuclear localization signal
nt	nucleotide
nTreg	naturally occurring regulatory T cell
PA	phosphatidic acid
PAG	phosphoprotein associated with glycosphingolipid-enriched microdomains
PD-1	programmed death 1
PDK1	phosphoinositide-dependent kinase-1
PEI	polyethylenimine
PEP	proline-enriched protein tyrosine phosphatase
PHLPP	PH domain leucine-rich repeat protein phosphatase
PI3-K	phosphatidylinositol 3-kinase
PIKE-A	phosphatidylinositol 3-kinase enhancer-activating Akt
PIP2	phosphatidylinositol-4,5-bisphosphate
PIP3	phosphatidylinositol-3,4,5-trisphosphate
PKA	protein kinase A
PKB	protein kinase B
PKC	protein kinase C
PLCγ	phospholipase C gamma
PMA	phorbol 12-myristate 13-acetate
PML-nb	promyelocytic leukemia nuclear body
PMSF	phenylmethylsulfonylfluoride
PP2A	protein phosphatase 2A
PRAS40	proline-rich Akt substrate of 40 kDa
PTEN	phosphatase and tensin homologue localized on chromosome ten
PTPα	receptor protein tyrosine phosphatase alpha
RasGRP	Ras guanyl nucleotide-releasing protein
RHR	REL-homology region
rpm	rounds per minute
Rsk	ribosomal S6 kinase
RT	room temperature
Sam68	Src associated in mitosis 68 kDa

SAP	SLAM-associated protein
SDS	sodium dodecyl sulfate
SDS-PAGE	sodium dodecyl sulfate polyacrylamide gel electrophoresis
sec	second
SH	Src homology
Shc	SH2 domain-containing transforming protein
SHP-1	SH2 domain-containing phosphatase 1
SKAP55	Src kinase-assosciated phosphoprotein of 55 kDa
SLAM	signaling lymphocyte activation molecule
SLAP	SLP76 associated protein
SLP76	Src homology 2 domain-containing leukocyte protein of 76 kDa
SOS	son of sevenless
SP box	serine-proline box
SRR	serine-rich region
STAT	signal transducer and activator of transcription
SUMO	small ubiquitin-like modifier
TAD	transactivation domain
TCA	trichloroacetic acid
TCR	T cell receptor
TEMED	tetramethylethylenediamine
tg	transgenic
TGF-β	transforming growth facor beta
Th cell	T helper cell
ThF	follicular T helper cell
TNF-α	tumor necrosis factor alpha
TNF-β	tumor necrosis factor beta
Treg	regulatory T cell
TSC2	tuberous sclerosis complex 2
Tsg101	tumor susceptibility gene 101 protein
Unc119	uncoordinated 119
vc	vector control
WASP	Wiskott-Aldrich syndrome protein
XLP	X-linked lymphoproliferative syndrome
ZAP-70	zeta-associated protein of 50 kDa

9 List of figures and tables

10 Curriculum vitae

Personal details:

Name:	Thomas Drewes
Current address:	Blumenberger Straße 12, apartment 32
	39122 Magdeburg
Date of birth:	22.06.1975
Place of birth:	Steinheim (Westphalia, Germany)
Nationality:	German

Academic education:

2004- 2009:	PhD student
	Institute for Molecular and Clinical Immunology
	Otto-von-Guericke University, Magdeburg, Germany
1999- 2004:	Dipl.-Biol. Univ.
	Faculty of Biology
	Julius-Maximilians University, Würzburg, Germany

Professional education and activities:

1998- 1999:	Skilled worker
	Department of machine building
	Phoenix Contact GmbH & Co., Blomberg, Germany
1995- 1998:	Apprenticeship
	Industrial mechanic
	Phoenix Contact GmbH & Co., Blomberg, Germany

11 Publications

Bajbouj K, Poehlmann A, Kuester D, **Drewes T**, Haase K, Hartig R, Teller A, Kliche S, Walluscheck D, Ivanovska J, Chakrilam S, Ulitzsch A, Bommhardt U, Leverkus M, Roessner A, Schneider-Stock R;
Identification of Phosphorylated p38 as a Novel DAPK-Interacting Partner during TNFα-Induced Apoptosis in Colorectal Tumor Cells;
American Journal of Pathology 2009 Aug; 175(2):557-70

Patra AK, **Drewes T**, Engelmann S, Chuvpilo S, Kishi H, Hünig T, Serfling E, Bommhardt U;
PKB rescues calcineurin/NFAT-induced arrest of Rag expression and pre-T cell differentiation;
Journal of Immunology 2006 Oct 1; 177(7):4567-76

Alsheimer M, **Drewes T**, Schütz W, Benavente R;
The cancer/testis antigen CAGE-1 is a component of the acrosome of spermatids and spermatozoa;
European Journal of Cell Biology 2005 Mar; 84(2-3):445-52